Defining the Engineering Envelope of VMA Based Fogponics for Lunar Greenhouses

Framework Development and Boundary Evidence from Decontextualized Lab Venue Experiments

Thesis

Siert Hamers

Delft University of Technology

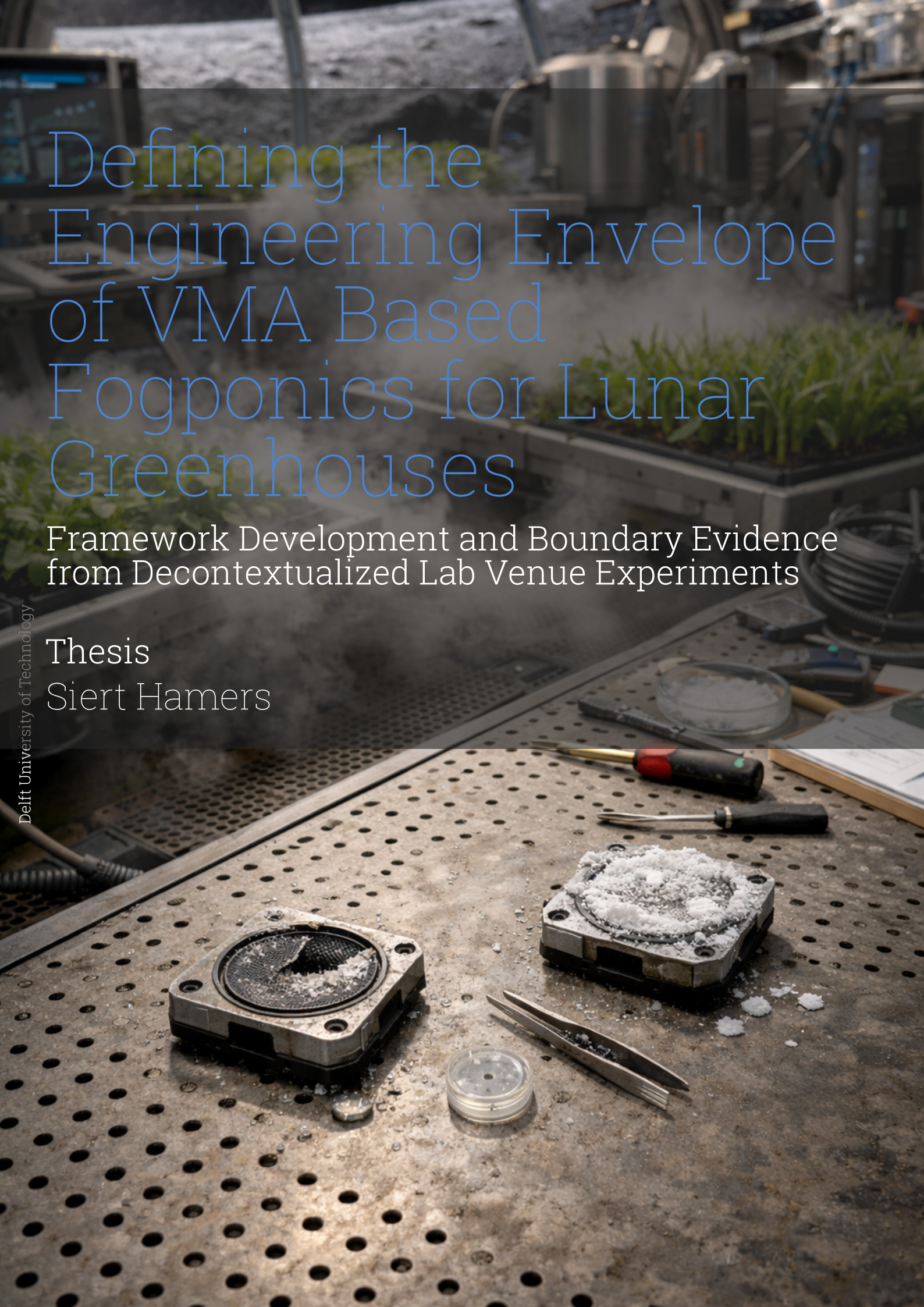

Defining the Engineering Envelope of VMA Based Fogponics for Lunar Greenhouses

Framework Development and Boundary Evidence from Decontextualized Lab Venue Experiments

by

Siert Hamers

—

Instructor: Dr. J. Guo
Prof. Dr. D. Schubert
Faculty: Faculty of Aerospace Engineering, Delft
Institution: German Aerospace Center, Institute for Space Systems, Bremen

TU Delft

Preface

I would like to express my sincere gratitude to everyone who supported me throughout this thesis.

First, I would like to thank my supervisors, Dr. Guo and Prof. Dr. Schubert, for their guidance during this work while giving me the freedom to explore, iterate, and learn through the process.

As this thesis marks the end of a long study career, I especially want to thank the people who sided me through this journey. I thank my parents and my sister. From my father I have always felt the curiosity and enthusiasm for fundamentals that shaped the way I approach engineering and research. I am grateful to my mother for her guidance in managing time, workload, and people. And I thank my sister for reminding me that it does not have to be perfect, it has to be finished first.

During my time at DLR, I would like to specifically thank, among my colleagues, Markus and Jess for taking the time to guide me and help me reflect on my work and its meaning. I am grateful to everyone who supported me in the day-to-day work, discussions, and practical help.

I would also like to thank Mark Weislogel. He did not know me beforehand, but he still made time to discuss my research and, in doing so, transmitted a remarkable enthusiasm for doing science. That energy genuinely kept me going.

Siert Hamers
Bremen, February 18, 2026

Summary

Bioregenerative life support systems (BLSS) are essential for long-duration lunar missions that require resupply independence. Current aeroponic architectures exhibit operational vulnerabilities including high-pressure pump related issues and biofilm proliferation. This research investigates fogponics as an alternative by utilizing Vibrating Mesh Atomizers (VMA) to deliver nutrient solutions. Adopting a Research through Design (RtD) framework, the study decontextualized the nutrient delivery problem by developing a custom prototype as a formal research instrument. This methodological approach enabled the isolation of mechanical and chemical variables through controlled duty cycles and intentional design moves. Experimental results identified salt precipitation and structural mesh rupture as dominant failure modes that define the current operational boundaries of VMA technology. Quantitative analysis demonstrated that gravimetric flowrate serves as a reliable health metric for VMA performance. Specifically, $25\ \mu m$ *modules exhibited catastrophic mesh rupture while* $2.9\ \mu m$ *modules experienced significant delivery degradation due to salt deposition. These failures led to substantial nutrient retention within the system. Furthermore, the findings reveal a strong coupling between pH and temperature, where thermal loads directly influenced chemical signal integrity. This thesis contributes a laboratory-validated research platform and an evidence-based characterization of dominant failure mechanisms. By establishing first-order design rules and defining a bounded engineering knowledge base, this work provides a standardized framework for VMA research in lunar crop production. The results emphasize the necessity of measuring parameters at both the reservoir and drain to maintain system stability and inform future high-technology readiness level (TRL) lunar greenhouse architectures.*

Contents

List of Figures

List of Tables

Nomenclature

Abbreviations

Abbreviation	Definition
BLSS	Bioregenerative Life Support System
DLR	Deutsches Zentrum für Luft- und Raumfahrt (German Aerospace Center)
EDEN ISS	Evolution and Design of Environmentally closed Nutrition sources – International Space Station demonstrator
LAM-GTD	Lunar Agricultural Module – Ground Test Demonstrator
EDEN LUNA	EDEN Lunar Analog (successor to EDEN ISS)
NDS	Nutrient Delivery System
EVE	EDEN Versatile End-Effector
C.R.O.P.	Combined Regenerative Organic food Production (Biofilter system)
RtD	Research through Design
CDR	Constructive Design Research
VMA	Vibrating Mesh Atomizer
EC	Electrical Conductivity
pH	Potential of Hydrogen (acidity/alkalinity)
RH	Relative Humidity
TRL	Technology Readiness Level
ESA	European Space Agency
NASA	National Aeronautics and Space Administration
CSA	Canadian Space Agency
MTF	Mobile Test Facility
SES	Service Section
FEG	Future Exploration Greenhouse
UV	Ultraviolet
CAD	Computer-Aided Design
IRR	Infrastructure Reliability and Robustness (requirement category)
CC	Contamination Control (requirement category)
SC	System Complexity (requirement category)
MC	Monitoring and Control (requirement category)
FPF	Fine Particle Fraction
TDS	Total Dissolved Solids
MHz	Megahertz
kHz	Kilohertz
µm	Micrometer
°C	Degree Celsius
ISS	International Space Station

Symbols

Symbol	Definition	Unit
t	Time	[s]
m	Mass	[kg]
$\dot{m}$	Mass flow rate	[kg/s]
Q	Volumetric flow rate	[m^3/s]
A	Area	[m^2]
d	Droplet diameter	[µm]
X_{10}, X_{50}, X_{90}	Percentile droplet diameters for distribution width	[µm]
Span	Droplet size distribution width factor $(X_{90}-X_{10})/X_{50}$	[-]
FPF	Fine Particle Fraction (fraction of 1–5 µm droplets)	[-]
f	Atomization or driving frequency	[Hz]
DC	Duty cycle (on/off ratio)	[min on / min off]
I	Electric current	[A]
U	Electric voltage	[V]
P_{el}	Electrical power input	[W]
E	Energy	[J]
η	Efficiency	[-]
EC	Electrical conductivity of nutrient solution	[mS/cm]
pH	Acidity or alkalinity index (hydrogen potential)	[-]
TDS	Total dissolved solids	[mg/L]
λ	Wavelength of surface oscillation	[m]
γ	Surface tension or specific heat ratio (context-dependent)	[N/m] or [-]
ΔT	Temperature difference	[K]
ΔEC	Change in electrical conductivity over time	[mS/cm]
N	Number of modules or sensors	[-]
k	Empirical constant or calibration coefficient	[-]
μ	Dynamic viscosity	[Pa·s]

1

Introduction and Problem Space

This chapter establishes the necessity of advancing life support technologies for the upcoming era of lunar exploration. As international space agencies transition from short-term mapping missions to the establishment of permanent lunar bases, the development of bioregenerative life support systems becomes a critical requirement for resupply independence. By analyzing the operational heritage of the German Aerospace Center (DLR) and projects like EDEN ISS, this introduction identifies the specific mechanical and biological failures of current aeroponic architectures. These limitations, ranging from biofilm proliferation to high-pressure pump vulnerabilities, define the problem space for this research. The following sections outline the engineering requirements and the constructive design research stance used to investigate fogponics as a simplified, high-reliability alternative for sustainable lunar agriculture.

1.1. Why Return to the Moon?

Returning to the Moon is an endeavor that extends far beyond exploration. The Moon offers a unique environment for scientific advancement, resource development, and technological innovation. It serves as a stepping stone toward a permanent human presence outside of Earth. The lunar surface holds valuable resources such as water ice confirmed at the poles. This ice can facilitate future life support and fuel systems [1]. Furthermore, the rare isotope Helium-3 could play a role in future fusion energy development [2].

With no atmosphere, the lunar surface allows telescopes to observe the full electromagnetic spectrum. Cold and stable regions near the poles could passively cool infrared instruments to below 40 K. This enables long-term, high-precision space observation without the need for cryogenic fluids [1]. Unlike Earth orbit, the Moon's far side remains free from radio interference and satellite congestion. It provides an ideal platform for deep-space astronomy. Finally, the ancient geology of the Moon preserves a history of the early solar system that has been lost on Earth due to tectonics and erosion. Studying its surface provides insight into the origins of our own planet [1]. Together, these factors make the Moon a gateway to a new paradigm of space exploration.

In recent years, global interest in the Moon has accelerated. Historically, the United States and the Soviet Union dominated lunar missions. Today, a broader group of nations (including China, India, Japan, South Korea, Russia, and the United Arab Emirates) is investing heavily in new lunar projects [3]. Upcoming missions range from surface mapping and precision landings to water-ice prospecting. China's space roadmap (2024–2050) aims to land astronauts on the Moon before 2030. It seeks to establish a sustained human and robotic presence through the International Lunar Research Station in the 2030s [4].

Concurrently, NASA's Artemis program aims to return humans to the lunar surface to lay the foundation for sustainable exploration. In its 2016 roadmap, the European Space Agency (ESA) identified sustaining human life in hostile environments as a fundamental pillar of its long-term strategy [5]. The central question within this pillar concerns which technologies can deliver the highest and most efficient

nutrient production. This motivates the development of Bioregenerative Life Support Systems (BLSS). These systems use biological processes to recycle air, water, and nutrients while producing food. For long-duration human exploration, BLSS are widely regarded as the only viable pathway to achieve sufficient autonomy and resupply independence at scale.

1.2. The German Aerospace Center (DLR)

Since 2011, the German Aerospace Center (DLR) has been investigating optimal crop production as a core element in BLSS. This research, led by the Institute of Space Systems in Bremen, is embedded in the Evolution and Design of Environmentally closed Nutrition sources (EDEN) initiative. The focus lies on developing and validating crop production systems capable of operating reliably in harsh and isolated environments [6]. These efforts are embodied in three primary projects and are explained in the following section.

1.2.1. EDEN ISS

The EDEN ISS project was a four-year, EU-funded program aimed at validating Controlled Environment Agriculture (CEA) technologies. To provide a research platform, the Mobile Test Facility (MTF) was developed. This facility demonstrated near-closed loop food production with the primary objective of supplying crews with fresh crops.

Figure 1.1: EDEN ISS Mobile Test Facility (MTF), a previous DLR Bremen project demonstrating controlled environment crop production as part of bioregenerative life support systems (BLSS). The facility was deployed near Neumayer III Station in Antarctica for a three year campaign and produced more than 1000 kg of fresh crops for the station crew. Source: [7].

The MTF as shown in Figure 1.1 was successfully deployed near the Neumayer III Station in Antarctica. It produced over 1000 kg of fresh crops and demonstrated the feasibility of cultivation in one of the most hostile environments on Earth [8]. The facility provides a cultivation area of 30 m^2 and consists of two sections. The Service Section (SES) houses the essential subsystems (including air monitoring, data handling, and control). The second section, the Future Exploration Greenhouse (FEG), contains the plant cultivation area. The roots of the plants are suspended in trays and are sprayed with nutrients by a specialized delivery system [8].

1.2.2. LAM-GTD

Building upon the work of EDEN ISS, DLR is collaborating with the Canadian Space Agency (CSA) to develop the Lunar Agricultural Module - Ground Test Demonstrator (LAM-GTD) [9]. The LAM-GTD follows an integrated approach where atmospheric revitalization, food production, and water recycling are combined within a single habitat module.

The internal layout provides approximately 30 m^2 of cultivation area. An early impression of a similar lunar variant is shown in Figure 1.2. Its production rate is aimed at 90 kg of fresh produce per month. This output should cover a significant percentage of the nutritional needs for a six-person crew. DLR

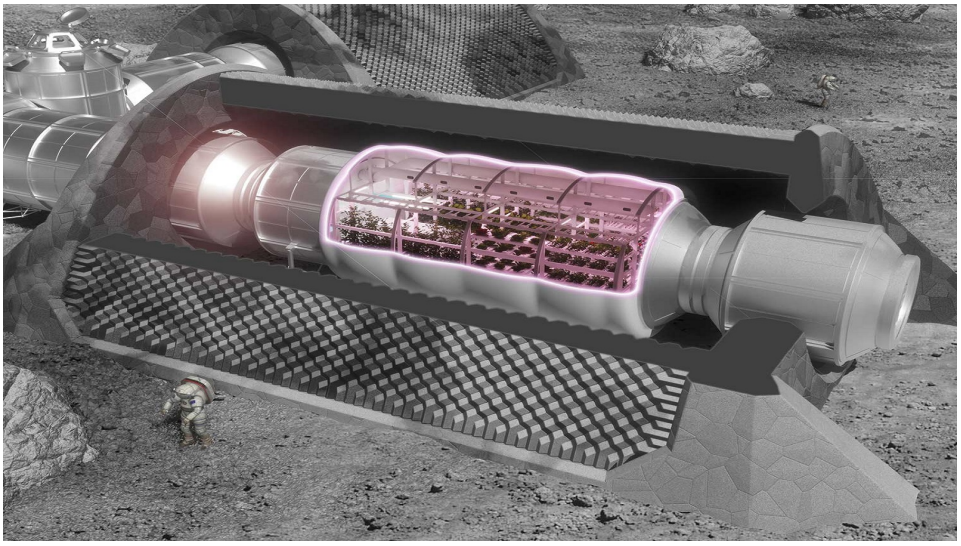

Figure 1.2: Concept rendering of the Lunar Agricultural Module – Ground Test Demonstrator (LAM-GTD), a flagship DLR Bremen project currently in the design phase. LAM-GTD is intended to be built as a lunar greenhouse analogue, reproducing the architecture and operational concept of a Moon deployed system while using non space grade materials for ground testing. It represents the next development step after EDEN ISS and a bridge towards a first lunar greenhouse implementation, and is developed in collaboration with the Canadian Space Agency (CSA). Source: [10].

aims to finalize this flagship project in the 2030s [9].

1.2.3. EDEN LUNA

After the Antarctic campaign of EDEN ISS, the MTF was refurbished into EDEN LUNA. In collaboration with ESA, this project simulates a lunar crop production facility. It acts as an intermediate step between EDEN ISS and future lunar systems [11].

Figure 1.3: Impression of EDEN LUNA, the successor of EDEN ISS, planned for deployment at the ESA LUNA facility in Cologne. The figure shows the EDEN LUNA greenhouse container placed at the ESA LUNA analogue site. Source: [12, 13].

One of the most significant upgrades concerns the Nutrient Delivery System (NDS). Experience gained in Antarctica revealed that pumps represent a dominant failure mode. In response, the NDS was redesigned to reduce the pump count and simplify the hydraulic architecture. Additionally, the piping layout was optimized to eliminate stagnant volumes and reduce microbial growth risk. Enhancements also include the EDEN Versatile End-Effector (EVE) [14], which is a robotic arm designed to perform plant health monitoring and physical tasks. Furthermore, the C.R.O.P.® Biofilter [15] was introduced to convert human urine into a nitrate-rich nutrient solution, thereby further closing the resource loop [16].

1.3. Nutrient Delivery Systems in BLSS

Within BLSS, the NDS represents a complex and interdisciplinary subsystem. It operates at the interface of engineering, plant biology, and chemistry. Its primary function is to deliver water and dissolved nutrients to plant roots in a reliable and hygienic manner [17]. Achieving this over long durations with minimal crew intervention remains a major challenge for space-based food production [18].

The EDEN projects utilize an aeroponics system [17]. In this configuration, plant roots are suspended in air and periodically sprayed with a fine mist of nutrient solution. This allows for high oxygen availability at the root surface. Figure 1.4 shows the flow of the nutrient solution. When starting in the left top corner; The nutrient solution is prepared in batch mixing tanks and adjusted to a target pH between 5.8 and 6.0 to allow for optimal nutrient exchange with the roots.[19].

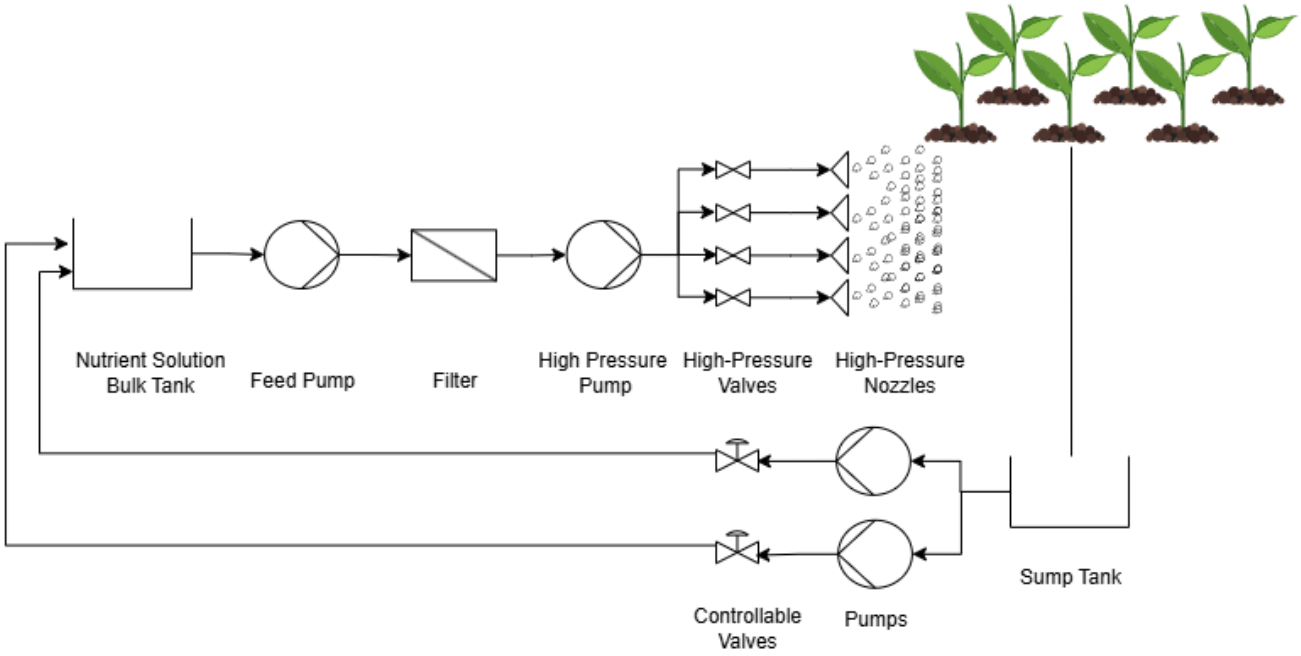

Figure 1.4: Annotated schematic of the EDEN Nutrient Delivery System (NDS) used in EDEN ISS and EDEN LUNA, showing the closed loop route of the nutrient solution. Solution is mixed in a bulk tank, filtered and pumped, pressurized and regulated by a high pressure pump and valves, and then sprayed onto the roots through nozzles. Excess solution is collected in a sump tank and returned to the mixing tank with redundant pumps for pH and EC control. In the EDEN FEG, 40 trays are supplied, with four nozzles per tray and about 6 to 8 L per day per tray. Biofilm mitigation and sterilization subsystems are not shown.

Once prepared, the solution is transported by a *feed pump* through the *filters*. It is pressurized using *high-pressure pumps* to a maximum of 10 bar. *Valves* ensure equal pressure distribution whereafter the nutrient solution reaches the cultivation tray equipped with four *high pressure nozzles* that break the solution into droplets with a diameter of approximately 600 μm.

Excess solution is collected through a drainage in the sump tank. Included redundancy has 2 *pumps* leading the nutrient solution through *controllable valves*. Before entering the nutrient solution Bulk Tank, the nutrient solution is filtered, and sterilized via UV radiation[17].

Challenges of the EDEN ISS NDS

Operation of the NDS during the EDEN ISS mission exposed critical challenges in contamination, reliability, and complexity. These issues required significant crew intervention, which presents a major hurdle for long-duration bioregenerative life support systems.

Biological Contamination and Biofilm Growth One primary challenge was extensive biofilm growth within the reservoirs, piping, and spray infrastructure. This biological contamination restricted flow rates and caused nozzle clogging, necessitating intensive full-system cleanings every eight weeks that occupied entire workdays [18].

Sensor Vulnerabilities and Software Risks In addition to biological issues, sensor and software vulnerabilities posed operational risks. A malfunction in the EC control sensor led to unstable dosing behavior, eventually depleting nutrient and water stocks and forcing a system shutdown [18].

Mechanical Failure of High-Pressure Components Mechanical failures in the pumps and piping represented another significant vulnerability. Pumps proved prone to failure due to continuous high-pressure operation and wear from precipitated salts or biofilm fragments [17]. Furthermore, the use of glued pipe connections under high operating pressures resulted in several leakages that required unplanned repairs [18].

System Complexity and Crew Time Demands Ultimately, the NDS exhibited high system complexity characterized by a large number of mechanical components and integrated subsystems like UV sterilization. The resulting maintenance demands (including cleaning, leak repair, and component replacement) consumed substantial crew time. This reliance on manual intervention is a critical limitation for future missions where crew availability remains a premium resource [18].

1.4. Requirements for a Lunar Nutrient Delivery System

The cultivation area of the EDEN projects, which covers approximately 30 m², serves as the baseline for this research. Based on this benchmark, a set of quantitative NDS requirements has been derived from existing research on lunar crop production facilities. These requirements originate from the EDEN ISS system design, operational data, the LAM-GTD and EDEN LUNA developments, and structured interviews with experts. Collectively, these sources provide essential constraints on mass, volume, power consumption, system reliability, and contamination control. They reflect critical lessons learned from long-duration operations in extreme environments [20, 17].

In the context of this thesis, these requirements are presented to define the boundaries of the design space. They establish the technical envelope within which the initial concepts and subsequent design choices are formulated. By identifying these heritage-based targets, the research ensures that any proposed alternative NDS concepts are evaluated against realistic operational benchmarks during the trade-off analysis. These requirements act as the foundational constraints that are later mapped into the Research through Design (RtD) framework to evaluate the viability of the protective belt hypotheses. The resulting requirements are summarized in Table 1.1, where each is assigned a structured identifier following category-based requirement engineering conventions.

Table 1.1: General Nutrient Delivery System (NDS) Requirements Derived from Heritage Data and Expert Interviews

Req. ID	Requirement Description	Verification Method
Contamination Control and Hygiene		
CC-01	The system shall have mitigation measures for biological contamination, including biofilm formation and pathogen growth, within all fluid-contact components.	Testing, inspection
CC-02	The system shall avoid stagnant fluid volumes through proper drainage and continuous circulation.	Design, inspection, CAD review
CC-03	The system shall include an active decontamination method to sterilize the nutrient solution during recirculation.	Functional testing
CC-04	All fluid-contact materials shall be selected to minimize microbial adhesion and support chemical cleaning.	Material inspection
Infrastructure Reliability and Robustness		
IRR-01	The system shall tolerate single-component failures without resulting in complete loss of irrigation.	Fault injection testing
IRR-02	The system architecture shall minimize reliance on failure-prone components, particularly pumps and high-duty-cycle actuators.	Design analysis
IRR-03	All fluid-handling interfaces shall prevent leakages under nominal and transient operating pressures.	Pressure testing
IRR-04	The system shall operate within an allocated mass budget of 766 kg for approximately 30 m^2 of cultivation area [20].	Mass budget analysis
IRR-05	The system shall operate within a nominal power consumption below 660 W during steady-state operation [20].	Electrical testing
System Complexity and Resource Efficiency		
SC-01	The system shall minimize overall part count, mass, and volume while maintaining required functionality.	Design analysis
SC-02	The system shall fit within an allocated volume of 4.52 m^3, including bulk solution tanks and storage [20].	CAD verification
SC-03	The system shall support autonomous operation over extended periods without crew intervention.	Long-duration testing
SC-04	The system shall be designed for ease of maintenance and cleaning, minimizing required crew time.	Operational assessment
Monitoring, Control, and Autonomy		
MC-01	The system shall continuously monitor critical nutrient parameters, including pH, EC, and temperature.	Sensor testing
MC-02	The system shall detect sensor and control faults and prevent unstable control behavior.	Fault simulation
MC-03	The system shall provide data outputs compatible with higher-level control and monitoring systems.	Interface testing
MC-04	The system shall support closed-loop control of nutrient delivery parameters.	Functional testing

1.5. Mapping Requirements to the Design Implementation

The requirements derived in Table 1.1 functioned as the primary drivers for the transition from a traditional aeroponic architecture to the fogponic prototype. This mapping defines how high-level engineering constraints were translated into specific design choices and research boundaries.

Contamination and Hygiene Drivers Requirements CC-01 through CC-04 provided the theoretical motivation for this shift. While the actual microbial impact of fogponics on Requirement CC-01 remains outside the scope of this thesis, the architectural simplified nature of a one-way system directly addresses the risks mentioned in CC-02, CC-03, and CC-04. By removing the complex drain infrastructure and recirculation loops, the design inherently avoids the stagnant fluid volumes and sterilization complexities that characterized the EDEN ISS mission.

Reliability and Robustness Constraints Infrastructure reliability and robustness requirements (IRR) shape the physical configuration of the apparatus. IRR-02 motivates an early focus on passive delivery aids such as wick materials to reduce reliance on failure prone actuators. IRR-01 requires tolerance to single component failures, which guides redundancy and fault cases during iteration, and any remaining single point vulnerability that could cause loss of irrigation will be treated as a defined deviation and a key reflection point. Reduced mass (IRR-04) is assumed as a baseline advantage of fogponics over high pressure systems, while power implications (IRR-05) are evaluated once the design is fixed.

Complexity and Autonomy Goals The system complexity and autonomy requirements (SC-01 through SC-04) guide the initial design iterations. The goal is to minimize part counts while supporting autonomous operation and ease of maintenance. The pursuit of SC-03 and SC-04 drive the selection of integrated misting modules and prototype architecture.

Monitoring and Control Boundaries Monitoring and control requirements (MC-01 through MC-04) are implemented by designing the nutrient delivery system around a small set of continuously sampled sensors for pH, EC, and temperature, integrated into a robust data acquisition chain with logging and time stamping. Fault detection is addressed through plausibility checks.

1.6. Trade-Off Soilless NDSs

In the previous sections, NDSs were discussed at a general level. Within this domain, two principal categories can be distinguished: soil-based and soilless cultivation systems. The next paragraphs explain why, soil-based approaches are excluded from consideration.

Lunar regolith is considered unsuitable for crop cultivation because its extremely high alkalinity disrupts nutrient availability and inhibits normal plant growth. It is also severely nutrient-poor and abrasive, lacking essential elements such as reactive nitrogen and organic matter, and inhibits root growth, which prevents sustained nutrient cycling and healthy biomass development. From a physical standpoint, the regolith has poor water-holding capacity, causing rapid drying and dehydration stress for plants. In addition, the presence of toxic metals such as aluminium further impairs root function and can lead to high plant mortality [21].

Alternative soil-like systems do exist, such as the substrates in the Veggie Project, where plant roots are supported in pillows filled with porous ceramic particles with characteristic sizes between approximately 600 µm and 2 mm. While this approach offers advantages for biological sampling, allowing root systems to be preserved and returned to Earth for analysis, it is less suitable when the primary objective is sustained crop production. Substrate-based systems introduce additional challenges related to cleaning, root removal, and long-term maintenance, which are undesirable in a crewtime-constrained lunar environment [22].

Consequently, the focus of current and near-term lunar greenhouse research lies on soilless cultivation systems. Within soilless agriculture, three distinct nutrient delivery approaches can be identified: hydroponics, aeroponics, and fogponics. Each method differs in its approach to nutrient delivery, resource efficiency, system complexity, and susceptibility to contamination. The following section provides an overview of these three approaches and presents a comparative trade-off analysis to assess their suitability for lunar crop production.

In the literature, fogponics is often treated as a subcategory of aeroponics, and aeroponics as a subcategory of hydroponics. In this thesis, these three approaches are treated separately because they differ in ways that matter for lunar greenhouse requirements and for the design of a nutrient delivery system. Here, hydroponics is used as an overarching term that includes NFT, ebb and flood, and DWC. Aeroponics refers to the spray based aeroponic systems used in the EDEN systems. Fogponics refers to nutrient delivery by ultrasonic atomization.

1.6.1. Hydroponics

Hydroponics encompasses several soilless cultivation methods in which plants grow in nutrient-enriched water, with or without inert substrates for mechanical support. Common implementations include Nutrient Film Technique (NFT), ebb-and-flood systems, and Deep Water Culture (DWC), as illustrated in

Figure 1.5 respectively. By decoupling plant growth from soil, hydroponics enables precise nutrient control, high yields, and efficient resource use, while avoiding soil-related constraints such as salinity and poor drainage [23].

While hydroponics is a mature and widely applied technology in terrestrial controlled-environment agriculture, its applicability to lunar crop production is limited by the constraints of space habitats, including water scarcity, strict mass and volume budgets, and the need for high system reliability.

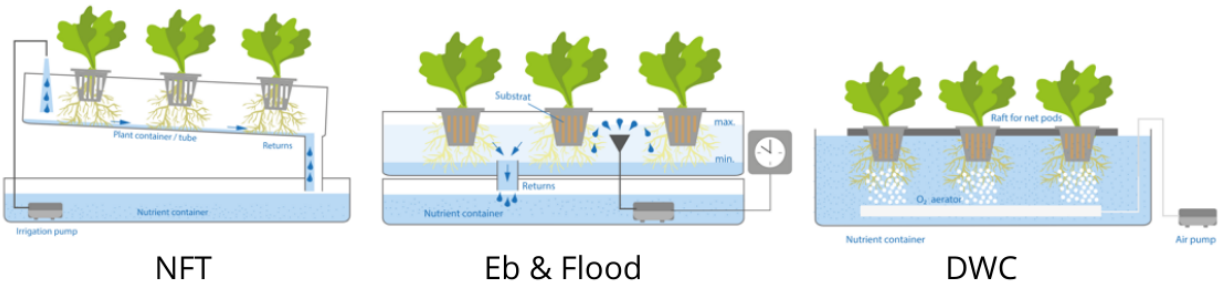

Figure 1.5: Schematic representation of hydroponic systems. From left to right: Nutrient Film Technique (NFT), ebb and flood system, and Deep Water Culture (DWC). Plant roots are periodically irrigated by a nutrient solution and drained back into a shared reservoir. Source: [24].

Contamination risks
Contamination risks in hydroponic systems are inherent to the use of a shared, recirculating nutrient solution, which connects all plants through a common transmission pathway. Root exudates enrich the solution and promote microbial growth and biofilm formation, while oxygenation supports aerobic pathogens. In addition, pathogens can be internalized through the roots and transported into plant tissues, rendering surface sanitisation ineffective. Once introduced, contamination can rapidly propagate throughout the system via the shared reservoir [25].

System reliability
System reliability is strongly dependent on the continuous operation of pumps and aeration devices, as plant roots remain fully immersed in the nutrient solution. Failures in circulation or oxygenation can quickly induce hypoxic stress and crop loss. Because many plants are hydraulically coupled, hydroponic systems exhibit high sensitivity to single-point failures [26].

Operational and system complexity
Operational complexity arises from the need for extensive fluid-handling infrastructure, including large reservoirs, circulation pumps, aeration systems, and associated piping. These subsystems increase part count, power consumption, and potential failure modes. In addition, large water volumes are required to buffer nutrient concentrations and maintain stable operation, which is unfavorable under the mass and volume constraints of lunar greenhouse systems [26].

Monitoring and control
Monitoring and control impose a substantial crew time burden, as biofilm mitigation primarily relies on structural cleaning rather than sensor-based detection. Maintenance typically requires draining large volumes of nutrient solution, disassembling components, and refilling the system. Ongoing inspection and servicing of multiple active subsystems further reduce autonomy, conflicting with the operational constraints of lunar greenhouse applications.

1.6.2. Aeroponics
Aeroponics, officially a subset of hydroponics, is a soilless cultivation technique in which plant roots are suspended in air and intermittently sprayed with a nutrient solution, enabling high root zone oxy-

gen availability and efficient uptake [27]. A schematic overview is shown in Figure 1.6. The EDEN implementation of this architecture is described in 1.3.

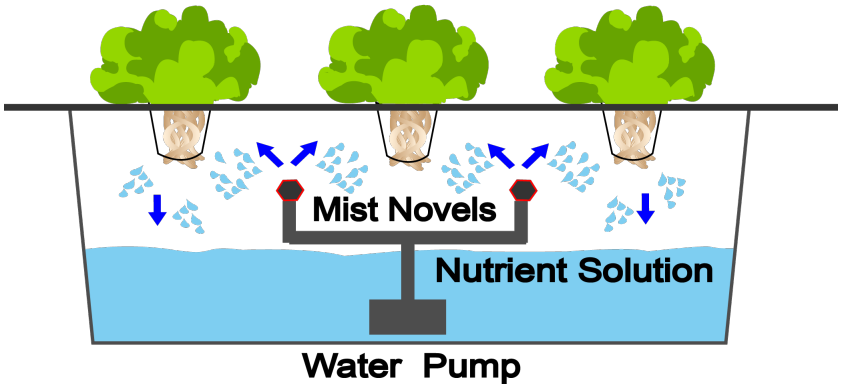

Figure 1.6: Schematic representation of an aeroponic cultivation system, where plant roots are suspended in air and intermittently sprayed with nutrient solution. Source: [28].

Contamination risks
Contamination risks are reduced compared to hydroponics because plants are not immersed in a shared liquid volume, limiting direct pathogen transfer; however, EDEN ISS still showed substantial biofilm formation within the NDS (1.3), and nutrient recirculation can distribute upstream contamination system-wide unless sterilization and maintenance are applied.

System reliability
System reliability is dominated by spray continuity, since short interruptions can rapidly desiccate exposed roots, and progressive nozzle clogging can remain unnoticed until plant stress occurs (1.3), implying low fault tolerance without fast detection and robust redundancy.

Operational and system complexity
Operational complexity is driven by the high-pressure spray infrastructure, including many nozzles, fine filtration, pressure regulation, and UV sterilization to mitigate biofilm and clogging, which increases part count, leak risk, mass, power, and maintenance effort.

Monitoring and control
Monitoring and control require substantial crew time because partial nozzle blockages are difficult to detect automatically, and EDEN ISS required full-system cleaning approximately every eight weeks (1.3), with additional time for leak repair and component replacement [18].

1.6.3. Fogponics

Fogponics, is a specialized form of aeroponics in which nutrients are delivered to plant roots as a fine mist at low pressure. Typical droplet sizes range from approximately 1 to 50 µm, allowing nutrients to form a thin film on the root surface rather than accumulating as bulk liquid. The basic workings are shown in Figure 1.7. This approach enables highly efficient water use by minimizing runoff and overspray, while roots remain suspended in air and continuously exposed to atmospheric oxygen. The resulting high oxygen availability supports root respiration and energy-dependent nutrient uptake processes, making fogponics theoretically attractive for resource-constrained environments [29].

Although fogponics is frequently identified in the literature as a promising nutrient delivery concept, it is currently considered insufficiently mature for direct application in operational space greenhouses. In the thesis on NDSs the author calls the Technology Readiness Level (TRL) of fogponics to be too low for further consideration [20]

In an EDEN-like implementation, a fogponic system would still consist of elements such as a nutrient mixing tank, filtration, and a feed pump. However, unlike aeroponics, no high-pressure pump would

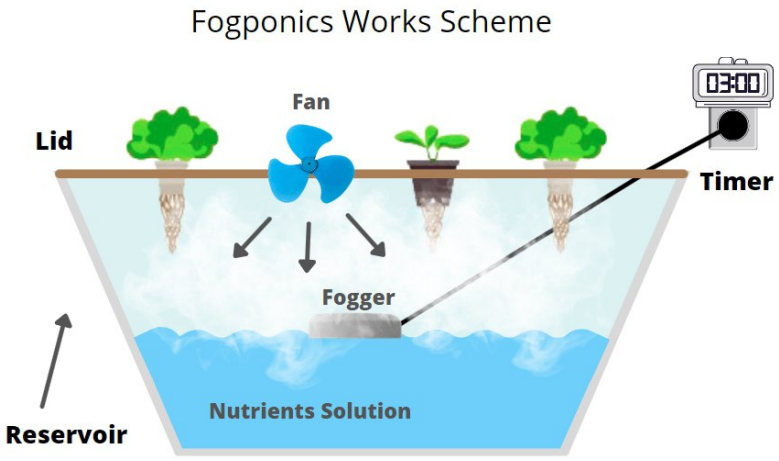

Figure 1.7: Schematic overview of a fogponic nutrient delivery system, illustrating fog generation, root zone exposure to nutrient mist, and intermittent operation controlled by a timer. Source: [30].

be required. Instead, the nutrient solution would be supplied via low-pressure (1 - 2 bar) feed lines to fine misting units located in each cultivation tray. A schematic of a fogponics based NDS in the EDEN system is shown in Figure 1.8 below. Nutrients are applied directly to the roots as a fine fog. Depending on system tuning, excess solution is either locally collected within the tray and remisted or the supply rate is matched to plant transpiration. This enables a one-way operation without full system recirculation. This non-recirculating architecture represents a fundamental difference from existing EDEN systems and has direct implications for contamination control, system reliability, and system complexity, which are explored in the following sections.

Contamination risks in fogponic systems are reduced by the absence of nutrient solution recirculation. The fogponic system as proposed is designed without a recirculation loop. This one-way delivery, as shown in Figure 1.8, limits the potential for pathogen spreading through shared reservoirs. In addition, the reduced amount of wetted infrastructure decreases the available surfaces for biofilm formation. Together, these characteristics inherently lower contamination risks compared to recirculating hydroponic and aeroponic systems.

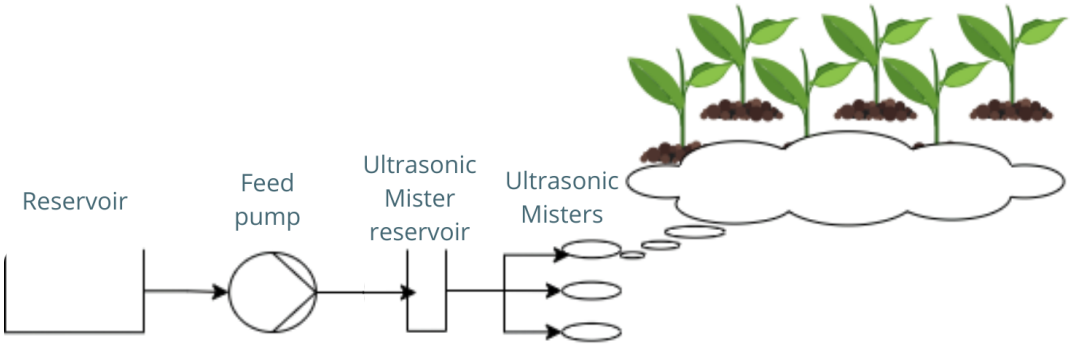

Figure 1.8: Conceptual schematic of a fogponic Nutrient Delivery System (NDS). Nutrient solution is prepared in a bulk tank, filtered, and supplied via a low-pressure feed pump to ultrasonic misting units, which generate a fine nutrient fog for direct root zone application. When compared to the recirculating EDEN NDS in Figure 1.4, the advantages become clear in this one-way nutrient delivery excluding recirculation infrastructure and contamination mitigation measures.

Reliability in fogponic systems depends on the performance of the misting units, as failure of nutrient delivery can rapidly lead to plant loss, similar to aeroponic systems. The long-term reliability and degradation behavior of fogponic misters remain unknown, introducing uncertainty at component level.

However, at system level, fogponics benefits from a simplified fluid architecture, as the absence of high-pressure pumps and drain-based recirculation reduces the risk of leakages and mechanical failures. With fewer active components, fogponic systems are expected to offer improved overall reliability compared to aeroponics or hydroponics, despite their sensitivity to localized mister failures.

Operational and system complexity in fogponic systems is reduced compared to conventional aeroponic implementations due to the simplified. The absence of high-pressure pumps reduces system mass, volume, and power consumption. In addition, the lack of a drain-based recirculation loop removes the need for dedicated tanks, pumps, filters, and piping. The low operating pressure (« 10 bar) reduces the risk on leakages. Due to the reduced amount of wetted infrastructure, fogponic systems may also require fewer biofilm mitigation measures, such as continuous UV sterilization, as needed in aeroponic systems.

Monitoring and control in fogponic systems remain largely driven by the performance of the misting modules. These require regular inspection similar to aeroponic spray nozzles. Blockages or degradation of misting elements can directly affect nutrient delivery and must therefore be monitored closely. However, due to the absence of extensive wetted infrastructure, fewer components are subject to biofilm formation and structural cleaning. The reduced risk of biofilm development may allow for less frequent cleaning cycles, although this remains an assumption given the limited operational heritage of fogponic systems. Overall, while monitoring of misting performance remains, the expected reduction in cleaning effort suggests lower crew time compared to recirculating aeroponic systems.

1.6.4. Trade-Off

In 1.4 the requirements were discussed. This section will show a trade-off between the above mentioned NDSs based on these requirements.

Based on the challenges identified in 1.4 and the resulting system-level requirements formulated in the previous section, a comparative evaluation of the soilless cultivation methods is conducted. The trade-off analysis assesses hydroponics, aeroponics, and fogponics against criteria including contamination risk, infrastructure reliability, system complexity, and the level of monitoring, control, and autonomy required. These criteria directly reflect the operational limitations observed in EDEN ISS. They define the performance for NDSs intended for lunar crop production. Below the results are listed in Table 1.2

Table 1.2: Qualitative trade-off between soilless cultivation methods for lunar NDS applications. High indicates an unfavorable characteristic, Medium a moderate impact, and Low a favorable characteristic.

Category	Sub-criterion	Hydroponics	Aeroponics	Fogponics
Contamination	Pathogen spread risk	High	Medium	Low
	Biofilm susceptibility	High	High	Medium
Reliability	Failure susceptibility	High	High	High
	Failure impact severity	High	High	High
	TRL uncertainty	Low	Medium	High
Complexity	Component count & interfaces	Medium	High	Medium
	Mass / power implications	High	High	Medium
Monitoring & crew	Monitoring intensity	Medium	High	Medium
	Cleaning & maintenance burden	High	High	Medium

The trade-off shows fogponics as a potentially superior alternative nutrient delivery system for the set requirements. Research will show to what extent fogponics can provide a more effective way of nutrient delivery.

1.7. Research Program

This thesis contributes a laboratory-validated research platform for fogponic nutrient delivery and uses it to generate first-order evidence on the feasibility limits of ultrasonic misting. The work delivers (i) a

fogponic NDS prototype architecture derived from EDEN heritage constraints, (ii) a measurement and verification approach to quantify fog output stability, nutrient-solution parameter drift (pH/EC/temperature), and operational reliability, and (iii) an evidence-based characterization of dominant degradation and failure mechanisms over defined runtimes.

Research Approach and Methodological Stance

By applying a Constructive Design Research (CDR) approach [31], this thesis addresses the primary unknowns in fogponics, which concern integrated system behavior rather than isolated parameter values. The core method is constructive, utilizing a fogponic prototype designed and built as a formal research instrument. Laboratory experiments are subsequently employed to generate bounded evidence regarding feasibility limits, performance retention, and dominant failure mechanisms.

Decontextualization and Evidence Limits

To isolate mechanical and chemical behavior, experiments are performed in a decontextualized lab venue. The scope of this inquiry focused on nutrient solution chemistry drift, deposition and clogging mechanisms, fog production stability, and the operational reliability of the misting modules. The resulting evidence yields a first-order design envelope and failure-mode evidence for fogponic nutrient delivery in nutrient-rich solutions, intended to inform subsequent higher-TRL system iterations and future BLSS architecture decisions.

The resulting evidence does not constitute a full-scale validation of a lunar greenhouse NDS. Instead, it yields a first-order design envelope and failure-mode evidence for fogponic nutrient delivery in nutrient-rich solutions. These findings are intended to inform future space-relevant architectures and subsequent higher-TRL system iterations.

Thesis outline

The structure of this thesis follows a Research-through-Design program in which the prototype is treated as a research instrument for mapping feasibility limits rather than as a finalized lunar product. Chapter 1 introduces the lunar BLSS motivation and defines the problem space using EDEN heritage, including the reliability, contamination, and complexity challenges of high-pressure aeroponic nutrient delivery. Chapter 2 reviews fogponics literature to identify the governing parameters and, crucially, the gaps that prevent a standardized evaluation of VMA-based nutrient delivery (e.g., retention behavior, chemistry drift attribution, and thermal load effects).

Chapter 3 formulates the main and supporting research questions and positions the methodological stance of Constructive Design Research, including the Lab Venue strategy and the negative heuristic (explicit exclusions) used to protect internal validity. Chapter 4 translates the research questions into the physical *Design Thing*: it details the apparatus logic, measurement chain, experimental protocols, and verification plan that make the prototype usable as a reproducible research platform. Chapter 5 presents the resulting datasets and observations as bounded evidence, including delivery performance metrics, nutrient-solution dynamics, temperature behavior, and operational reliability events.

Chapter 6 interprets these results within the RtD framing by extracting an initial design envelope and synthesizing evidence-based design rules, while keeping claims explicitly bounded by the verification objectives and observed failure modes. Chapter 7 concludes the thesis by summarizing the contribution and the extent to which the research questions are answered. Chapter 8 provides recommendations as the forward RtD pathway, outlining prioritized design moves and follow-up experiments required to harden the instrument, close the key knowledge gaps, and support later recontextualization toward lunar-relevant architectures.

2

Literature Study

The purpose of this chapter is to map the reported relations between atomization parameters, nutrient solution stability (pH, EC, and temperature), delivery performance (flow rate), and the subsequent plant response. By synthesizing these relationships, this review identifies which links are currently evidenced in literature and where research gaps necessitate the decontextualized experimental approach of this thesis.

2.1. Fogponics: Definitions and Conceptual Framework

Across the reviewed literature, fogponics is consistently positioned as a specialized subset of aeroponic cultivation rather than as a fundamentally distinct cultivation category [32]. The primary distinction between fogponics and conventional aeroponics is the atomization regime used to generate the nutrient delivery medium. Conventional aeroponic systems typically employ mechanical sprayers or high-pressure nozzles to disperse nutrient solution into relatively coarse droplets. Fogponic systems, by contrast, predominantly utilize ultrasonic atomization, commonly achieved using piezoelectric ceramic transducers [32]. These transducers operate at ultrasonic frequencies ranging from approximately 20 kHz to 3 megahertz [33], inducing capillary waves at the liquid surface that result in the formation of fine droplets. As a consequence, definitions of fogponics in the literature are often based on a combination of atomization method and the resulting droplet size regime. Terminology used to describe atomized nutrient delivery media varies across studies and is not applied consistently. In general, “spray” refers to droplets larger than approximately 100 µm [34] , typically generated by high-pressure mechanical nozzles. The term “fog” is commonly used to describe droplets in the micrometer range, frequently cited as spanning 1–100 µm [34]. The term “mist” is sometimes defined within a similar or overlapping size range, for example between 1 and 35 µm [34]. These overlapping definitions reflect the absence of a standardized classification framework within the fogponics literature. Depending on the application, different terminology is used. Despite the agreement on the technological shift from mechanical spraying to ultrasonic atomization, divergence exists in how fogponic systems are classified and described. Some sources apply hierarchical distinctions between spray, mist, and fog, referring to micro and ultra-fine atomization regime and are based strictly on droplet diameter, while others define fogponics primarily by the use of ultrasonic fog generators, independent of the reported droplet size. Figure 2.1 below shows an indication of droplet size terminology and its correlated size distribution.

Given these inconsistencies, it is necessary to explicitly define the scope and terminology adopted in this thesis. Throughout this research, fogponics is treated as a subset of aeroponics characterized by ultrasonic atomization of nutrient solution into fine droplets within the micrometer range. In particular, the term mist or fog is used to describe atomized droplets with characteristic diameters between 1 and 100 µm, independent of the specific atomization technology employed. Nutrient delivery in this regime results in a suspended mist that hydrates the roots without bulk liquid wetting or high-pressure spraying.

This functional definition is adopted to ensure terminological consistency when comparing experimental results, atomization technologies, and plant responses across the reviewed literature. While droplet

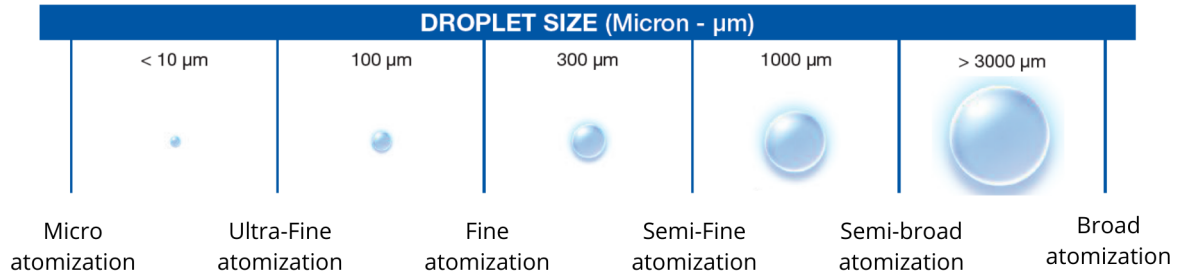

Figure 2.1: Classification of spray droplet sizes and associated atomization regimes, ranging from micro atomization (<10 µm) to broad atomization (>3000 µm). The figure illustrates typical droplet diameters produced by different nozzle types and highlights the large variation in atomization scales relevant for aeroponic and fogponic nutrient delivery systems. In this context, fog is typically considered to fall between micro and fine atomization regimes. Adapted from [35].

size constitutes a central distinguishing parameter of fogponic systems, it does not fully characterize their operational behavior. Additional parameters and performance metrics such as fogging frequency, flow rate, and nutrient solution stability play a critical role in determining system performance and are therefore introduced and discussed in the following section.

2.1.1. Parameters and Performance Metrics in Fogponics

This section introduces the key parameters and performance metrics used in the literature to characterize fogponic nutrient delivery systems and relates them to the general Nutrient Delivery System requirements derived in Section 1.4. In the chapter two parameter categories are distinguished. It explains the parameters and metrics on system level, referring to hardware and architecture. On the other hand on plant level parameters are discussed, referring to metrics or parameters that are biologically determined by the crops.

Fogponics Parameters

Droplet size refers to the characteristic diameter of atomized nutrient solution particles delivered to the plant roots and represents the primary physical parameter distinguishing fogponic systems from spray-based aeroponics. It is typically reported in *micrometers* and, where available, described as a distribution rather than a single mean value [36]. Droplet size influences liquid residence time in air and settlement probability on the root surface and nutrient transport mechanisms, and therefore strongly influences both plant response. In addition smaller droplets can be generated at lower operating pressures without extensive recirculation infrastructure.

To describe the width of the droplet size distribution, the span number is commonly used and is defined as

$$\text{Span} = \frac{X_{90} - X_{10}}{X_{50}}. \tag{2.1}$$

Where X_{90} represents the droplet diameter of which 90% of the droplets are sized in. X_{10} represents the diameter of which 10% of the droplets are sized in, and X_{50} the diameter of which half of the droplets are sized in. A lower span value indicates a narrower and more uniform droplet size distribution, which is generally desirable for controlled fogponic nutrient delivery.

In addition, the fine particle fraction (FPF) is often reported as a performance metric and is defined as the fraction of droplets with diameters between 1 μm and 5 μm. This metric provides a measure of the proportion of droplets within the size range typically associated with fog-like behavior and high suspension stability.

Duty cycle describes the temporal pattern of fog generation, defined by the on–off intervals of nutrient delivery to the root zone. Typically the duty cycle is measured in *minutes ON / minutes OFF*. It regulates the balance between root hydration and root-zone oxygen availability. An appropriate duty cycle ensures sufficient nutrient uptake while preventing prolonged wetting that could limit oxygen uptake. Because plant response and root-zone conditions depend on both droplet characteristics and

delivery timing, the optimal duty cycle must be considered in conjunction with droplet size and delivery rate, and may vary between fogponic technologies and operating conditions [34, 33].

Operating frequency refers to the electrical excitation frequency at which the piezoelectric atomizer is driven to generate ultrasonic capillary waves at the liquid surface. Mainly the frequency is measured in kHz or MHz. This parameter governs the wavelength of surface oscillations and thereby influences both mist generation rate and characteristic droplet size. The droplet size depends on fluid properties such as surface tension and density [33], which vary with fertilizer concentration, implying that operating frequency droplet size relationships must be determined empirically and may differ between nutrient formulations and atomizer technologies. As a result, operating frequency constitutes a technology control parameter that directly affects fog output.

Fogponics Performance Metrics

Thermal behavior refers to heat generation and temperature changes associated with ultrasonic atomization during fogponic operation. Electrical energy supplied to piezoelectric transducers is partially converted into heat, leading to localized warming of the nutrient solution and the root-zone environment. This temperature is generally measured in the root zone and expressed in *degrees Celsius*. Temperature variations influence nutrient solution chemistry and root physiology, and may thereby affect nutrient stability and plant performance [32]. From a system perspective, thermal behavior links atomizer operation to broader system requirements related to chemical stability and reliability and must be considered when evaluating fogponic technologies for long-duration and autonomous operation.

Atomizer lifetime describes the duration over which a fogponic atomization device maintains stable and repeatable performance within acceptable operational limits. Rather than being defined by a sudden failure, lifetime is treated as a performance-retention metric, reflecting gradual degradation of atomization quality due to mechanisms such as mineral deposition or fatigue of piezoelectric components. In literature limited information is available. Therefore this parameter will be expressed in *hours.* Because continuous measurement of droplet size distributions is rarely reported, changes in effective nutrient solution delivery rate are commonly used as a practical indicator for degradation over time. Atomizer lifetime directly influences system requirements related to reliability and maintenance demand, as limited lifetime increases replacement frequency, system complexity, and crew time.

Electrical Conductivity is used as a system-level metric to quantify the total ionic concentration of the nutrient solution and thereby assess nutrient solution stability in fogponic systems. Because mineral nutrients are dissolved as charged ions, EC serves as a proxy for the overall strength of the nutrient solution rather than for individual nutrient composition. EC is typically measured using a digital EC probe, often with temperature compensation to a reference temperature (commonly 25 °C), and is reported in *mS/cm*. An increase in EC generally indicates concentration of ions due to water loss, whereas a decrease may result from dilution or deposition [37]. Monitoring EC is particularly important in closed-loop fogponic nutrient delivery systems because small imbalances in ionic concentration can rapidly propagate throughout the system. In recirculating or partially closed nutrient loops, changes in EC are not naturally dissipated and can accumulate over time if left uncorrected. This makes EC a key indicator for maintaining chemical stability and preventing progressive nutrient drift that could compromise plant health or system reliability. Continuous EC monitoring therefore enables timely correction through dilution or nutrient dosing. This supports autonomous operation and reduces the risk of crop loss due to incorrect nutrition concentration.

pH is a system-level metric describing the acidity or alkalinity of the nutrient solution, defined by the concentration of hydrogen ions (H^+), and plays a central role in nutrient availability and root-zone stability in crop cultivation systems. In soilless cultivation, pH is particularly critical because the nutrient solution lacks the natural buffering capacity of soil, making it sensitive to chemical and operational disturbances. pH is typically measured using a digital pH probe integrated into the nutrient reservoir or base chamber and is reported on a logarithmic scale going from 0 to 14 where 0 is most acidic and 14 most alkaline. Deviations in pH directly affect the solubility and bioavailability of macro- and micronutrients and can impair root function when values fall outside crop-specific tolerance ranges. In closed-loop fogponic nutrient delivery systems, pH can drift over time due to nutrient uptake, evaporation or thermal

effects. Continuous pH monitoring therefore supports stable nutrient delivery, enables automated correction through dosing or dilution, and is essential for maintaining chemical stability, system reliability, and autonomous operation during long-duration cultivation. [38]

Flow rate is a system-level perforance metric that describes the effective rate at which nutrient solution is delivered to the root zone in fogponic systems, typically expressed as mass or volume of atomized liquid per unit time [34]. In this research it is expressed as *ml/min* or sometimes in *g/min* . It reflects the effect of atomizer output and determines whether sufficient hydration and nutrient availability are maintained. Flow rate directly influences resource efficiency and system reliability, as under-delivery can rapidly lead to root desiccation, while excessive delivery may result in local pooling or unintended wetting causing undesired microbial growth. In addition, changes in flow rate under constant operating conditions can indicate atomizer performance degradation, linking this parameter to lifetime and maintenance-related system requirements.

Root morphology is a plant-level performance metric that describes the structural development of the root system and provides direct insight into how plants respond to nutrient delivery and aeration conditions in nutrient delivery systems. Root morphology is therefore a sensitive indicator of how effectively the system balances oxygenation with intermittent nutrient supply. It is commonly quantified through destructive harvest measurements as well as through high-throughput digital image analysis using software such as GiA Roots, which extracts parameters including total root length, surface area, volume, average diameter, and root count. In fogponic and aeroponic systems, pronounced root development is often interpreted as a compensatory response to temporally discontinuous nutrient delivery, whereby plants increase root surface area to maximize uptake during misting events [39]. Root morphology can thus define both system success and failure: enhanced root growth is advantageous for root and rhizome crops and reflects effective aeration, whereas excessive or imbalanced root proliferation may indicate inefficient nutrient delivery.

Yield and biomass are plant-level metrics that quantify the amount of plant material produced by a crop production system and represent the primary indicators of cultivation performance. In small scale systems as discussed in this research, biomass is expressed in *grams* Biomass is typically distinguished between shoot biomass, corresponding to the above-ground plant parts, and root biomass, corresponding to the below-ground system, with the harvestable fraction defining yield depending on crop type. Biomass is commonly measured through destructive harvesting, where fresh weight is recorded immediately after harvest and dry weight is determined after oven-drying to remove water content, providing a measure of accumulated biological matter. In fogponic and aeroponic systems, biomass outcomes must be interpreted in relation to system objectives, as enhanced root development does not necessarily translate into increased shoot yield. High root biomass and elevated root-to-shoot ratios are frequently observed as adaptive responses to intermittent nutrient delivery, indicating that plants allocate resources to root expansion to compensate for temporal limitations in water and nutrient availability. Yield and biomass metrics therefore serve both as measures of productivity and as diagnostic indicators of whether system parameters such as droplet size, delivery frequency, and nutrient availability are aligned with the intended crop and cultivation strategy [39].

2.1.2. Fogponic Technologies

Often in literature on fogponics agriculutre the used ultrasonic technology is not clearly specified. Therfore, the goal of this section is to explain the different technologies that are commonly used in ultrasonic atomization and can be used for fogponics. Three main categories are distinguished. The Vibrating Mesh Atomizer (VMA), the submerged ultrasonic atomizer and the ultrasonic horn atomizer. Below, Figure 2.2 provides an overview of these fogponic atomization technologies explained in this section.

(a) Vibrating mesh atomizer (VMA) using a piezoelectrically actuated perforated membrane. Source: [40].

(b) Submerged ultrasonic atomizer (piezoelectric transducer). Source: [41].

(c) Ultrasonic horn atomizer. Source: [42].

Figure 2.2: Ultrasonic atomization technologies relevant to fogponics.

Submerged Ultrasonic Atomizers

Submerged ultrasonic atomizers consist of a piezoelectric transducer that is fully submerged in the liquid to be atomized. When actuated, the transducer vibrates at ultrasonic frequencies, typically in the megahertz (MHz) range, and generates droplets through the capillary wave mechanism at the liquid–air interface. These systems generally operate at relatively high power levels, ranging from approximately 1 to 100 W, and are capable of producing high flow rates.[43]

The droplet breakup and resulting aerosol formation depend strongly on the actuation frequency of the transducer and on the physicochemical properties of the liquid, including surface tension and density. Extensive research has been conducted on the influence of capillary waves and liquid properties on the droplet size distribution produced by ultrasonic atomization. Despite this, submerged ultrasonic atomizers are reported to suffer from several limitations, including settling of suspensions, deterioration of heat-sensitive materials due to heat generation, residual formation, expensive electronic components, low output rate in certain configurations, and the production of non-uniform droplet size distributions.[43]

Ultrasonic Horn Atomizers

Ultrasonic horn atomizers use a piezoelectric transducer coupled to a horn that vibrates in the fundamental (0,1) acoustic mode at frequencies from 60 kHz. An exemplary image is shown in Figure 2.2c. Atomization occurs through the capillary wave mechanism, although the exact physics behind droplet formation remain discussed as of today. The mechanism is similar to other ultrasonic approaches, but is localized at the vibrating horn surface. This configuration produces polydisperse droplets, meaning that the resulting aerosol contains a wide range of droplet sizes rather than a narrowly controlled distribution. Ultrasonic Horn Atomization finds its use in many applications such as additive manufacturing where molten aluminum is atomized into fine droplets [44]. Such devices are often complex as they require precise manufacturing and assembling methods, increasing cost.

Vibrating Mesh Atomizers

Vibrating mesh atomizers (VMA), also referred to as mesh atomizers, were originally developed for inhaled drug delivery as an advancement over conventional ultrasonic atomization. Compared to submerged ultrasonic devices, VMA offer improved atomization efficiency, lower power consumption, higher atomization rates, and enhanced control over droplet size distribution.

The process of vibrating mesh atomization (VMA) represents a high-frequency mechanical method for generating consistent aerosols by transforming electrical energy into kinetic motion. This cycle is

driven by a piezoelectric ring, typically composed of lead zirconate titanate (PZT), which serves as the mechanical motor of the assembly. When a sinusoidal voltage is applied, the ring undergoes lateral vibrations that are transferred through a specialized holder to a central membrane, often fabricated from silicon. This mechanical coupling forces the membrane to oscillate vertically at ultrasonic frequencies, typically reaching approximately 100 kHz.

Effective atomization relies on a high-speed pumping action within the micro-nozzle geometry of the membrane. This cycle is divided into two distinct phases. During the upward cycle, the membrane creates negative pressure that pulls the bulk liquid from the reservoir into the wider inlet of the pyramidal nozzles. As the membrane moves downward, the pressure shifts to positive, squeezing the liquid through the narrow outlet, which is often tapered at a specific angle of 54.74°, and pinching it off into individual droplets. The size of these droplets is ultimately determined by the diameter of the nozzle exit. The fundamental principles are shown in Figure 2.3

While simpler vibration patterns like the (0,1) mode provide significant movement, their lower frequencies fail to provide the momentum required to overcome the surface tension of the nutrient solution. Consequently, the system must operate in the (0,2) vibration mode to achieve a threshold velocity of approximately 1.02 m/s. This high-velocity movement allows silicon-based membranes to generate mist with displacements as small as 0.7 μm, offering superior energy efficiency compared to traditional metallic alternatives.

The efficiency of this atomization process is further influenced by the material stiffness and voltage application. Increasing the peak-to-peak voltage linearly correlates with higher vibration speeds, which in turn accelerates the mist flow rate. Furthermore, the use of silicon provides a stiffer substrate that supports higher resonance frequencies in smaller, thicker membranes. By optimizing these physical factors, the VMA can maintain a stable nutrient aerosol with significantly lower power consumption than compressed-air systems, establishing it as a viable technology for mass-constrained lunar life support architectures. [45]

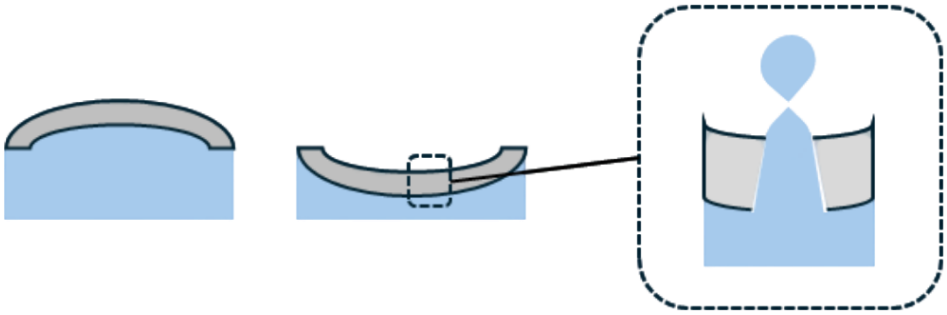

Figure 2.3: Schematic illustration of the working principle of a vibrating mesh atomizer (VMA). A piezo ceramic ring drives the mesh membrane to vibrate up and down, deforming the liquid surface at the mesh apertures. During the downward motion, liquid is extruded through the holes and pinches off into droplets. The resulting droplet size is primarily related to the mesh hole size.

Table 2.1 shows the parameters and performance metrics per fogponic technology.

2.2. Requirements from a plant perspective

In the context of space-based and bio regenerative life-support systems, plant production requirements fundamentally differ between terrestrial economic efficiency and independent optimal control of yield and nutritional availability. Whereas terrestrial controlled-environment agriculture prioritizes yield consistency, scalability, and operational cost, space-relevant cultivation systems must operate under extreme constraints of mass, volume, and power while maintaining near-continuous reliability to sustain human life. In such closed-loop environments, plant growth is not only a matter of productivity but of system stability [46]. This section covers parameters that influence the plant yield and development. The parameters are then linked to fogponic related parameters.

Table 2.1: Qualitative comparison of ultrasonic atomization technologies for fogponic nutrient delivery, comparing submerged ultrasonic atomizers, ultrasonic horn atomizers, and vibrating mesh atomizers (VMA) across mechanism, frequency, droplet size characteristics, flow rate, thermal behavior, fouling, lifetime, complexity, and suitability.

Parameter	**Submerged Ultrasonic Atomizer**	**Ultrasonic Horn Atomizer**	**Vibrating Mesh Atomizer (VMA)**
Atomization mechanism	Capillary wave breakup at liquid–air interface	Capillary wave breakup at vibrating horn surface	Liquid extrusion and pinch-off through vibrating micro-apertures
Operating frequency	MHz range (typically $\sim$1–3 MHz)	kHz range (typically $\geq$60 kHz)	kHz range (typically $\sim$100–200 kHz)
Droplet size distribution	Highly polydisperse; simultaneous ultrafine (< 1 μm) and large (> 100 μm) droplets	Polydisperse distribution	Narrow distribution; controllable median droplet size
Droplet size control	Poor	Limited	High (especially for MEMS-based VMA)
Flow rate	High (up to $\sim$900 mL h^{-1})	Application-dependent; not typically optimized for low-flow operation	Moderate (reported $\sim$200 mL h^{-1} for metallic VMA)
Thermal behavior	Significant heat generation; risk to heat-sensitive solutions	Localized heating at horn surface	Lower heat generation due to lower power operation
Fouling and residue formation	High susceptibility (residual formation, settling of suspensions)	Susceptible due to surface exposure	Reduced for MEMS-based VMA; metallic VMA show residue near apertures
Atomizer lifetime	Limited by fouling and thermal degradation	Limited by mechanical and manufacturing complexity	Potentially improved; MEMS VMA benefit from smooth surfaces
System complexity	High (power electronics, cooling considerations)	High (precision manufacturing and alignment)	Moderate; MEMS VMA enable compact and integrated designs
Suitability for fogponics	Low (poor droplet control)	Limited	High (particularly MEMS-based VMA)

Droplet size is a critical parameter, as it directly influences root wetting, oxygen availability, and nutrient uptake efficiency [47, 48]. In fogponic systems, droplet size determines whether nutrients are effectively deposited onto the root surface while preserving an oxygen-rich root environment. For most plant species, the literature identifies an effective droplet size range between approximately 30 and 100 μm. Within this range, droplets are sufficiently large to adhere and form thin liquid films on the root surface, yet small enough to remain airborne and avoid water logging of the roots [49].

Droplets smaller than approximately 2 μm tend to remain suspended in the air and behave primarily as aerosols rather than direct nutrient carriers. Due to their low mass, such droplets exhibit limited deposition efficiency on the root surface, reducing nutrient delivery and potentially promoting excessive root hair formation without supporting adequate lateral root development [50]. At the opposite extreme, droplets larger than approximately 100 μm fall rapidly and settle at the bottom of the cultivation chamber, leading to uneven nutrient distribution, localized oversaturation, and displacement of air in the root zone, which induces hypoxic conditions and impairs nutrient uptake [51, 52, 53, 54]. Maintaining droplet sizes within the optimal intermediate range is therefore essential for healthy root development.

Spray interval determines how often the nutrient mist is applied to the root system and is critical for balancing nutrient delivery with root-zone aeration. If misting occurs too frequently, excess liquid accumulates around the roots, displacing air and causing hypoxic stress [51, 54]. Conversely, overly long spray intervals may lead to root desiccation, reduced nutrient absorption, and physiological stress [48]. Experimental studies indicate that spray intervals between approximately 15 and 60 minutes can support healthy growth, depending on droplet size and environmental conditions [47, 48]. The optimal spray interval must therefore be considered in conjunction with droplet size to ensure consistent nutrient uptake while maintaining adequate oxygen availability.

Root-zone temperature is a critical factor governing plant metabolism, oxygen availability, and yield, and can ultimately determine crop viability under thermally challenging conditions. Elevated ambient air temperatures, particularly in tropical or enclosed environments, can severely inhibit plant development; maintaining a cooler root zone enables plants to sustain physiological function despite adverse air temperatures. Cooler nutrient solutions exhibit a higher oxygen-binding capacity, and when atomized into fine droplets, the increased surface area further enhances oxygen availability at the root surface, supporting root respiration and metabolic activity. Due to the higher specific heat capacity of the nutrient solution compared to air, root-zone cooling provides thermal stability, with cooled droplets maintaining reduced temperatures for 15–20 minutes after misting ceases. Precise root-zone temperature control has been shown to be a primary determinant of yield, as demonstrated by potato cultivation in tropical lowlands where root-zone cooling enabled substantial tuber production, while the absence of cooling resulted in complete crop failure. Similar benefits have been observed in crops such as lettuce, cucumbers, strawberries, and spinach. Optimal root-zone temperature is crop- and environment-dependent; effective growth has been reported when the root zone is maintained approximately 2–6 °C below air temperature, with broader ranges for mineral uptake typically cited between 26 and 34 °C, provided plants are not subjected to extreme heat stress. From a system perspective, controlling root-zone temperature is also energetically favorable compared to cooling the entire cultivation volume [55].

2.3. Results from research papers

This section synthesizes experimental findings from aeroponic and fogponic cultivation studies with the aim of identifying how key system parameters influence nutrient solution stability, droplet behavior, and plant performance. Rather than treating individual experiments in isolation, the reviewed literature is evaluated comparatively to extract consistent trends and limitations across different system configurations. Particular attention is given to the role of ultrasonic operating frequency, droplet formation mechanisms, nutrient solution chemistry, and plant response, as these factors directly relate to the parameters and metrics defined in the preceding sections.

2.3.1. Droplet formation, transport, and deposition limitations

Several studies demonstrate that droplet formation and transport in fogponic and ultrasonic aeroponic systems are governed by coupled effects of atomization physics, fluid properties, airflow, and system geometry. Mirzabe et al. [43] showed that droplet size generated by piezoelectric ultrasonic atomizers depends strongly on excitation frequency as well as liquid surface tension and density, with higher frequencies producing smaller droplets according to an analytical model based on Rayleigh instability theory. However, this work focused on droplet formation at the atomizer surface and did not address downstream transport, spatial distribution, or deposition efficiency within the root zone.

Limitations related to droplet transport and deposition are illustrated by the experimental observations of Yang et al. [56], who investigated mist distribution in a vertical ultrasonic aeroponic system operating at 1.7 MHz. Uneven droplet settlement was observed across vertical levels, with increased moisture accumulation at lower sections, likely due to gravitational settling and mist trajectory effects. Although fan-assisted airflow was applied to improve mist distribution, droplet deposition remained non-uniform and was evaluated only qualitatively. Continuous fogging further resulted in a gradual increase in root-zone temperature, indicating interactions between mist transport, airflow, and thermal effects. Together, these findings indicate that controlling droplet size at the atomizer alone is insufficient to ensure uniform nutrient delivery at the root surface, and that gravitational effects, airflow configuration, and thermal buildup represent critical limitation in fogponic set-ups.

2.3.2. Influence of atomization parameters on nutrient solution stability

Several experimental studies indicate that ultrasonic atomization parameters exert a strong influence on nutrient solution stability, particularly with respect to EC and pH. Jamshidi et al. [57] investigated the combined effects of ultrasonic operating frequency and fogging duration in a vertical aeroponic tomato system and observed that both EC and pH increased with increasing frequency. The strongest changes were reported when operating at higher frequencies, while lower-frequency operation (50 kHz) consistently produced more stable nutrient conditions and superior plant growth and yield. Fogging duration further affected pH, with longer misting periods leading to greater increases, whereas frequency remained the dominant factor governing chemical shifts.

Complementary findings were reported by Lakhiar et al. [53], who systematically evaluated the effects of frequency, spray time, and interval time on EC and pH using a uniform design approach. Their results confirmed that ultrasonic frequency and spray time significantly influenced both EC and pH, while interval time showed no statistically significant effect. High-frequency operation (1.7 MHz) produced the largest deviations in EC and pH, whereas low-frequency atomization (28 kHz) resulted in minimal chemical drift. Regression analysis further demonstrated that frequency was the primary contributor to nutrient instability, irrespective of spray interval.

Together, these studies identify ultrasonic operating frequency as the dominant control parameter affecting nutrient solution chemistry in fogponic systems, particularly in recirculating configurations. While increased atomization intensity may enhance mist generation, high-frequency operation can destabilize EC and pH beyond optimal ranges for plant growth. These findings highlight the need to balance atomization performance with chemical stability, especially in closed-loop nutrient delivery systems where deviations can accumulate over time.

2.3.3. Plant performance and yield trends

Experimental studies investigating fogponic and ultrasonic aeroponic systems indicate that plant performance and yield are strongly influenced by atomization parameters, particularly operating frequency and fogging duration. Jamshidi et al. [57] reported clear reductions in growth and yield metrics, including plant height, root weight, and fruit size, with increasing ultrasonic frequency. The highest tomato yields were obtained at the lowest tested frequency (50 kHz) combined with an intermediate fogging duration of 15 minutes, while higher frequencies and longer fogging periods consistently resulted in poorer plant performance.

These findings suggest that increased atomization intensity does not translate directly into improved biological outcomes. Although higher frequencies generate finer droplets, the associated destabilization of nutrient solution chemistry, as reflected by elevated EC and pH, appears to outweigh potential benefits of enhanced misting. This reinforces the observation that optimal plant response arises from a balance between sufficient nutrient delivery and chemical stability rather than from maximizing mist generation alone.

Other studies provide indirect support for these trends. Yang et al. [56] observed that continuous ultrasonic fogging led to elevated root-zone temperatures, which may negatively affect nutrient uptake and plant development. Similarly, Lakhiar et al. [53] demonstrated that high-frequency ultrasonic operation caused significant EC and pH shifts, conditions known to impair plant growth when sustained. Together, these results indicate that plant performance in fogponic systems is governed by coupled interactions between atomization parameters, nutrient stability, and root-zone environment, rather than by droplet size or fog density in isolation.

2.4. Experimental Synthesis and Identified Gaps

Recent studies identify ultrasonic operating frequency as a dominant control parameter. Higher frequencies are consistently reported to produce finer droplets; however, they are also associated with increased EC and pH drift, and these studies frequently report reduced growth or yield at these higher frequencies [57, 53].

Limitations in spatial wetting distribution have also been observed. In vertical systems, moisture accumulation is reported to be non-uniform across levels due to gravitational settling, suggesting that controlling droplet size at the atomizer is insufficient to ensure uniform root-zone conditions [56].

Table 2.2: Synthesis of experimental findings on fogponic and ultrasonic aeroponic systems, highlighting the influence of atomization parameters on droplet behavior, nutrient solution stability, and plant performance.

Parameter	Observed effects	Experimental evidence	Implications for fogponic design
Operating frequency	Smaller droplets at higher frequencies; increased EC and pH drift; reduced plant growth and yield	Mirzabe et al. [43]; Jamshidi et al. [57]; Lakhiar et al. [53]	Frequency is the dominant control parameter; high-frequency operation risks chemical instability and reduced plant performance
Droplet size	Strongly frequency- and fluid-dependent; wide distributions in ultrasonic systems; non-uniform deposition	Mirzabe et al. [43]; Yang et al. [56]	Droplet size control at the atomizer does not ensure uniform root delivery; transport and settling must be considered
Fogging duration	Longer fogging increases EC and pH shifts; excessive durations reduce plant performance	Jamshidi et al. [57]; Lakhiar et al. [53]	Moderate fogging durations are required to balance nutrient delivery and chemical stability
Spray interval	No statistically significant effect on EC or pH within tested ranges	Lakhiar et al. [53]	Interval timing is secondary to frequency and duration for nutrient stability control
Airflow and system geometry	Uneven mist distribution across vertical levels; gravitational settling dominates	Yang et al. [56]	Vertical systems require careful airflow design to mitigate non-uniform nutrient delivery
Thermal effects	Continuous fogging increases root-zone temperature, affecting nutrient uptake	Yang et al. [56]	Thermal management must be considered alongside atomization to prevent adverse plant response

Knowledge Gaps

The synthesis of the reviewed literature reveals the following structural gaps:

- **Inconsistent reporting:** Droplet size distributions are often not reported or are measured using non-comparable methods across different technologies.
- **Recirculation confounding:** Most studies utilize recirculating architectures, which prevents the attribution of chemistry drift specifically to the atomization process versus cumulative solution reuse.
- **Performance retention scarcity:** Long-duration drift in flow rate and module performance in nutrient-rich solutions is rarely quantified under controlled conditions.
- **Thermal load isolation:** Thermal behavior is seldom treated as a primary independent variable, despite its known influence on root health.
- **Stability $\leftrightarrow$ Chemistry coupling:** A correlation between fogponic technology and nutrient drift is suggested, but the causal link to droplet size and chemical drift is not proven.

2.5. Summary

This chapter has mapped the relationships between atomization parameters and system outcomes. The literature indicates that while fogponics offers architectural simplifications, it introduces complex couplings between ultrasonic frequency, thermal load, and chemical stability.

Therefore, the apparatus developed for this research must independently measure pH, EC, temperature, and fog output across different module types. This is necessary to decontextualize the atomization process and isolate thermal and chemistry effects from recirculation artifacts. Accordingly, experiments are designed to exclude biological effects so that measured drift can be attributed directly to atomization and module operation. This yields the bounded evidence required to characterize the feasibility limits of fogponic nutrient delivery.

3

Research Approach: Research through Design

The development of a lunar fogponic system presents a ”wicked problem” where the technical requirements and environmental constraints (low gravity, salt precipitation, and hardware longevity) are poorly defined in existing literature. Traditional linear engineering models, such as the waterfall or V-model, assume a stable set of requirements that can be systematically validated. However, in the absence of a standardized framework for lunar fogponics, a linear approach risks optimizing the wrong variables.

Therefore, this thesis adopts the methodology of Research through Design, specifically utilizing the Lab Venue. This chapter proposes the Research Questions and the methodological framework of Constructive Design Research by Koskinen [31]. This chapter details the research questions derived from gaps pointed out by literature, explains the RtD framework and details how this framework is integrated in this particular research.

3.1. Research Questions

The literature review in Chapter 2 identifies a critical lack of standardized evaluation protocols for fogponic systems in lunar environments. While the theoretical benefits of ultrasonic atomization are well-documented, the mechanical boundaries and the technology’s impact on the immediate growth environment remain largely unexplored. To address these gaps and provide a reliable baseline for the German Aerospace Center (DLR).

3.1.1. Knowledge Gaps to Research Questions

The research questions formulated in this chapter follow directly from the knowledge gaps identified in Chapter 2, in particular Section 2.4. The literature indicates that fogponics can offer high oxygen availability and potentially improved resource efficiency, but existing experimental evidence cannot yet be used to guide design decisions for lunar crop production facilities because key variables are reported inconsistently and several confounding effects are not separated.

A first gap concerns droplet size. As stated in Section 2.4, droplet size distributions are often not reported or are measured using non-comparable methods across different technologies. At the same time, the literature indicates an approximate optimal droplet-size range of 30 to 100 μm for effective root wetting while preserving oxygen availability. Since droplet size strongly governs deposition and transport in the root zone, this inconsistency motivates an investigation of distinct operating regimes using vibrating mesh aperture size as a controlled hardware descriptor. This leads to *RQ1: How do different vibrating mesh aperture sizes (2.9 μm and 25 μm) influence the mechanical reliability and droplet sedimentation behavior in a controlled environment, and what are the resulting implications for future system design?*

A second gap concerns nutrient chemistry attribution. As identified in Section 2.4, most studies utilize recirculating architectures, which prevents attribution of chemistry drift specifically to the atomization process versus cumulative solution reuse. Reported EC and pH drift in fogponic systems may therefore reflect technology effects, architecture-driven accumulation effects, and plant-driven effects such as root exudation. This results in *RQ2: To what extent does the atomization technology affect the electrical conductivity (EC) and pH stability of the nutrient solution over prolonged operational cycles?*

A third gap concerns thermal behavior. Section 2.4 highlights that thermal behavior is seldom treated as a primary independent variable, despite its known influence on root health. Because fog generation hardware can introduce thermal loading and thereby confound plant-response interpretation, this motivates *RQ3: How does the operation of the ultrasonic fogponic apparatus affect the root zone temperature within the growth chamber?*

Finally, plant performance trends reported in the literature remain difficult to interpret because they are embedded in the same limitations described above. As discussed in Section 2.3.3, multiple studies report reduced yield, but it remains unclear whether this reflects inherent limitations of fogponics or boundary conditions of specific implementations (droplet delivery, thermal coupling, chemistry drift, and mechanical reliability). This motivates *RQ4: To what extent can the observed differences in plant viability and growth be attributed to the mechanical and environmental boundary conditions identified in the fogponic apparatus?*

Taken together, these gaps indicate that the central limitation is not the absence of promising effects, but the absence of a concise and reproducible framework that defines what to measure, where to measure it, and how to relate system behavior to plant outcomes. This leads to the main research question: *How can a standardized research framework be developed to evaluate the technical boundaries and impacts of VMA-based fogponics for lunar agricultural applications?*

3.1.2. Research Questions

Main Research Question

MRQ: How can a standardized research framework be developed to evaluate the technical boundaries and impacts of VMA-based fogponics for lunar agricultural applications?

Technical Research Questions

RQ 1: How do different vibrating mesh aperture sizes ($2.9\mu m$ and $25\mu m$) influence the mechanical reliability and droplet sedimentation behavior in a controlled environment, and what are the resulting implications for future system design?

RQ 2: To what extent does the atomization technology affect the electrical conductivity (EC) and pH stability of the nutrient solution over prolonged operational cycles?

RQ 3: How does the operation of the ultrasonic fogponic apparatus affect the root zone temperature within the growth chamber?

RQ 4: To what extent can the observed differences in plant viability and growth be attributed to the mechanical and environmental boundary conditions identified in the fogponic apparatus?

Together these research questions will define the direction of this research

3.2. Methodological Framework: Research through Design

Standardized engineering practices typically rely on established ”design envelopes” within which a system is expected to perform. However, as identified in Chapter 2, the interaction between concentrated nutrient solutions and vibrating mesh interfaces in a closed-loop growth chamber represents an undefined design space. By utilizing CDR, the focus of the thesis is redirected toward uncovering the hidden variables of this space. The methodology justifies the use of the prototype as a ”probe” rather than a final deliverable, allowing the researcher to map the mechanical and chemical boundaries of the technology before optimization can occur.

The Research Program: Hard Core and Protective Belt

Following the logic of research programs in design, this inquiry is structured around a central hard core and an evolving protective belt. The hard core represents the fundamental and non-negotiable assumptions of the research, which in this context is the belief that mass-efficient, soilless nutrient delivery systems are essential for sustainable lunar habitation, and that fogponics promises a more efficient and contamination resistant nutrient delivery system. Surrounding this core is the protective belt, consisting of auxiliary hypotheses that are subjected to experimental testing and iterative refinement. These hypotheses concern the specific technical variables of fogponic atomization, such as the relationship between ultrasonic frequency, mesh aperture size, and the chemical stability of nutrient solutions. By organizing the research in this manner, the thesis distinguishes between the permanent mission objectives and the technical variables that are being systematically investigated.

The Lab Venue: Strategy of Decontextualization

The primary setting for this research is the lab venue, characterized by the methodological principle of decontextualization. In this approach, the fogponic phenomenon is removed from the eventual system context of a full lunar greenhouse and studied in a controlled setting to isolate specific causal relationships at the technology–material interface. The intent is to establish reproducible, engineering-relevant relationships between the atomization hardware, the nutrient solution, and the immediate root-zone environment. And provide a platform and baseline for further research.

Accordingly, biological variability is treated as indication of causal attribution: where plant cultivation is used, it functions as a qualitative boundary probe to indicate whether the technical operating conditions are plausibly compatible with plant survival, rather than as a controlled agronomic performance study. The objective of the lab venue is to identify conditional laws i.e., transferable principles describing how the hardware behaves under specified physical and chemical parameters that can underpin a standardized testing framework for future aerospace research.

The Artifact as Knowledge Instrument

Within this framework, the physical prototype is not treated as a final engineering product but as a testrig, a ”design thing” or an experimental apparatus. This artifact serves as a knowledge instrument designed to facilitate a dialogue between the researcher and the material reality of lunar agriculture. The construction and testing of this apparatus are intended to provoke specific moments of reflection-in-action, where technical hurdles are documented as formal research data. Rather than viewing system limitations as project failures, this methodology frames them as critical design episodes that define the boundaries of the technology. Consequently, the artifact acts as a carrier of scientific information, where its physical evolution and the resulting failure modes constitute the primary academic contribution of the thesis, leading to a robust and justified positive heuristic for future lunar system design.

3.2.1. Study Logic

The study logic in this thesis starts from an uncertain technology space in which the engineering envelope for VMA based fogponics is not defined. A decontextualized lab venue is then used to constrain the evidence space and to construct a research instrument that enables repeatable operation and measurement. Observed performance retention and documented failure signatures are interpreted as boundary evidence and translated into conditional statements that define feasibility limits and motivate subsequent design iterations, indicated by the feedback loop. Figure 3.1 summarizes the study logic of this thesis.

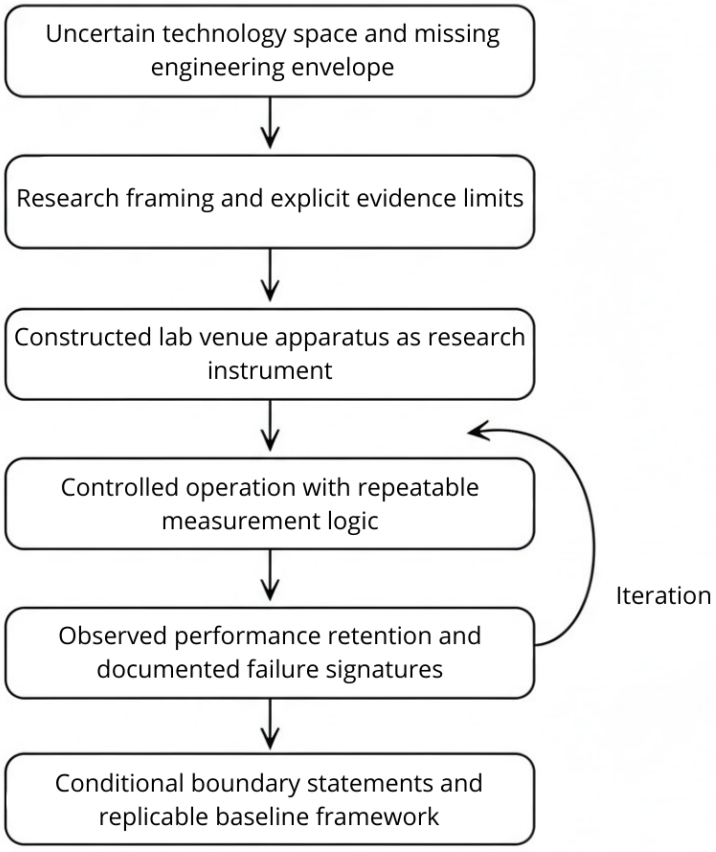

Figure 3.1: Study logic of the thesis based on a Research through Design approach, where the prototype is treated as the central research instrument. The diagram shows how an initially uncertain technology space is narrowed through explicit framing, construction of a lab venue setup, controlled repeatable operation, and observation of performance and failure signatures, which then inform iterative design moves and lead to conditional, replicable boundary statements. Source: [31].

3.3. Research Boundaries and Limitations

In accordance with the RtD framework, the boundaries of this study are defined as a ”negative heuristic”, a strategic exclusion of variables to protect the internal validity of the laboratory inquiry. By establishing these limits, the research program moves from broad system speculation to the extraction of specific ”conditional laws” governing fogponic atomization within a controlled environment.

Methodological Shift: From Growth to Technical Rupture

The primary boundary of this thesis is the decontextualization of the nutrient delivery process from a full-scale, long-term biological lunar production cycle. The research is bounded to an investigation. Plant cultivation is included only as a qualitative boundary to reveal technical feasibility limits, and no

causal attribution to biological mechanisms or quantitative agronomic performance is claimed in this thesis.

Environmental Limitation: Absence of Reduced Gravity

A significant boundary of this research program is the exclusion of direct reduced-gravity simulation. While the "Hard Core" of the thesis is centered on lunar applications, the physical experiments were conducted entirely within a terrestrial 1-g environment. Consequently, the research does not account for the complex fluid dynamics, such as the absence of buoyancy-driven convection or the altered droplet coalescence patterns, that would occur in a 1/6-g lunar environment. This study serves as a 1-g baseline characterization.

Technological and Experimental Scope

The technical scope is limited to the comparative analysis of two specific vibrating mesh apertures ($2.9\mu m$ and $25\mu m$) integrated into a single-unit experimental test rig. This boundary was set to isolate the effects of droplet size on system reliability and root zone temperature without the interference of varying mesh materials or large-scale multi-tray complexities. Furthermore, while the research is framed within a lunar "hard core," experimental testing was conducted under terrestrial gravity. The implications for low-gravity performance are therefore extrapolated from sedimentation theory.

Temporal and Chemical Parameters

The inquiry is bounded by test cycles ranging from 10 to 14 days, providing a high-fidelity window into the early-stage stability of the system. The chemical investigation is limited to the behavior of two specific nutrient solutions: a standard Hoagland solution and a Priva-based laboratory solution. While factors such as airflow velocity were excluded from the measurement matrix to maintain the focus on the atomization-material interface, environmental parameters including relative humidity, ambient temperature, and Photosynthetically Active Radiation (PAR) were monitored to ensure a stable baseline for the Lab Venue.

4

Tools and Methods

4.1. The Initial Concept (The Design Thing)

The primary objective of the implementation is to manifest the research program through a physical Design Thing. From the Lab Venue strategy of Constructive Design Research, the apparatus is not intended as a final lunar product, but as a specialized research instrument optimized for inquiry. The logic of this apparatus is governed by the need to bridge the gap between theoretical lunar requirements and the material reality of ultrasonic atomization.

To achieve the rigor required by the Lab Venue, the apparatus utilizes a strategy of strategic decontextualization. By isolating the technology-material interface within a controlled laboratory setting, the complexities of a full-scale lunar greenhouse, such as reduced airpressure and 1/6th gravity, are temporarily removed. This decontextualization allows for the clear observation of the fundamental conditional laws governing the Vibrating Mesh Atomizer (VMA). It ensures that the technical feedback provided by the rig is a clean signal, which is directly attributable to the hardware configuration rather than environmental noise.

4.1.1. EDEN laboratory Environment

All experiments were performed in the EDEN laboratory environment, which provides controlled growth conditions for comparative testing. Ultimately, two nutrient delivery architectures were evaluated under matched conditions: a recirculating aeroponic baseline and a VMA-based fogponics prototype. Both systems used the same cultivation tray and plant holder geometry to minimize non-architectural differences.

The EDEN lab is a controlled cultivation environment, here plants are cultivated using the same aeroponics system as shown in Section 1.4. Air temperature, relative humidity, and lighting conditions are set through facility control and logged. In Figure 4.1a the lab is shown. Figure 4.1b shows the designated area for the experiment. Nutrient solution is prepared and maintained by a dedicated mixing system and supplied to the cultivation systems from a reservoir this specific mix will be referred as the Priva nutrient solution. Facility logs were used to confirm stable ambient conditions during experiments, while system-specific variables (EC/pH, root-zone temperature, and delivery performance) are logged independently.

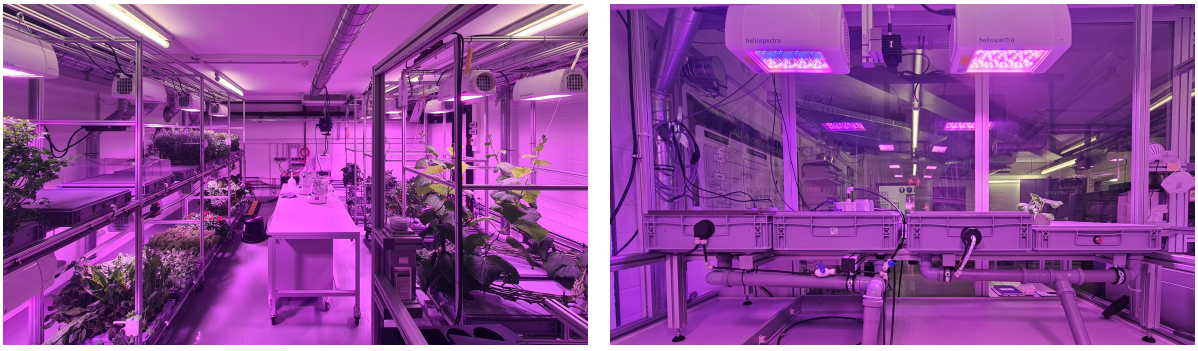

(a) EDEN cultivation laboratory at DLR Bremen.

(b) Designated area for experiments inside the EDEN cultivation laboratory.

Figure 4.1: EDEN laboratory environment used for comparative cultivation experiments. The figure shows the EDEN laboratory on the left with plants growing, and a designated area for experiments with growth trays, nutrient solution infrastructure, and LED grow lights.

4.1.2. System Architecture: Requirements and Selection Heuristics

The following section explains the requirements involved the design of a research prototype for fogponics in lunar agriculture. These are later used to validate decisions made during the design moves.

Design objectives

The design objectives for a prototype, resulting from the research questions in Section 3.1 are:

- Enable separated monitoring of nutrient chemistry before and after delivery by implementing reservoir and drain measurement points (EC/pH/temperature).
- Provide automatic, time-stamped data logging for the variables required for time-series analysis and comparison between systems.
- Allow controlled operation of the atomization process (misting frequency / duty cycle) to support comparative experiments.
- Fit the EDEN cultivation form factor (40×60 cm tray, sufficient root-zone height) and ensure reliable drain function without root obstruction.
- Allow for research on variety in modules and misting nature.

Key prototype requirements

To keep the requirements section compact, the design is driven by a limited set of requirements that directly affect measurement validity and experimental comparability. These key requirements are:

- **Timely monitoring (REQ-01):** monitor and control EC, pH, and temperature before and after fogging.
- **Automatic data logging (REQ-02):** time-stamped logging of solution parameters (and, where applicable, air temperature, PAR, and humidity above the plants).
- **Chemical compatibility (REQ-07):** wetted components compatible with nutrient solution and cleaning agents.
- **Fog distribution (REQ-10):** provide fog delivery to all roots with acceptable uniformity.
- **Tray constraints (REQ-20):** 40×60 cm tray compatibility and minimum root-zone height.
- **Drain placement (REQ-21):** drain positioned to avoid root congestion.
- **Root intrusion prevention (REQ-22):** prevent roots entering and blocking the drain.
- **Lab integration (REQ-24):** allow integration with lab infrastructure (mounting/interfaces).

In addition to the requirement set above, prototype-specific requirements derived from EDEN LUNA and expert input were used to guide implementation choices, including support for inline sensing and time-stamped EC/pH logging (P-21, P-26) and adjustable misting frequency (P-11). Requirements that

conflict with the measurement objective (e.g., full runoff recirculation) are treated as out of scope for this prototype and are deferred to follow-up work.

Requirement handling and scope

The complete requirement list with sources are provided in Appendix B. Within the main text, requirements are referenced only where they directly motivated a design decision or a verification step, to avoid an extensive requirement-by-requirement discussion.

4.1.3. Initial Concept Design Approach

This thesis develops a fogponics prototype as a research instrument. The design process is structured in two steps. First, a conceptual design is established to define the overall architecture and the main subsystems. Second, the selected concept is translated into a detailed design and iterated based on implementation constraints and verification tests. The conceptual design step is documented in this section; detailed design choices and subsequent scope reductions are documented in Section 4.2.

Concept generation using a morphological chart

To translate the derived prototype requirements into concepts, a morphological chart was used to structure the design space. The system was decomposed into key subfunctions (nutrient solution storage and routing, atomization and fog delivery, drain handling, sensing and logging, and operational support), and multiple solution principles were identified per subfunction. The chart was used to ensure complete coverage of relevant options, and can be found in Appendix A.

At the conceptual level, the morphological chart was used to combine compatible solution principles into a limited set of candidate concepts. At this stage, concepts were defined by their architecture (e.g., separation of reservoir and fog tray, drain collection strategy, and monitoring locations) rather than by final component selection.

Concept selection logic

The candidate concepts were evaluated against the key prototype requirements defined in Section 4.1.2. Safety and lab integration were treated as pass/fail gates. Concepts that could not be operated safely in the EDEN laboratory environment or could not be integrated within the available tray form factor were excluded.

For the remaining candidates, selection was performed using a structured, criteria-based engineering judgment rather than a formal scoring method. The concepts were weighed against a prioritized set of criteria reflecting the primary purpose of the prototype as a research instrument. The criteria, listed from highest to lowest priority, were: *reproducibility, measurability and observability, validity and traceability, reliability and operational robustness, maintainability and serviceability, and reduced complexity*. In practice, concepts were preferred when they supported repeatable construction and operation, enabled clear and separated measurement points, and provided unambiguous interpretation of recorded data, while remaining sufficiently robust to run for multi-day trials with practical access for inspection and cleaning. Complexity was treated as a secondary consideration and only accepted when it directly improved measurement capability or operational stability.

Selected initial concept

Following this selection approach, the initial concept was chosen to best support the measurement objectives of this thesis within the practical constraints of the EDEN lab. The concept separates the nutrient reservoir from the fog tray and collects the drain in a dedicated tank. This enables separate EC and pH monitoring in the reservoir and in the drain, which is essential to distinguish bulk-solution trends from changes introduced by the delivery chain and the root zone.

Figure 4.2 provides an overview of the initial prototype concept and its intended functional blocks. The cultivation tray includes plant holders in the lid, while nutrient delivery is provided by an ultrasonic atomizer integrated into the reservoir body. Fog produced by the atomizer is directed toward the root zone through a fog-guidance channel. The nutrient solution is monitored using pH and EC sensors, and an additional pH/EC control unit is indicated for adjusting the solution when required.

To support safe operation and repeatable testing, the concept includes an overflow valve to prevent overfilling and a return filter to capture particles before recirculation. Flow delivery is monitored with a

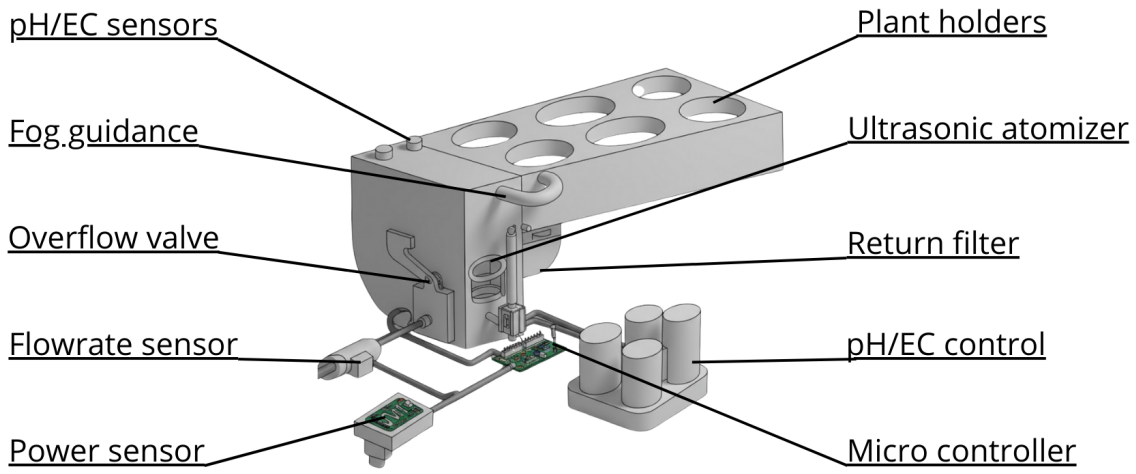

Figure 4.2: Annotated rendering of the first fogponic prototype concept, derived from the requirements and the morphological chart as an integratable module for the EDEN tray based infrastructure. The concept shows the intended integration of fog generation and guidance, plant holders, return filtration, drain and overflow routing, and embedded sensors and control electronics. The main design aims are monitoring and controlling EC, pH, and temperature before and after fogging with automatic time stamped data logging, ensuring chemical compatibility of wetted components, achieving uniform fog distribution across the root zone, and fitting the 40×60 cm tray constraints with a drain layout that limits root intrusion and supports integration with lab mounting and interfaces.

flow-rate sensor, and electrical input to the atomizer is monitored with a power sensor. A microcontroller is shown as the central unit for actuating the atomizer and logging sensor data, enabling time-stamped monitoring of solution behavior and system performance during experiments.

4.1.4. Technical Specifications (The Design Envelope)

The transition from the conceptual design documented in Section 4.1 to the final as-tested apparatus was not a linear assembly process. Instead, it was characterized by a series of design moves necessitated by the material resistance of the nutrient solution and the physical behavior of the atomized droplets. This section documents the starting point archictecture of the apparatus.

Chamber Geometry and Standardization

The primary containment for the atomization process is a PVC tray measuring 60 x 40 x 12 cm. The selection of these specific dimensions is a strategic design move intended to align the research with standardized formats used in current lunar crop production studies [16]. By utilizing a standard geometry, the apparatus ensures that the results regarding fog density and thermal accumulation are directly transferable to existing Bio-regenerative Life Support System architectures. This choice represents the integration of a mission-critical constraint into the Lab Venue, ensuring that while the technology is decontextualized, it remains grounded in the physical realities of space-based agricultural modules.

Ultrasonic Module Selection

The research investigates two distinct vibrating mesh aperture sizes to map the operational boundaries of fogponic delivery. In consultation with the supplier, the 25 μm modules were selected to align with existing literature, which identifies an optimal droplet range between 30 μm and 100 μm for root-zone nutrient uptake. In contrast, the 2.9 μm modules were chosen to represent the industry standard for ultrasonic atomization, despite their limited documentation in fogponic plant growth contexts. The inclusion of both sizes allows the apparatus to serve as a comparative instrument, revealing how varying droplet spectra influence system-wise behavior and mechanical longevity. This technical configuration allows for the testing of auxiliary hypotheses regarding the trade-off between biological requirements, represented by larger droplets, and mechanical standardization, represented by smaller droplets.

Sensor Integration and Fluid Monitoring Strategy

To monitor the chemical stability of the nutrient solution, pH and EC sensors were integrated into both the primary reservoir and the drainage system. A collection beaker was positioned at the drain to cap-

ture condensed nutrient solution, facilitating continuous measurement of the solution after it had undergone the atomization and condensation cycle. Because these sensors require constant submersion to maintain calibration and accuracy, a thin baseline layer of Reverse Osmosis water was maintained within the beaker. This configuration ensures the tracking of chemical drift, which is a critical dependent variable in the research program. The placement of these sensors is a methodological requirement of the Lab Venue, providing the empirical data necessary to define the conditional laws of nutrient stability under high-frequency vibration.

4.2. Iterative Development of the Test Rig

The test rig was built through a sequence of design changes. Each change followed directly from what was observed during testing with nutrient solution and atomized droplets. Practical issues were treated as inputs for the next iteration, consistent with a Constructive Design Research approach.

Isolation of Chemical Variables

To ensure that the data collected regarding pH and EC stability was an accurate reflection of the technology's impact, the nutrient solution was subjected to baseline testing to exclude drift caused by the solution itself. Preliminary observations of the Priva solution indicated an inherent increase in pH after five days of stagnation, independent of any ultrasonic excitation. Consequently, a Hoagland solution was selected for the primary research program to isolate the technology's influence. This methodological choice ensures that any observed chemical drift can be attributed directly to the atomization process and its interaction with the apparatus, fulfilling the Lab Venue requirement for the isolation of specific causal relationships.

Episode 1: External transport and plume characterization

Following the principles of the Lab Venue [31], the first prototype decontextualizes fog production and guidance into the root zone, without integrating other system functions. The setup used an external reservoir and a single 2.9 μm module supplied through a wicking cylinder. Fog was guided towards the growth tray through an external tube. This prototype provides space for pH and EC measurement probes in the lid of the reservoir. The physical setup is shown in Figure 4.3

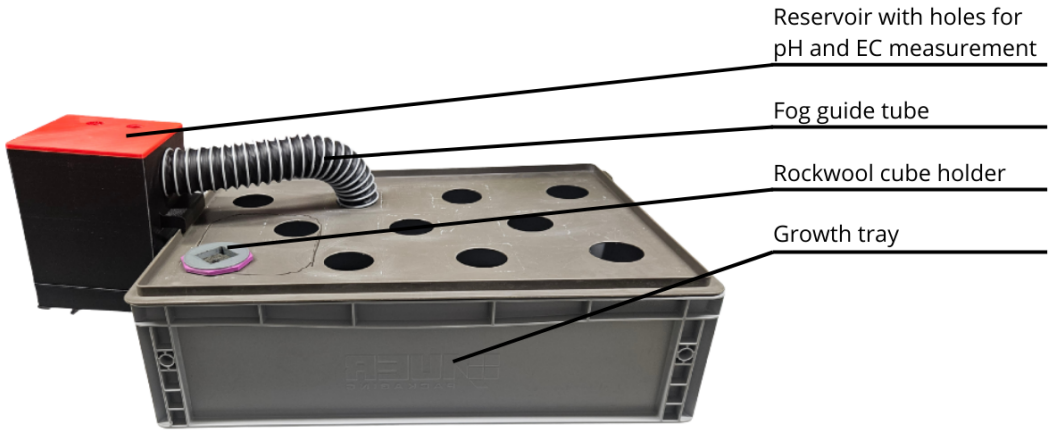

Figure 4.3: First prototype iteration with a separate nutrient reservoir and fog guided into the growth tray through an external tube, aimed at decontextualizing fog production and fog transport into the root zone. The reservoir lid includes access holes for pH and EC probes, and the tray lid provides plant holder openings. Initial tests identified two limitations: a single module did not generate enough fog to fill the tray volume, and fog entry through the guide tube was not reliable without forced flow. Since adding a fan or blower would increase system complexity, the external guide tube concept was abandoned and the next iteration placed the atomizer modules directly inside the root zone.

Initial tests showed two limitations. First, one module did not generate enough fog to fill the tray volume. Second, the fog did not enter the tray reliably through the guide tube. This would have required forced flow. Adding a fan or blower would add complexity, which is is in contradiction to complexity requirement *SC-01* as described in Table 1.1. Therefore, forced flow was not persued. Instead, the external guide

tube was removed and the next iteration internalized the atomizer modules directly into the root zone.

In parallel, the plume behavior of two VMA variants was compared to understand how droplet size affects transport and wetting. Figure 4.4 shows side and top views of the 2.9 μm and 25 μm variants. The 2.9 μm module produced a diffuse plume that spread and remained suspended long enough to contribute to volumetric filling. The 25 μm module, however, produced a directional spray with rapid deposition on the surfaces. This indicated that the 25 μm variant should be treated as a wetting and impingement mechanism, not as a suspended fog. Future orientations and placement of the modules had to account for directly aimed liquid application.

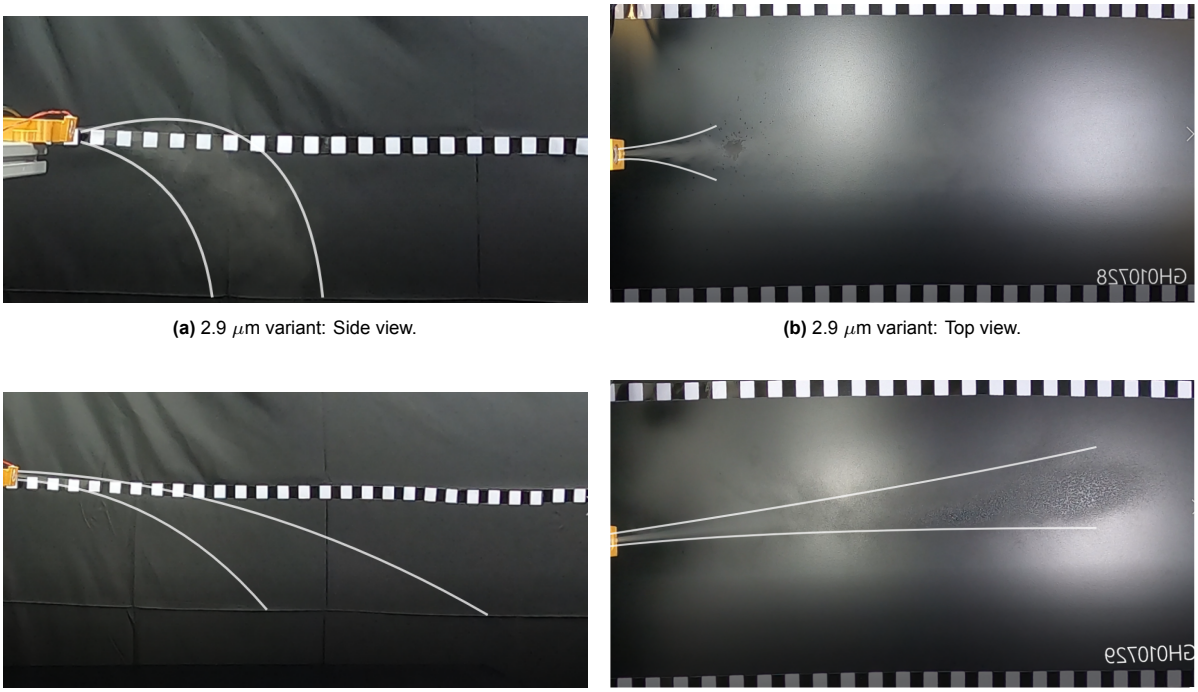

(a) 2.9 μm variant: Side view.

(b) 2.9 μm variant: Top view.

(c) 25 μm variant: Side view.

(d) 25 μm variant: Top view.

Figure 4.4: Comparative plume development of two VMA variants, shown in side and top view. (a) and (b) show the 2.9 μm module, producing a diffuse, fog like plume that spreads and remains suspended. (c) and (d) show the 25 μm module, producing a more directional spray with rapid deposition. In (c), the spray was difficult to distinguish due to non optimal lighting, so the spray pattern is enhanced for visibility, while (d) clearly shows direct impingement of liquid on the surface below.

At the end of this first development step, two issues remained unresolved and directly defined the next design move. First, the external transport concept did not work reliably: the 2.9 μm plume did not have internal pressure to consistently pass through the guide tube and enter the tray volume, and a single module also did not generate enough fog to fill the tray. Solving this with a fan or blower was rejected due to added complexity which is against the design requirements B. Second, the 25 μm variant did not behave as a volumetric fog source at all, but as a directional spray that impinged on nearby surfaces and caused local wetting.

These observations required two changes in the next iteration: (i) abandon the external guide tube and place the atomizer modules inside the growth tray directly at the roots, and (ii) Increase the number of atomization modules.

Episode 2: Top reservoir integration and dual module compatibility

The second iteration aimed to increase fog production while keeping access for pH and EC measurements at the tray lid. A second goal was to keep the mechanical interface compatible with both the 2.9 μm and 25 μm modules, as required for droplet size comparisons. The resulting concept used a small top reservoir holding two modules. This reservoir was mounted in one of the plant holder openings, so the modules could operate inside the growth tray while the reservoir remained on top (Figure 4.5).

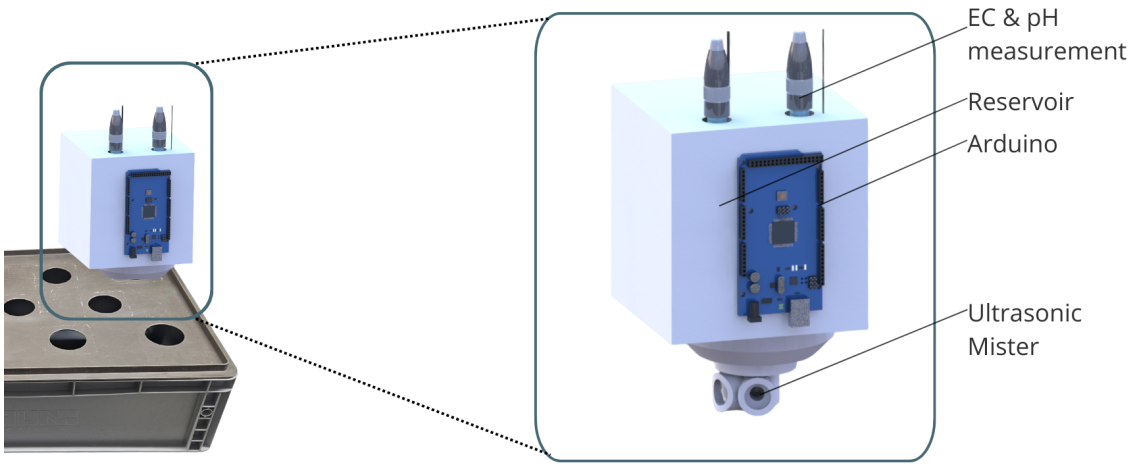

Figure 4.5: Top mounted reservoir concept from the second prototype iteration, used to increase mist output while keeping pH and EC access at the tray lid and allowing interchange between 2.9 μm and 25 μm VMA modules. Two modules operate inside the tray while the reservoir sits above the lid. Tests confirmed that the 25 μm variant can deliver droplets directly to roots when aimed at the root entry locations, but the concept was rejected due to leakage and pooling, loss of a plant position, potential light obstruction, and insufficient uniformity when using only two modules.

.

Two aspects worked well. In this orientation, the 25 μm variant behaved as expected and provided a directed spray at the roots. When the spray was aimed at a plant opening, droplets were delivered directly to the roots entering through the lid. This confirmed that the spray like modules can be used effectively, but only if they are aimed at the root entry locations.

However, several issues made the design unsuitable as a research prototype. The top reservoir occupied a plant position, reducing usable growing area. It also leaked nutrient solution along the module bodies into the tray, causing direct liquid flow and local pooling instead of delivery as fog. This violated the no leak requirement IRR-03 in Table 1.1, since stagnant nutrient solution on surfaces can promote microbial growth. Placing a reservoir above the plants was also not acceptable because it would block the light path. Finally, distribution would not reach all plants as 2 modules in the corner would not be enough. For the 25 μm variant, the spray had to be directed at the roots to be effective. This implied that uniform supply would require one module per plant position, at least for this droplet size range.

Episode 3: The Wick Based Prototype

Based on these observations from Episode 2, the next prototype moved the reservoir underneath the growth tray and placed the modules fully inside the growth tray. To supply all plants, the baseline configuration became one module per plant. This resulted in a six plant prototype with six atomization modules. The reservoir under the tray had to supply nutrient solution to each module and allow practical cable routing and placement inside the tray. Since the modules and control boards are connected by cables of approximately 10 cm, a clustered layout was preferred to keep wiring feasible. Nutrient solution was supplied using a wick. The wick can lift liquid only over a limited height of approximately 10 cm, so the modules were positioned halfway up in the growth tray. They were angled slightly upward to aim droplets at the roots entering through the lid. This configuration is shown in Figure 4.6 and is the first test ready prototype. It is referred to as the wick based prototype.

Rupture of 25 μm modules and duty cycle

During initial testing, several 25 μm modules ruptured and cables broke loose from the modules, resulting in not enough remaining for a plant trial. Therefore, the wick based prototype used only the 2.9 μm modules. Literature commonly reports duty cycles around 15 minutes on and 15 minutes off for systems that create a fog that remains suspended [47]. Since this prototype also had to remain applicable to the less foglike, more spraylike modules, the initial duty cycle was set to 30 seconds on and 30 seconds off. This duty cycle was tuned based on observed root wetting and the amount of excess

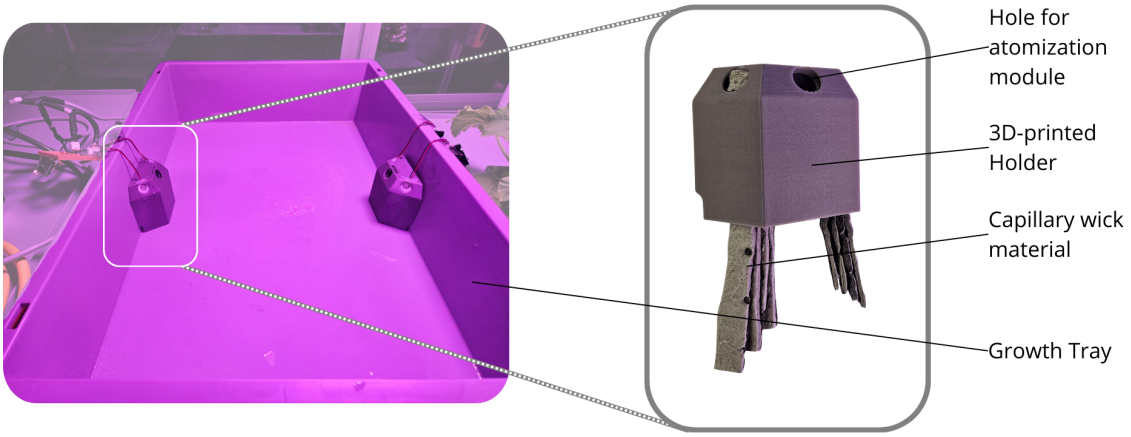

Figure 4.6: First prototype iteration showing the wick supplied module holders integrated into the growth tray root zone. Nutrient solution is drawn up from the reservoir below through tray holes, which are not visible in the figure, by capillary wick material and supplied to the atomization module location in the 3D printed holders. This configuration was used for the first cultivation trial with plants and Priva solution.

nutrient solution in the drain, with assessment supported by DLR cultivation experts. The wick based prototype was used for the first plant trial. Full results are discussed in Chapter 5. The observations that drove the subsequent iteration are discussed next.

The first cultivation trial showed two dominant failure mechanisms that limited stable operation over time. First, the capillary supply degraded. Over the course of the trial, the wicks progressively delivered less nutrient solution to the modules. This was observed as a decreasing wetting of the wick tips at the module interface and a reduction in visible fog output, eventually leading to intermittent or absent atomization for some modules. Second, the module interface itself became fouled. Part of the generated fog deposited back onto the module face and around the vibrating mesh. This back deposition concentrated dissolved salts locally as water evaporated. After ten days visible crystallization had formed on and near the mesh surface. As crystallization increased, atomization performance degraded further. In practice this was observed as a reduction in fog output.

Episode 4: Final Prototype

To achieve a nutrient supply that remains consistent over longer operating times, the wick based prototype was redesigned to an actively supplied configuration. A small liquid pump, shown in Figure 4.7a, was added to deliver nutrient solution to the atomization modules. The pump was controlled by the same Arduino used for the fogger duty cycle, allowing synchronized timing between supply and atomization. In this configuration, one pump supplied all six modules. The delivered volume was tuned iteratively by adjusting the pump on time until the supplied flow matched the amount the modules could atomize.

A second change addressed salt crystallization at the module interface. The module placement was moved from mid height with a slightly upward aiming angle to a position near the top of the growth tray, angled slightly downward. The intent of this orientation change was to reduce back deposition of fog onto the mesh and to limit droplet deposition on nearby surfaces around the modules. This redesign formed the next test ready configuration, which is evaluated in Chapter 5.

This resulted in the second fully functional prototype, which was used for the pilot cultivation trial and the comparative analysis against the aeroponics baseline. This resulted in the second fully functional prototype, which was used for the pilot cultivation trial and the comparative analysis against the aeroponics baseline. As within the venue of RtD the prototype is the result. The final prototype and findings are discussed in Chapter 5.

(a) Small liquid feed pump to supply liquid to the atomization modules.

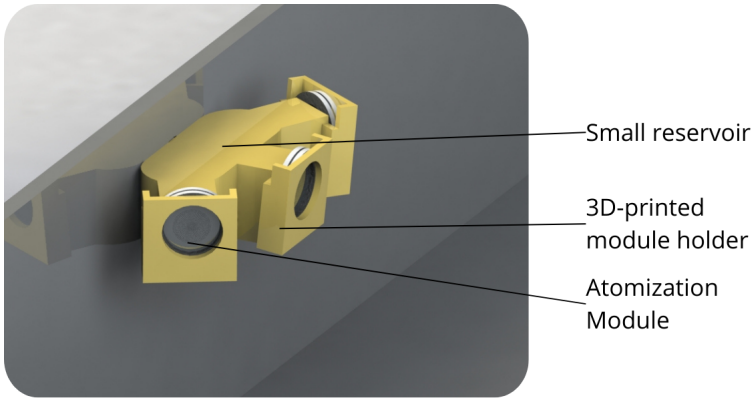

(b) CAD render illustrating the integration of the atomization modules and the custom mounting insert within the fogponics growth tray.

Figure 4.7: Hardware used in the final fogponics prototype. (a) Small liquid feed pump added to deliver nutrient solution to the atomization modules, controlled by the same Arduino as the fogger duty cycle to synchronize supply and atomization; one pump supplies all six modules and the pump on time is tuned so the delivered flow matches the atomization capacity. (b) Rendering of the atomization modules and mounting insert integrated into the growth tray. For the pilot cultivation trial and comparative evaluation.

4.2.1. Summary of Design Episodes

Below the iteration outcomes and following design choices have been formulated in Table 4.1. The table states the design episode, the decontextualized focus, if it has been used for a growth trial, outcomes and the subsequent design move.

Table 4.1: Prototype iterations, key outcomes, and cultivation use.

Ep.	Prototype focus	Cultivation use	Key outcome	Next design move
1	Contextualized testing of fog production and guidance.	No	Guide tube transport unreliable, single module insufficient. Plume study showed 25 μm behaves as spray.	Internalize modules in root zone, increase module count.
2	Module compatibility (2.9 and 25 μm).	No	25 μm spray delivers to roots when aimed. Top reservoir occupies plant spot, leaks, and distribution is insufficient.	Reservoir below tray. One module per plant baseline.
3	Wick based prototype.	Yes (first trial)	Wick supply degrades due to salt precipitation. Back deposition causes reduced output.	Replace wick with active supply. Change orientation to reduce back deposition.
4	Final prototype.	Yes (second trial)	Tuned pump timing, reorientation modules.	Final test ready configuration evaluated in Chapter 5.

4.3. Final Experimental Protocols and Research Operations

This section documents the experimental protocols used in this thesis. It describes how atomizer failure modes were identified and quantified, how measurements and data logging were implemented, and how nutrient solution preparation and plant material handling were conducted. It also defines the verification plan used to check that the prototype and instrumentation operated as intended and that the resulting datasets are interpretable within the stated boundaries.

4.3.1. Final as-tested configuration in EDEN lab

The experiments reported in this thesis were performed using the final as-tested configuration summarized in Figure 4.9.

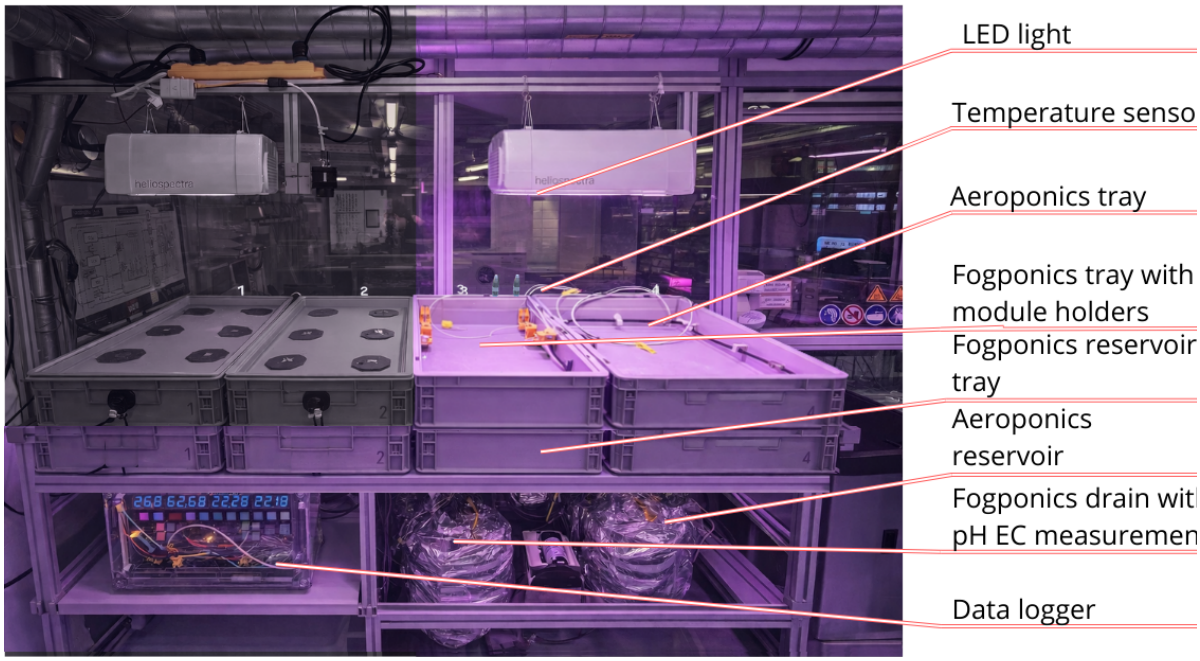

Figure 4.8: Final as tested fogponics prototype and instrumentation setup used for the pilot trial in the EDEN lab. The configuration consists of a cultivation tray with a six module VMA manifold, three modules per side, supplied by a low pressure pump from a reservoir tray located underneath. A dedicated drain collector enables separate monitoring of reservoir and drain solution, with pH and EC measured at both locations. Temperature is monitored at four locations: fogponics reservoir, fogponics drain, fogponics root zone, and the aeroponics root zone used as baseline reference. This setup is the reference configuration for the datasets reported as the second trial in Chapter 5.

The setup consists of a reservoir tray located beneath the cultivation tray, a low-pressure pump supplying nutrient solution to a six-module VMA manifold (three modules per side), and a dedicated drain collector enabling separated reservoir and drain monitoring. EC and pH are measured at both reservoir and drain locations, and temperature is measured at four locations (fogponics reservoir, fogponics drain, fogponics root zone, aeroponics root zone). This configuration is the reference for all datasets presented in Chapter 5.

4.3.2. Failure Modes Identification and Quantification

Two failure modes were observed during testing: rupture of the atomization modules and salt deposition. Rupture was observed during Episode 2 and Episode 3. Salt deposition was observed at the end of the first growth trial that was conducted with the Episode 3 prototype. These failure modes were further identified by microscope through optical inspection under a KERN OBL 137 transmitted light microscope (trinocular) at $4\times$, $10\times$, and $20\times$ magnification. The impact of these failure modes requires quantitative investigation. This investigation is described in the following section.

(a) Final prototype atomization module, closed top. With casing for electronics.

(b) Final prototype atomization module with open top (installed and working configuration).

Figure 4.9: Final prototype documentation images showing module configurations.

Atomizer gravimetric flow-rate measurement

Two vibrating-mesh atomizer (VMA) module variants were evaluated, defined by nominal mesh aperture size of 25 μm and 2.9 μm. Aperture size is treated as a hardware specification only. Droplet size was not measured and is not inferred from aperture size. Delivery performance is quantified as mass flow rate in g/min, measured gravimetrically by collecting atomizer output over a fixed interval and weighing the collected mass.

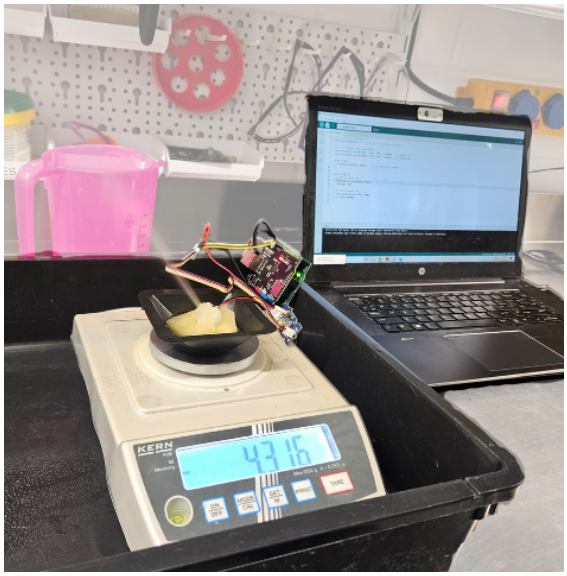

(a) Flow rate measurement setup with a 25 μm atomization module placed on a precision balance.

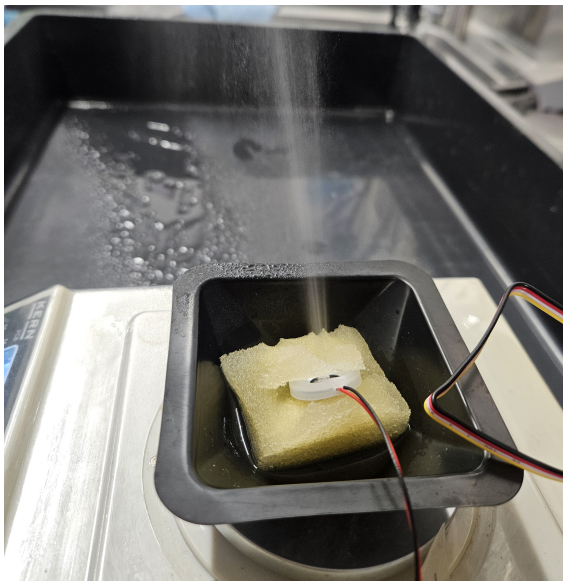

(b) Atomization module integrated in the sponge insert used during flow rate testing.

Figure 4.10: Experimental setup for gravimetric measurement of VMA mass flow rate. (a) Example setup with a 25 μm module, where atomizer output is collected over a fixed actuation interval and the collected mass is determined using a precision balance. (b) Atomizer integrated in the sponge insert used during testing, which supplies liquid to the module during actuation. Flow rate is reported in g/min as collected mass divided by the collection time, with repeated trials per module to quantify unit to unit variation and before and after performance changes.

Flow-rate measurements were performed on individual atomizers, with one active module at a time, to isolate module-to-module variation and to enable repeated testing of the same module over time. For the 25 μm modules, a sample size of $n = 5$ was used. For the 2.9 μm modules, a sample size of $n = 4$ was used. Each measurement was repeated three times per atomizer, and the mean value was used for subsequent analysis.

Test setup and actuation. A single atomizer was connected to an Arduino-based trigger circuit with a push-button that initiated actuation. A sponge was cut to fit the atomizer and placed in a small container with test liquid. The test liquid mass was measured before and after a defined actuation time. Figure 4.10 shows the test setup. The mass was measured without the atomizer module present on the balance.

Weighing procedure. The container was placed on the balance and tared, then removed for actuation. After actuation, the atomizer was removed again and the container was placed back on the balance to record post-test mass. This configuration was kept consistent between pre-test and post-test measurements.

Test durations and resolution. The balance resolution was 0.001 g. For the 25 μm modules, the collection interval was 60 s. For the 2.9 μm modules, the collection interval was 300 s. In addition to single-module characterization, tests were also performed for a nominal four-module configuration (four $\times$ 2.9 μm and four $\times$ 25 μm), while still measuring one module at a time.

Measurement points over the prototype lifetime. Each atomizer was measured in a fresh condition and measured again after failure, providing paired before and after data per unit. For the 25 μm modules, the post-failure condition corresponds to operation after an observed rupture event. For the 2.9 μm modules, the post-failure condition corresponds to operation after salt precipitation was observed together with loss of output. Imagery evidence of this is shown in Section 5.5.4.

Flow-rate computation. For each trial, the collected mass Δm was computed as the difference between post-test and pre-test mass. The mass flow rate was computed as

$$\dot{m} = \frac{\Delta m}{\Delta t}, \tag{4.1}$$

where Δt is the collection interval (60 s or 300 s). Reported flow rates are expressed in g/min. An overview of the evaluated module variants and datasets is given in Table 4.2.

Table 4.2: Overview of VMA module variants and datasets.

Module variant	Aperture size	Interval	Sample size	Fresh	Post-failure	Post-failure label
VMA-A	25 μm	1 min	$n = 5$	measured	measured	Rupture
VMA-B	2.9 μm	5 min	$n = 4$	measured	measured	Salt precipitation

4.3.3. Measurement Instrumentation and Data Logging

The data acquisition system transforms environmental variables into digital records through a three-stage process involving hardware signal conditioning, digital filtering, and a time-delayed storage protocol. The water quality parameters, pH and EC, were acquired using Atlas Scientific hardware. The probes and transmitters utilized in this setup are shown in Figure 4.11. For EC measurements, a standard K1.0 probe was used.

Data transmission was facilitated via a 4–20 mA current output of the transmitter boards. To interface with the Arduino Uno, this current passed through a 250 Ω shunt resistor to create a voltage drop between 1.0 V and 5.0 V. The Arduino Uno sampled this voltage through its 10-bit analog-to-digital converter (ADC). The conversion of the raw analog signal to the physical measurement is governed by the following linear relationship:

$$y = \left(\frac{V_{avg} \cdot 5.0}{1023} \cdot m \right) + b \tag{4.2}$$

Where V_{avg} represents the filtered ADC counts, m is the calibration slope, and b is the calculated offset.

For each channel, sampling was performed at 1 Hz. To mitigate electrical noise, each 1 Hz sample was obtained from a burst of 40 ADC readings. These readings were sorted to compute a trimmed mean from the average of the 10 median-centered values from indices 15 to 24.

Values were logged to an SD card once per 5-minute window. Each logged row represents the average of the 1 Hz filtered samples accumulated over that window. ADC values were mapped to pH and EC using implemented calibration relationships, specifically a two-point linear calibration for pH and a piecewise linear calibration for EC.

Nutrient solution and root-zone temperatures were measured using DS18B20 digital temperature sensors. Three sensors were used in the fogponics system: one submerged in the reservoir ($T_{\mathrm{res,fg}}$), one in the drain collector ($T_{\mathrm{drn,fg}}$) and one in the root-zone. Root-zone temperatures were monitored in both systems using sensors placed in the respective root chambers ($T_{\mathrm{rz,fg}}$ and $T_{\mathrm{rz,ae}}$).

Data storage was handled by the LAN-shield on the Arduino Uno. To ensure system stability, all data were timestamped using a DS3231 real-time clock (RTC) and written to daily CSV files. File rollover checks and header creation were performed at 60 s intervals. To prevent timing conflicts between the SD card power draw and sensitive sensor readings, a specialized flush protocol was implemented. CSV rows were written without immediate flushing; instead, flush operations were delayed and constrained to avoid execution within a 2.5 s safety gap of a temperature request.

Calibration from Transmitter to Arduino Procedure

The monitoring system underwent a multi-stage calibration process to maintain traceability across different nutrient formulations and sensor configurations. Because the firmware logic was updated to accommodate additional sensors and different sampling rates during the pivots between trials, providing every minor code iteration was deemed less reliable than documenting the hardware-level ground truth.

The calibration strategy focused on distinct verification layers including chemical-to-voltage mapping and voltage-to-digital integrity. Probes were calibrated using standard buffer solutions (pH 4.0 and 7.0) to establish the linear relationship between the chemical state and the transmitter analog output. To decouple sensor performance from software scaling, the raw voltage outputs from the transmitters to the Arduino ADC were monitored. These readings represent the hardware-level interface independent of the specific code versions used. Five reference datasets of these raw voltage outputs are provided in Appendix-B to ensure instrumental transparency.

Furthermore, the raw voltage output associated with the experimental results is documented in the same appendix to allow for post-hoc verification of the digital conversion. Documenting the raw electrical signals in this manner ensures that the results are not dependent on specific software scaling factors. This approach allows for independent verification of the sensor behavior and the identification of potential electronic noise or drift encountered during the trials.

4.3.4. Lighting uniformity (PAR measurements).

To document the local light environment at plant level and assess comparability between tray positions, PAR was measured at lid level at six edge locations on each tray. The measured values are reported in Table 4.3. The data indicate spatial variation across the tray edges and provide context for potential microclimate-driven differences between plant positions.

4.3.5. Nutrient solution and management

The first part of the experiments were done using the Priva solution from the EDEN cultivation Lab. Later experiments were performed using a Hoagland-type nutrient solution prepared from individual salt stocks and a micronutrient mix. RO water was used for all batches. The solution was mixed to a target electrical conductivity of 1.1 mS/cm and adjusted to a pH of 6.0 prior to operation.

(a) Atlas Scientific pH Transmitter.[58]

(b) Atlas Scientific pH Probe. [59]

(c) Atlas Scientific EC Transmitter.[60]

(d) Electrical Conductivity probe Atlas Scientific (K 1.0). [61]

Figure 4.11: Water quality sensing hardware used for pH and electrical conductivity measurements. The pH transmitter board and pH probe are shown in red, and the EC transmitter board and EC probe are shown in green (K = 1.0). The 4 to 20 mA output of each transmitter was converted to a voltage using a 250 Ω shunt resistor and read by the Arduino Uno for data logging.

Table 4.3: PAR measured at lid level at six edge locations (P1–P6) for both trays measured in μmol · m^{-2} · s^{-1}.

Point	Tray A		Tray B	
	Left	Right	Left	Right
P1	138	325	365	86
P2	181	448	430	167
P3	131	258	240	100

Two separate batches were prepared to avoid cross-use between systems: 20 L for the aeroponics baseline and 20 L for the fogponics trial. The fogponics reservoir capacity was limited to approximately 9–10 L; the remaining prepared solution was stored as stock. To reduce light exposure during storage, the stock container was covered to limit algae growth and photochemical changes.

During operation, nutrient chemistry was monitored at two locations (reservoir and drain) to distinguish bulk reservoir behavior from changes occurring along the delivery chain and root zone. The fogponics reservoir was replenished once using the stored stock solution after four days of operation. No pH adjustments were performed during the run.

4.3.6. Plant material and cultivation protocol

Lettuce (*Lactuca sativa*) was selected as test crop because it is widely used in controlled-environment cultivation and provides a well-characterized baseline for comparative trials. The experiments used leaf lettuce cultivar *Waldmann's Dark Green* (MTO OG) from Johnny's Selected Seeds (lot 65560, organic seed).

Seeds were germinated in rock wool cubes. The cube tops were covered with cheese wax to reduce microbial growth during cultivation. Prior to sowing, excess wax was removed using a needle and the seed hole was re-opened to ensure consistent placement depth. Cubes were soaked in water and placed in a germination tray with a shallow water layer. Seeds were placed into the cubes using tweezers; selected cubes were seeded with two seeds to ensure sufficient germination. The tray was covered with a transparent lid to maintain humidity. To limit light exposure and reduce undesired growth, the tray sides were covered with aluminium foil and a trash bag was wrapped around the tray for the first two days, after which the bag was removed. By then the plants had germinated and were exposed to the light. Figure 4.12 shows the sequence in development until transplanting into the experimental setup.

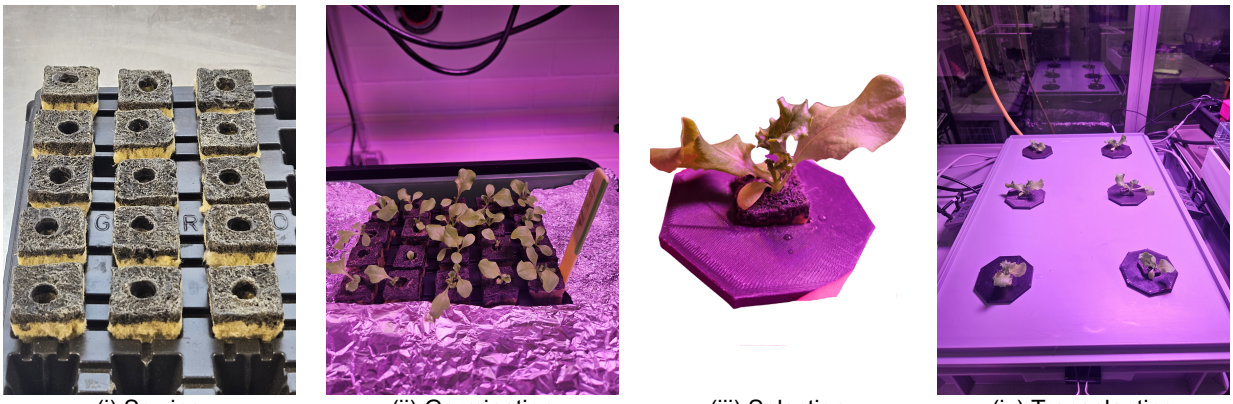

(i) Sowing (ii) Germination (iii) Selection (iv) Transplanting

Figure 4.12: Cultivation workflow stages for Lactuca sativa (cv. Waldmann's Dark Green): (i) Sowing: individual seeds placed in rockwool cubes treated with cheese wax to inhibit microbial growth; (ii) Germination: seedlings after the initial 2 day dark period, using aluminum foil and tray covers, and subsequent light exposure; (iii) Selection: identification of uniform, healthy individuals from the redundant batches to ensure consistent trial starting points; and (iv) Transplanting: final placement of six plants into the experimental tray.

To provide redundancy, a second batch of seedlings was prepared using the same procedure nine days after the first batch. On the same day, 100 mL of premixed Hoagland solution was added to the first batch.

Transplanting and cultivation. Seedlings were transplanted into the experimental trays on 24 November at a comparable early growth stage. Each tray contained six plants, matching the tray lid geometry and supporting comparability between the fogponics prototype and the aeroponics baseline.

The intended cultivation duration was one lettuce growth cycle (28 days). In practice, the planned full cycle was not completed due to experimental interruptions; the achieved cultivation duration and resulting plant response dataset are reported in the Results chapter.

4.3.7. Experimental campaign overview

The experimental campaign consists of two beaker tests and two prototype trials. The beaker tests isolate nutrient solution behavior without plants and without a delivery architecture. They serve two purposes: (i) a first validation of the data logging procedure, and (ii) a baseline for pH drift to support attribution of pH and EC trends to the fogponics delivery technology rather than to the nutrient solution alone. Beaker test 1 used Priva nutrient solution and monitored pH for 11 days using a single probe. Beaker test 2 repeated the same approach with Hoagland nutrient solution for 9 days.

Trial 1 used Priva solution and the first functional fogponics prototype with wick based nutrient supply (Design episode 3). The trial lasted 11 days and included plants. pH and EC were monitored in the reservoir, while root zone temperature was measured only during the last 5 days. Plant germination and transplanting followed the procedure described in Section 4.3.6.

Trial 2 used Hoagland solution and the final fogponics prototype with active nutrient supply (Design episode 4). In this trial, pH and EC were monitored continuously in both reservoir and drain. Temperature was monitored continuously in reservoir, drain, and root zone. An aeroponics baseline was

operated in parallel for plant development comparison. For the aeroponics baseline, pH and EC were recorded as point measurements before and after the trial.

Table 4.4: Overview of experiments, measurements, and prototype configuration.

	Beaker test 1	Beaker test 2	Trial 1 fogponics	Trial 2 fogponics	Trial 2 aeroponics
Nutrient solution	Priva	Hoagland	Priva	Hoagland	Hoagland
Duration	11 days	9 days	11 days	`15 days`	`15 days`
pH measurement location	Beaker, single probe	Beaker, single probe	Reservoir	Reservoir and drain	Reservoir, before and after only
EC measurement location	Not measured	Not measured	Reservoir	Reservoir and drain	Reservoir, before and after only
Temperature measurement location	Not measured	Not measured	Root zone, last 5 days only	Reservoir, drain, root zone	Reservoir
Prototype used	Beaker setup	Beaker setup	Episode 3, wick fed	Episode 4, active supply	Aeroponics baseline setup

4.3.8. Verification plan

Verification is conducted to ensure that the experimental prototype functions as a reliable research instrument for this thesis. The focus is not on qualifying a flight-like nutrient delivery system, but on demonstrating that the recorded datasets are traceable to defined measurement locations and are suitable for time-series interpretation and comparison between the fogponics and aeroponics architectures. Verification therefore addresses three aspects: (i) measurement meaning, by confirming calibration and separation of reservoir and drain sampling; (ii) data integrity, by confirming correct time-stamping and continuous logging over representative runs; and (iii) performance quantification, by confirming that the gravimetric flow-rate method is repeatable and sensitive enough to resolve delivery degradation associated with observed failure modes.

Verification items and evidence

1. **Nutrient chemistry measurement validity** pH and EC sensors are calibrated using the manufacturer's procedure prior to experiments. To bound measurement drift for trend interpretation, a spot-check is performed by re-measuring a calibration buffer/standard after a representative run (or at the end of the day). The deviation between the expected and measured value is recorded and reported as an uncertainty bound for interpreting the time series.
2. **Reservoir–drain separation** The separation between reservoir and drain measurements is verified through an EC step event during logging (e.g., during a refill/top-up or a controlled increase in reservoir EC). The reservoir signal is expected to change immediately, whereas the drain signal is expected to respond later and/or with a different magnitude due to transport through the delivery chain and interaction at the root zone. A short time-series excerpt is retained as evidence that the two sampling locations provide distinct information.
3. **Temperature measurement consistency** To establish that temperature readings can be compared across locations and over time, the temperature sensors are cross-checked by briefly co-locating sensors in the same water volume and recording the maximum observed offset. This defines a sensor-to-sensor consistency bound. Sensors are then returned to their fixed experimental locations (fogponics reservoir, fogponics drain, fogponics root zone, and aeroponics root zone) for the experiments.
4. **Channel-to-location traceability.** Sensor locations and identities are documented in an annotated photo or schematic of the final configuration. A simple stimulus check is performed during setup (e.g., temporarily moving one temperature sensor or briefly lifting a probe) to confirm that only the intended channel responds. This provides traceability between logged columns and physical locations.

5. **Logging integrity and timestamp validity.** Data logging is verified by reviewing a representative run (or the longest continuous run achieved) for timestamp correctness and continuity. The expected logging interval is compared with the recorded timestamps to confirm consistent spacing. Missing or corrupted rows are counted and reported as a fraction of the expected record count. This ensures the dataset can be interpreted as a continuous time series.
6. **Flow-rate measurement repeatability** The gravimetric flow-rate method is verified by repeating measurements three times for each atomizer in the "new" condition. The mean and scatter (standard deviation or coefficient of variation) are recorded. This establishes repeatability of the measurement procedure and defines the minimum resolvable change in delivered mass flow.
7. **Flow-rate sensitivity to degradation and failure modes.** To confirm that the flow-rate method captures performance decay relevant to the thesis, flow-rate measurements are repeated after observable degradation events. For the 25 µm modules, this is after rupture behavior is observed; for the 2.9 µm modules, after salt precipitation is observed. The magnitude of change relative to baseline is compared against the repeatability scatter. Microscopy images are used as supporting evidence to link performance changes to the observed degradation mechanism.

Verification outputs

The outputs of this verification plan are: (i) calibration and spot-check records for nutrient chemistry sensors, (ii) a short reservoir–drain response excerpt demonstrating measurement separation, (iii) an offset bound for temperature sensors, (iv) documented sensor placement for traceability, (v) a logging integrity summary for representative runs, and (vi) baseline and post-degradation flow-rate datasets with repeatability bounds. Together, these elements justify interpreting the recorded time series and degradation trends in the Results chapter.

4.4. Summary and Analysis Approach

This chapter defined the experimental systems, measurement chain, and prototype implementation used to generate the datasets analysed in the remainder of this thesis. The aeroponics baseline and VMA fogponics prototype were operated in the EDEN laboratory under matched growth conditions, using identical tray geometry and plant handling procedures.

The resulting data products consist of (i) time-stamped EC and pH measurements at reservoir and drain locations, (ii) nutrient solution temperature measurements at reservoir and drain locations, (iii) atomizer flow-rate measurements (g/min) collected at baseline (new) and repeated after observed degradation events, and (iv) qualitative failure evidence supported by microscopy and electrical measurements under operational conditions. These datasets form the basis for trend-level comparison between nutrient delivery architectures and for documenting degradation and failure mechanisms.

All results are interpreted within the scope and boundaries of an experimental prototype: the comparative trial is intended to provide controlled evidence on system behavior and degradation trends rather than statistically powered biological outcomes. The as-tested configuration and all deviations introduced by component failures (e.g. atomizer type substitution) are reported explicitly and considered in the interpretation of the Results.

Mapping Design to Research Questions

The architecture of the apparatus is a direct physical translation of the research questions. Each component and sensor placement is a deliberate design move intended to provide empirical answers to the following inquiries:

- **Methodological Mapping (MRQ):** The creation of the rig itself, which utilizes standardized tray dimensions and documented assembly protocols, serves as the initial answer to the development of a standardized framework.
- **Mechanical Mapping (RQ1):** The mounting system enables a comparison of 2.9 μm and 25 μm apertures, allowing for the direct measurement of sedimentation and mechanical reliability.
- **Chemical Mapping (RQ2):** The separation of the nutrient reservoir and the drain collection beaker is designed to capture the chemical drift allegedly caused by the atomization process.

- **Thermal Mapping (RQ3):** The placement of temperature probes within the root zone and the nutrient fluid allows for measuring the effect of the technology on the temperature.
- **Biological Mapping (RQ4):** The inclusion of a standardized growth lid allows the plants to act as biological sensors, which test the lethal boundaries of the environment generated by the hardware.

The following chapter presents the primary takeaways derived from the iterative design process. It details the positive and negative heuristics that define the practical envelope and operational requirements of the system. In addition to these qualitative lessons, the chapter documents the experimental timeline and the specific results used to validate the physical performance of the prototype. These findings establish the empirical evidence base required to characterize the nutrient delivery concept and identify its functional limitations.

5

Results

This chapter reports the outcomes of the research through design evaluation of the fogponics nutrient delivery concept and its prototype implementations as well as the results of the validation experiments. The transition from the implementation of the *design thing* to its experimental operation revealed critical boundary conditions in the nutrient delivery hardware. In accordance with the Lab Venue strategy, these observations are treated as rigorous experimental evidence that defines the limitations of current ultrasonic atomization technology for lunar life support systems.

The chapter first summarizes the design heuristics that emerged while developing the assessment approach. The positive heuristic captures practices that improved interpretability and robustness, while the negative heuristic documents pitfalls that repeatedly led to ambiguous outcomes. The executed experiments and available datasets are then documented using overview tables to make clear which planned measurements were achieved, which were partial, and which are out of scope due to missing or non comparable datasets. Next, environmental logging of the cultivation room is reported to contextualize system behavior during the trials. The core results then quantify the impact of dominant failure modes on delivery performance using paired gravimetric flow rate measurements, and report nutrient chemistry stability using EC and pH trends from both static beaker tests and prototype runs. The chapter closes by documenting limitations in data retrieval and completeness, which bound the interpretation and motivate the discussion and recommendations in Chapter 6.

5.1. Heuristics for fogponics research infrastructure

In alignment with the Research through Design (RtD) framework, the results in this section document the construction process in which the prototype functions as a research instrument. The following heuristics synthesize the design moves and the observed resistances encountered during the development and operation of the fogponics system. They are formulated as transferable engineering lessons that define the practical envelope for applying VMAs in controlled agriculture research.

5.1.1. Module orientation and plume management

One of the outcomes across iterations was that module orientation strongly influences operational stability. Upward facing configurations promoted local liquid retention near the mesh and surrounding surfaces. This coincided with mineral deposition and deterioration of atomization, which reduced output and increased the likelihood of module failure. As a negative heuristic, any configuration that allows for the retention of liquid on these surfaces must be designed against to prevent mineral-induced degradation.

Downwards angled mounting helped to prevent settlement of non atomized liquids from the vibrating element, which reduced local salt accumulation. In the context of research infrastructure, orientation should therefore be treated as a first order design variable, because it directly affects consistency and runtime.

5.1.2. Physical system architecture

The negative heuristic identified across prototype revisions was that passive wicking cannot guarantee a stable nutrient supply. Relying on capillary action often failed to keep the mesh interface wet, leading to ”dry running” where the atomizer operates without enough liquid. This made the fog output inconsistent and put unnecessary mechanical strain on the hardware, eventually leading to system failure.

In response, the positive heuristic for system architecture is the implementation of an active liquid supply tuned to the specific atomization rate. Furthermore, physically separating the nutrient reservoir from the root zone tray significantly improves researchability. This separated architecture allows for distinct drain-path measurements and reduces thermal coupling between the VMA hardware and the bulk solution, ensuring that observed changes in chemistry are attributable to specific delivery mechanisms rather than system-wide temperature bias.

5.1.3. Parameters that determine researchability

A negative heuristic is to define the atomization process solely by operating frequency or the generic label of ”fogponics,” as is often seen in existing literature. While droplet size is a critical performance parameter, it is frequently ignored when direct measurement methods are unavailable. Assuming that modules with different aperture sizes produce equivalent fog leads to significant errors in interpretation, as larger droplets exhibit different physical behavior and settlement patterns. Relying on hardware specifications without accounting for these differences prevents a clear understanding of how the nutrient plume interacts with the root zone.

The positive heuristic is to explicitly define the aperture size of the modules and design the infrastructure to monitor their specific effects. In this research, the 25 μm and 2.9 μm modules were positioned so that their distinct spray characteristics could be utilized effectively. The infrastructure was designed to be interchangeable, allowing hardware variants to be compared under identical conditions. Additionally, the system must support continuous monitoring of EC, pH, and temperature at the exact locations where delivery occurs. Prioritizing this level of accessibility ensures that the prototype functions as a transparent instrument for gathering evidence rather than a static growth container.

5.1.4. Redundancy and reliability for long duration trials

The negative heuristic is the reliance on single points of failure within the delivery and logging systems. Depending on a single pump, a single supply path, or a single data logging chain creates a high risk that a local event, such as a blockage, leakage, or sensor failure, will terminate the trial prematurely. Such failures do not just end the experiment; they remove the ability to interpret the results by creating gaps in observability. Furthermore, allowing the reservoir volume to decrease without a controlled refill mechanism introduces a negative heuristic where increasing nutrient concentration biases EC values and increases the likelihood of pump malfunction.

The positive heuristic is to treat redundancy as a core requirement for any research prototype intended for extended operation. This involves implementing parallel delivery paths and independent sensing or logging routes to ensure that at least partial datasets remain available if one component fails. While redundancy does not eliminate failure modes, it preserves the ability to localize the failure while retaining interpretable evidence. Additionally, automated or controlled refill should be utilized as an experimental control measure. This maintains liquid level stability, reduces disturbances caused by manual maintenance, and ensures comparability of nutrient chemistry across the duration of the trial.

5.1.5. Data infrastructure and robustness

The negative heuristic is the implementation of a data architecture where critical subsystems are interdependent, such as sharing communication protocols or storage interfaces without sufficient isolation. In this research, a significant constraint was identified when using a microcontroller with limited resources, such as the Arduino Uno, to process high-frequency sampling and averaging for a high number of sensors. This workload, combined with the lack of hardware isolation on the SPI bus, created conflicts that compromised the data logging process. Furthermore, leaving the system to operate autonomously for the full duration of a trial without intervention proved to be a failure in the research strategy, as it allowed undetected errors to persist until the endpoint.

The positive heuristic is to utilize a more capable microcontroller and more efficient protocols for data sampling and storage. This includes designing for strict isolation between communication lines to prevent hardware-level interference. In addition to these technical measures, the experimental protocol must include rigorous pre-trial testing and scheduled intermediate checkups. These checkups function as an essential control measure, ensuring that any sensor drift or logging failures are identified and corrected early. Prioritizing both hardware robustness and active monitoring ensures that the prototype remains a reliable tool for data retrieval throughout the mission duration.

5.1.6. Summary on heuristics

Overall, these heuristics summarize the practical conditions that must be met for a VMA-based fogponics platform to remain both operational and researchable. By categorizing these findings into negative pitfalls and positive design moves, the prototype serves as a tool for engineering knowledge. These lessons are used later in this thesis to interpret the observed failure modes and to motivate the design requirements for follow-up prototypes.

5.2. Overview of results and executed tests

This section summarizes which experiments were executed and which datasets are available. As noted in the chapter introduction, the final comparative cultivation trial did not yield a comparable plant-response dataset; therefore, this chapter focuses on the system-level measurements that were successfully obtained, complemented by qualitative growth-trial observations and endpoint spot measurements.

Operating environment logging (air temperature, RH, and light state)

Environmental conditions (air temperature, relative humidity, and light on/off state) were logged during the relevant periods for both systems and are used to document consistency of operating conditions and to contextualize observed system behavior. Summary statistics and time-series plots are provided in Section 4.1.1.

VMA delivery performance and degradation (flow-rate tests)

Two VMA module variants were evaluated, distinguished by nominal mesh/aperture size (25 μm and 2.9 μm). Aperture size is treated as a hardware specification; droplet size distributions were not measured and are therefore not inferred from the aperture size. Gravimetric flow-rate measurements (g/min) were performed for both module variants in their fresh state to quantify initial delivery performance. In addition, post-failure flow-rate measurements were performed for the 25 μm modules following rupture and for the 2.9 μm modules following salt precipitation. Where repeated flow-rate measurements are available, this chapter reports the associated decrease in delivered mass flow through direct comparison between fresh and post-failure conditions; these results should be interpreted before–after failure comparison, not a lifetime curve.

Nutrient chemistry monitoring (EC/pH)

For fogponics, EC and pH were recorded as a reservoir-only time series over a 10-day pre-trial period using an earlier prototype configuration and a Priva nutrient solution (not Hoagland). These data provide time-resolved evidence of bulk-reservoir chemistry evolution under fogponics operation, but are not directly comparable to the later cultivation trial due to differences in hardware configuration and nutrient formulation. Drain-path measurements were not recorded during this time series, so reservoir–drain attribution of chemistry drift is not possible from the continuous dataset. For the pilot cultivation trial, reservoir–drain separation is available only as start/end spot measurements in the fogponics reservoir and drain using the final prototype and a Hoagland-type solution. For the aeroponics baseline, EC and pH measurements are available at two time points separated by approximately two weeks, providing a trend-level indication of baseline reservoir chemistry evolution rather than a continuous time series.

Thermal observations (root-zone temperature)

Root-zone temperature data are available only for the final five days of operation of the preliminary test with the earlier prototype configuration and are therefore reported as limited thermal observations rather than a complete thermal characterization.

Summarized Table of obtained data

The table below summarizes the available data streams from the experiments with the correlated dates and brief descriptions.

Table 5.1: Data availability matrix categorized by experimental phase and measurement stream. All measurements refer to Fogponics (VMA) unless specified as Aeroponics baseline.

Experimental Phase	Data Streams and Availability
Continuous Environmental Monitoring (05 Sep – 06 Jan)	• **Parameters:** Full-duration time-series of Air Temperature (T_{air}), Relative Humidity (RH), and Light state (binary on/off). • **Scope:** Background monitoring providing environmental context for all phases, identifying anomalies and verifying operating envelope consistency.
Standalone Hardware Characterization	• **Delivery Performance:** Gravimetric mass flow (g/min) for 2.9 μm and 25 μm variants. • **Degradation Analysis:** Comparison of fresh versus post-failure (rupture/salt) flow rates. • **Physical Specs:** Aperture size reported from specifications; droplet size distribution was not measured.
Phase 1: Beaker Test (05 Sep – 16 Sep)	• **Chemistry:** Continuous time-series of pH and EC (Priva solution, reservoir-only). • **Environment:** Continuous air temperature, RH, and light logging to contextualize stability.
Phase 2: Beaker Test (15 Nov – 24 Nov)	• **Chemistry:** continuous time-series of pH for Hoagland-type solution baseline. • **Environment:** Continuous air temperature, RH, and light logging.
Phase 3: First Trial (Priva solution) (24 Nov – 05 Dec)	• **Chemistry:** 10-day continuous time-series (reservoir-only); no drain path data available. • **Thermal:** Root-zone temperature (T_{rz}) monitored for the final four days only. • **Reliability:** Qualitative evidence of sensor fouling and VMA state through event logs.
Phase 4: Second Trial (Hoagland solution) (20 Dec – 06 Jan)	• **Fogponics (VMA):** Spot measurements for reservoir and drain chemistry; no time-series due to SD-card corruption. • **Aeroponics Baseline:** Comparative trend-level EC/pH (two-point comparison over trial duration). • **Biological:** Qualitative observations and photographic series only; no harvest mass metrics recorded.

5.3. Experimental Timeline

The following section documents the timeline of the performed experiments and the chronological structure of the research campaign. Environmental parameters such as air temperature and humidity were monitored throughout the entire experimental phase to maintain a consistent boundary condition dataset. The sequence of prototype design episodes progressed consecutively from episode 1 through episode 4. The first system trial using the Priva solution marked the conclusion and validation of design episode 3, while the second trial using the Hoagland solution served as the final validation for design episode 4. In parallel with these prototype iterations, standalone beaker tests were conducted to evaluate nutrient chemistry stability. These tests appear far apart in the chronology because the Hoagland solution required specific formulation and preparation before the second validation phase could begin. The full duration and overlap of these activities are visualized in the Gantt chart in Figure 5.1.

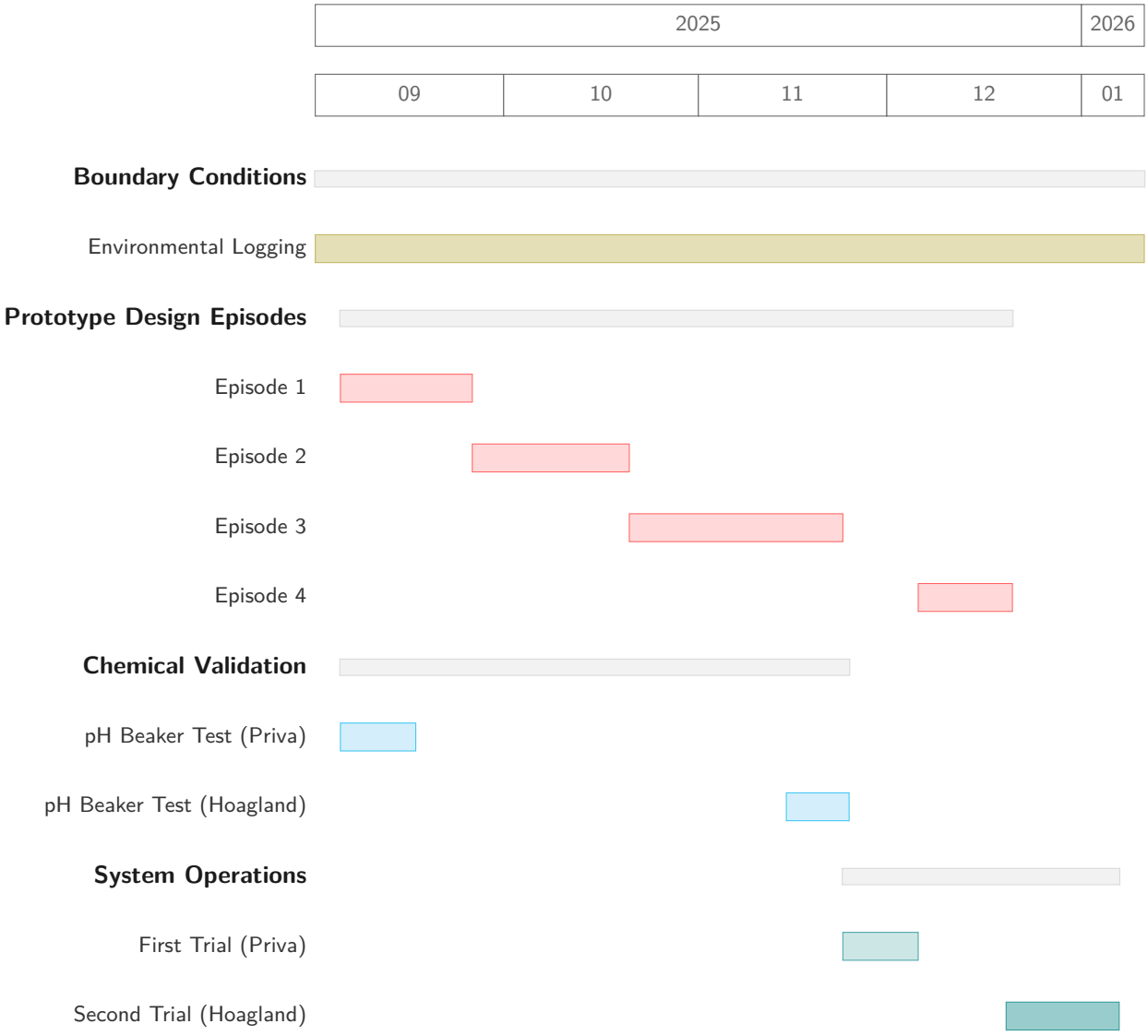

Figure 5.1: Experimental timeline showing the sequence of prototype design episodes and validation activities. The chart relates the four prototype episodes to the chemical beaker tests conducted in parallel and to the two system trials. The first cultivation trial was performed after Episode 3 using the wick based prototype, after which further iteration in Episode 4 led to the second trial. Environmental conditions were logged continuously throughout the full research period as a boundary condition dataset for interpreting the experiments.

5.4. Operating environment logging (air temperature, RH, and light state)

Air temperature, relative humidity (RH), and light state were logged during the relevant periods for both systems. The EDEN cultivation room is equipped with sensors to monitor environmental parameters. The data was retrieved from the database and processed. These records were then used to assess whether operating conditions were broadly consistent and to identify potential anomalies that may contextualize observed behavior in delivery performance and nutrient chemistry. Light is reported as the recorded on/off state (or equivalent binary/logged representation). Because the cultivation room temperature of these periods is shown together with the results of the correlated experiments, the temperature and humidity measurements as discussed are also shown separately in the Appendix without pH measurements.

Four environmental time-series plots are provided in Appendix C, corresponding to the four experimental periods: (i) *beaker test (Priva solution)* (05 Sep–16 Sep), (ii) *beaker test (Hoagland solution)* (15 Nov–24 Nov), (iii) *preliminary trial (Priva solution)* (24 Nov–06 Dec), and (iv) *pilot trial (Hoagland solution)* (20 Dec–05 Jan).

5.5. Delivery performance degradation associated with observed failure modes

This section reports how atomizer delivery performance changes when the two dominant failure modes observed in this work occur. Delivery performance is quantified as gravimetric mass flow rate (g/min), using the measurement protocol as defined in Section 4.3.2 (25 μm: 1 min; 2.9 μm: 5 min). Results are presented as within-case consequences: (i) rupture in the 25 μm module variant and (ii) salt precipitation in the 2.9 μm module variant. Because the absolute delivery rates differ by orders of magnitude between these module variants, flow-rate results are shown on separate scales per failure mode; cross-case comparison is limited to normalized metrics (retention) where appropriate. The effect of the wick based prototype on the flow rate was tested as well and is discussed below in Section 5.5.1.

5.5.1. Iteration change from Wick to direct supply

With two foggers installed in the prototype and wick-assisted feeding, the combined fog production rate ($PD_6 + PD_7$) was measured under identical conditions in three repeat trials. The resulting mass flow rates were 7.501, 7.920, and 6.468 g/min, corresponding to a mean total output of 7.296 g/min. The measurements indicate that the dual-fogger configuration consistently produced on the order of 7.3 g/min total fog output, with trial-to-trial variation of 1.452 g/min between the minimum and maximum values (6.468–7.920 g/min). Notably, two trials clustered around 7.5–7.9 g/min, while one lower value reduced the overall mean, suggesting moderate repeatability under nominally identical conditions. These results supported the move from a wick based prototype to a controlled direct supply of nutrient solution to the atomization modules.

5.5.2. Rupture case: 25 μm modules

This subsection quantifies the delivery performance before and after rupture events observed in the 25 μm VMA modules. Fresh performance was measured for five units (PD_1–PD_5). For PD_1–PD_4, three repeated 1-minute measurements were performed and averaged per unit. For PD_5, only one fresh measurement was available (22.7 g/min); after this measurement a wire broke loose and the unit stopped working. This was later resolved by soldering the cable back to the module. Post-rupture performance was quantified for four units (PD_2–PD_5) using three repeated 1-minute measurements per unit.

Fresh performance (baseline). Across PD_1–PD_4, fresh flow rates ranged from 22.1 to 28.0 g/min, with a mean of 25.5 g/min (unit-to-unit standard deviation 2.94 g/min). PD_5 showed a fresh flow rate of 22.7 g/min based on a single measurement. Of the first four measurements the standard deviation was 3.51 g/min. These values show the high-flow operating regime of the 25 μm modules prior to failure.

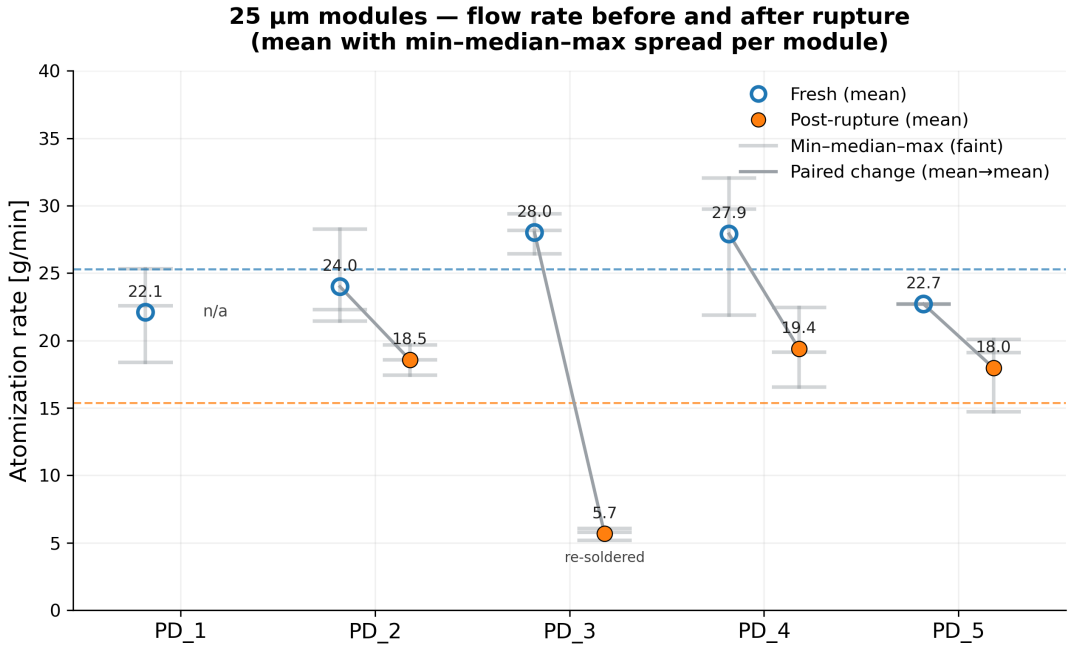

Figure 5.2: Paired gravimetric flow rate of five 25 μm VMA modules (PD_1 to PD_5) measured in fresh condition and after mesh rupture. Markers show the mean per module, faint bars show the min median max spread of repeated measurements, and connecting lines show the paired change. Fresh flow rates are 22.1 to 28.0 g/min (PD_1 to PD_4), with PD_5 at 22.7 g/min from a single measurement. After rupture, PD_2, PD_4, and PD_5 retain reduced but measurable output (18.55, 19.38, and 17.96 g/min), corresponding to about 70 to 80% retention. PD_3 is shown but its post rupture value follows re soldering and is not interpreted.

Post-rupture performance. After rupture, PD_2, PD_4, and PD_5 continued to produce measurable output, but at reduced flow rates: 18.55 g/min (PD_2), 19.38 g/min (PD_4), and 17.96 g/min (PD_5), based on three repeated measurements each. PD_3 was re-measured after the electrical connections were re-soldered and showed a substantially lower flow rate of 5.67 g/min. Because this post-rupture value was obtained after rework, PD_3 is shown for completeness but is not used for interpreting rupture-driven performance loss in this study. The average standard deviation of all measurements was 1.85 g/min.

Paired reduction and retention. For units with both fresh and post-rupture data and without rework (PD_2, PD_4, PD_5), the paired change in flow rate corresponds to a retention of 77.3% (PD_2: 23.99 $\rightarrow$ 18.55 g/min), 69.5% (PD_4: 27.90 $\rightarrow$ 19.38 g/min), and 79.1% (PD_5: 22.7 $\rightarrow$ 17.96 g/min), resulting in a mean of 18.63 g/min. PD_3 is reported with a retention of 20.3% (28.01 $\rightarrow$ 5.67 g/min), but this value is not considered representative of rupture-driven degradation because the module was re-soldered in a way that was not considerded properly, prior to the post-rupture measurement. Table 5.2 summarizes the unit averages and retention values. Figure 5.2 presents the flowrate measurements before and post-rupture.

Table 5.2: Summary of 25 μm module flow rates before and after rupture.

Fogger ID	Fresh (g/min)	Post-rupture (g/min)	Retention (%)
PD_1	22.09	–	–
PD_2	23.99	18.55	77.3
PD_3	28.01	5.67†	20.3†
PD_4	27.90	19.38	69.5
PD_5	22.70‡	17.96	79.1

†Post-rupture value obtained after re-soldering; shown for completeness but excluded from rupture interpretation.

‡Single fresh measurement; unit stopped working after a wire broke loose.

5.5.3. Salt precipitation case: 2.9 μm modules

This subsection quantifies delivery performance before and after salt precipitation observed in the 2.9 μm VMA modules. Fresh performance was measured for four units (F-A1–F-A4) using three repeated 5-minute measurements per unit. Post-precipitation performance was quantified using the same measurement procedure after visible salt deposition was observed together with loss of output.

Fresh performance (baseline). Fresh flow rates for the 2.9 μm modules were in the low-flow regime. Unit-average flow rates ranged from approximately 0.36 to 0.61 g/min with an average baseline of 0.45 g/min, based on three repeated measurements per unit. These values establish the baseline delivery level of the 2.9 μm modules prior to precipitation. Over the measurements of all 4 atomizers a standard deviation of 0.023 g/min was calculated.

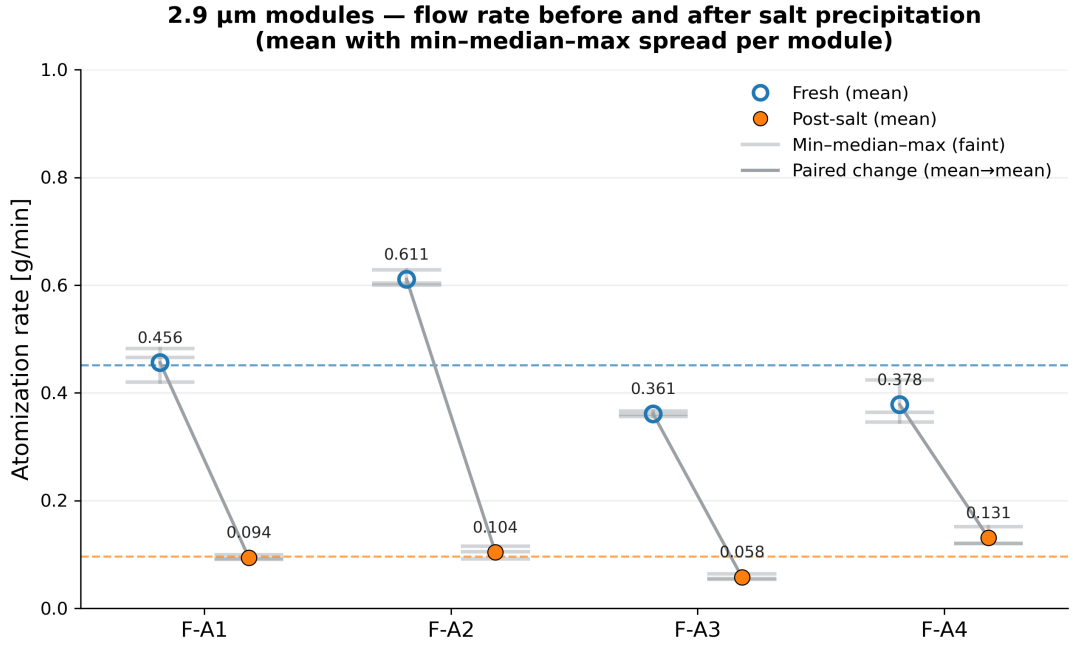

Figure 5.3: Paired gravimetric flow rate of four 2.9 μm VMA modules (F-A1 to F-A4) measured in fresh condition and after salt precipitation. Markers show the mean per module, faint bars show the min median max spread of repeated measurements, and connecting lines show the paired change. Fresh flow rates are in the low flow regime (0.36 to 0.61 g/min; mean 0.45 g/min). After visible salt deposition, flow rates drop to 0.058 to 0.131 g/min (mean 0.097 g/min), corresponding to about 16 to 35% retention. Post precipitation measurements were taken after storage in an uncleaned state and therefore represent performance after drying and crystallization rather than immediate in situ behavior.

Post-precipitation performance. After salt precipitation, the measured flow rates decreased to 0.058–0.131 g/min (unit-average range across F-A1–F-A4), with an overall mean of 0.097 g/min. This corresponds to a strong reduction in delivery performance under the recorded precipitation condition. Post-precipitation measurements were performed in a stored post-trial state (modules removed from the system and stored uncleaned for an extended period), and therefore represent performance after drying/crystallization rather than immediate in-situ behavior at the time precipitation was first observed. Of all four atomizers measured a standard deviation of 0.01 g/min was calculated.

Paired reduction and retention. For each unit (F-A1–F-A4), the paired before–after change corresponds to a retention of 16.1% to 34.7% relative to the fresh condition. Table 5.3 summarizes the unit averages and retention values. Figure 5.3 presents the paired before-after flow rates per unit; Figure 5.3 visualizes the corresponding retention.

5.5.4. Failure evidence and microscopy imagery

This section provides visual evidence supporting the failure-mode labels used in Section 5.5 and documents qualitative differences in atomization appearance between the two VMA module variants. Mi-

Table 5.3: Summary of 2.9 μm module flow rates before and after salt precipitation. Fresh values are unit averages based on three 5-minute trials for F-A1–F-A4 with a fresh mean of 0.45 g/min. Post-precipitation values are unit averages based on three 5-minute trials per unit (measured in a stored post-trial, uncleaned condition) with an average of 0.097 g/min. Retention after salt precipitation is shown in last column, resulting in an average retention of 22.1%.

Fogger ID	Fresh (g/min)	Post-precip (g/min)	Retention (%)
F-A1	0.456	0.094	20.6
F-A2	0.611	0.104	17.0
F-A3	0.361	0.058	16.1
F-A4	0.378	0.131	34.7

croscopy imagery is used to confirm the presence and morphology of rupture features and salt deposition.

Microscopy evidence of failure modes

Microscope imagery was recorded for both identified failure modes at multiple magnifications to characterize the material degradation of the VMA components. These images serve as observational confirmation of the mechanical and chemical resistances that led to the flow-rate degradation discussed in the preceding sections.

Structural fatigue and mesh rupture. For the 25 μm module variant, the primary failure mode was identified as structural fatigue. This manifested as visible cracks and ruptures within the stainless steel mesh structure, as shown in Figure 5.4. At 10$\times$ magnification, these fractures are clearly defined, particularly in modules PD4 and PD5. These structural breaks resulted in a significant reduction in flow rate.

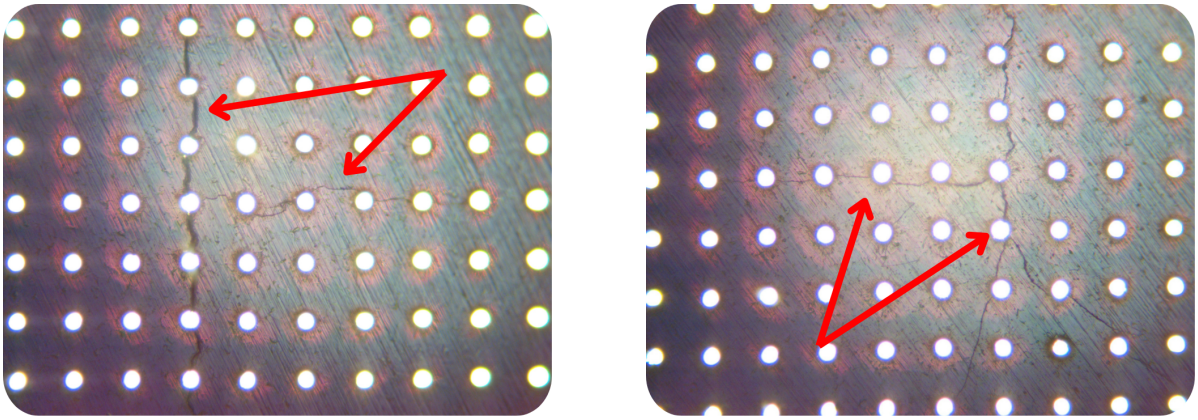

(a) Visible crack in Module PD4 (10$\times$).

(b) Visible cracks in Module PD5 (10$\times$).

Figure 5.4: Microscopic inspection of 25 μm VMA mesh integrity at 10× magnification, showing crack formation and propagation in modules PD4 and PD5. The observed rupture pattern is consistent with reduced structural margin due to the large aperture size and may have been exacerbated by dry running conditions during operation.

Salt deposition on the mesh In contrast, the 2.9 μm module variant exhibited a failure mode dominated by chemical interference rather than structural fracture. Figure 5.5 on the next page illustrates the extent of salt precipitation on the mesh surfaces following the preliminary test run. The accumulation of mineral deposits effectively blinded the microscopic pores, increasing the mechanical load on the piezoelectric element and eventually ceasing atomization. The comparison between the macro-scale observation and the 4$\times$ magnification reveals a pervasive crust that formed across the active vibrating area of the module.

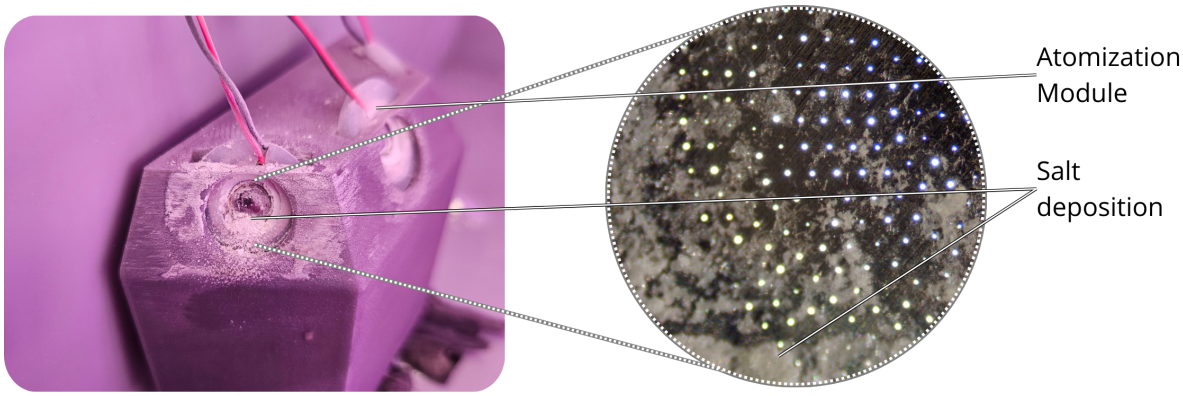

Figure 5.5: Inspection of VMA mesh condition showing mineral blinding caused by salt precipitation. The composite image shows a macroscopic view of the atomization module on the left and the corresponding mineral deposits at 4$\times$ magnification on the right. The deposits are consistent with back deposition of fog onto the mesh and surrounding surfaces, followed by evaporation and crystallization that progressively blocks the apertures and reduces output.

5.5.5. Observations of Plume Morphology and Momentum

Before the quantification of mass flow rates, the 25 μm and 2.9 μm VMA modules were evaluated for their qualitative delivery characteristics. Images are shown in Figure 4.4. The intent of these observations was to determine the compatibility of the generated plumes with the internal geometry of the growth tray and the proposed guide-tube architecture. This stage of the research represents a critical point where the behavior of the hardware necessitated a shift in direction from earlier designs.

5.6. System Stability: Nutrient Chemistry and Thermal Trends

The stability of the nutrient solution serves as a critical indicator of the technology-material interface. This section presents the observations from the static baseline tests, the preliminary trials, and the final comparative run. These results highlight the divergence between theoretical expectations and the operational behavior of the Vibrating Mesh Atomizer.

5.6.1. Static pH beaker test 1 (Priva solution: 5 - 15 September)

Before the introduction of ultrasonic excitation, a nutrient solution baseline was established to isolate the inherent chemical drift of the medium. A pH-only dataset was logged from 5 September to 15 September using approximately 800 mL of Priva nutrient solution in an open beaker, shaded from the light, and maintained without mixing or stirring. The pH probe remained immersed and measurements were recorded continuously. A separate environmental logger recorded laboratory conditions; short-term pH spikes are visible in the time series and will be discussed in relation to laboratory temperature variations in Chapter 6.

Overall, the beaker test demonstrates a clear upward drift in pH over the ten-day measurement period, rising from approximately 4.9 at the start to approximately 5.9 at the end, superimposed with distinct daily spikes.

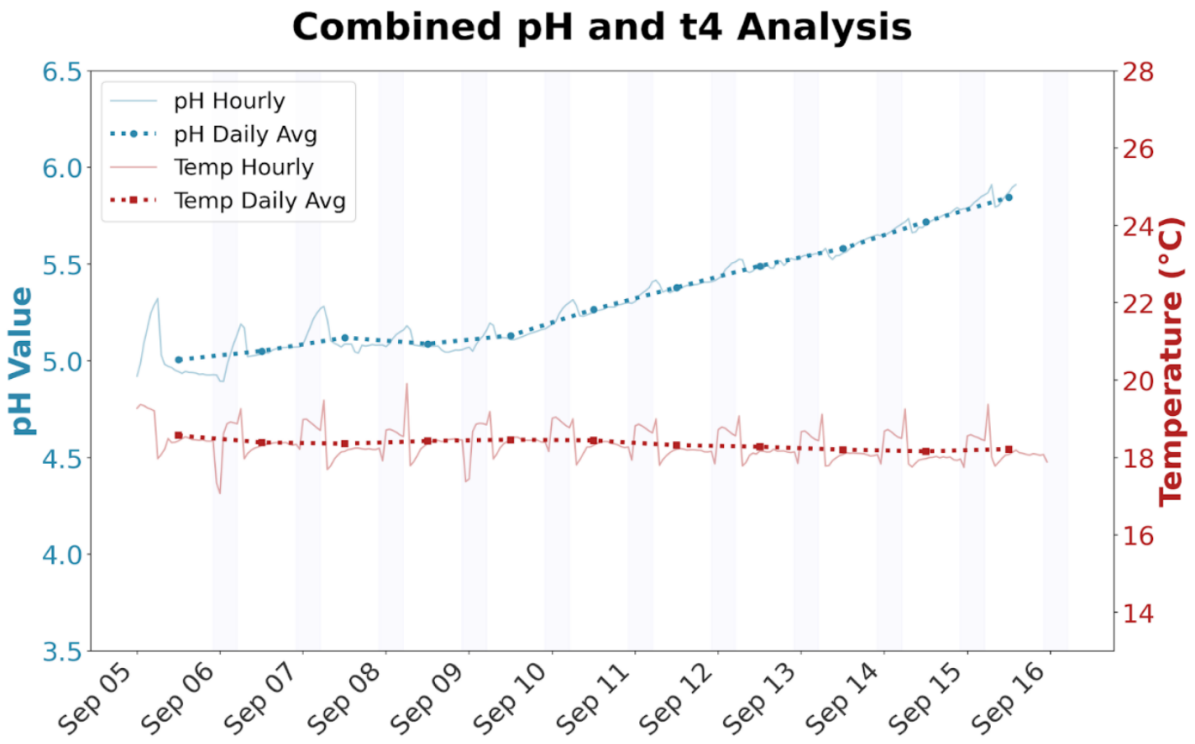

Figure 5.6: pH time series during static beaker test 1 using 800 mL of Priva nutrient solution (5 to 15 September). The beaker was open and not mixed; pH was logged continuously. Short term spikes are visible and are discussed in relation to laboratory conditions in Chapter 6. Temperature T4 refers to the temperature sensor in the cultivation room.

5.6.2. Static pH beaker test 2 (Hoagland Solution; November 15-24)

During the Hoagland static beaker test (15–24 November), the pH development initially indicated a stable chemical environment, as supported by Figure 5.8. This baseline was characterized by minor, short-term peaks. However, after five days of operation, the system recorded a sudden and unrealistic upward drift in pH that did not correspond to any known chemical reaction within the bulk solution.

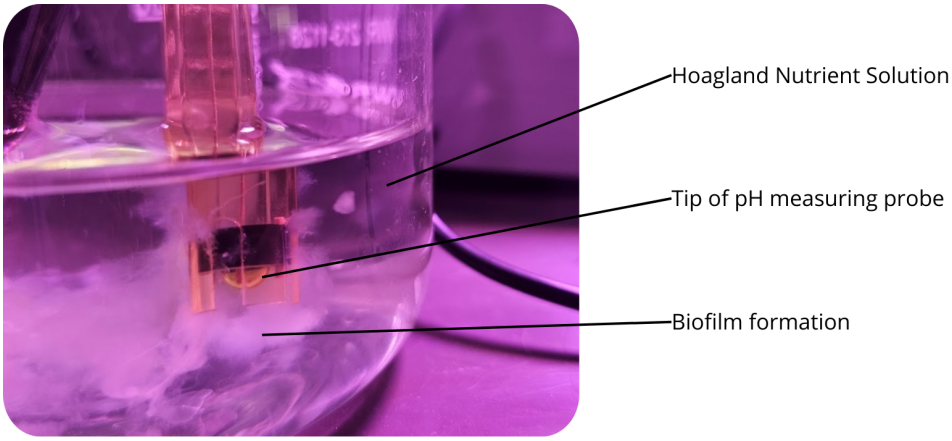

Figure 5.7: Biofilm formation shown in the nutrient solution and on the pH probe during a beaker test with Hoagland solution

This shift provides evidence for ”sensor blindness” rather than actual chemical instability. As illustrated in Figure 5.7, a thick and gelatinous biofilm formed on the active surfaces of the pH probe, creating a physical barrier between the sensing glass and the nutrient solution. This layer isolated the sensor, leading to the corrupted readings documented in Section 5.6.3 and masking the true chemical state of the reservoir.

The proliferation of this biofilm is attributed to light leakage where the pH sensor enters the reservoir.

In an aerospace bio-regenerative life support system, this incidental light provides the energy for photosynthetic growth, which directly threatens the interpretation of chemical stability. These results demonstrate that the measurement chain itself can become a failure mode within the first week of operation if light containment is not absolute. Consequently, future designs must treat light-baffled sensor ports as a primary requirement to ensure that pH-based stability assessments remain valid over long-duration missions.

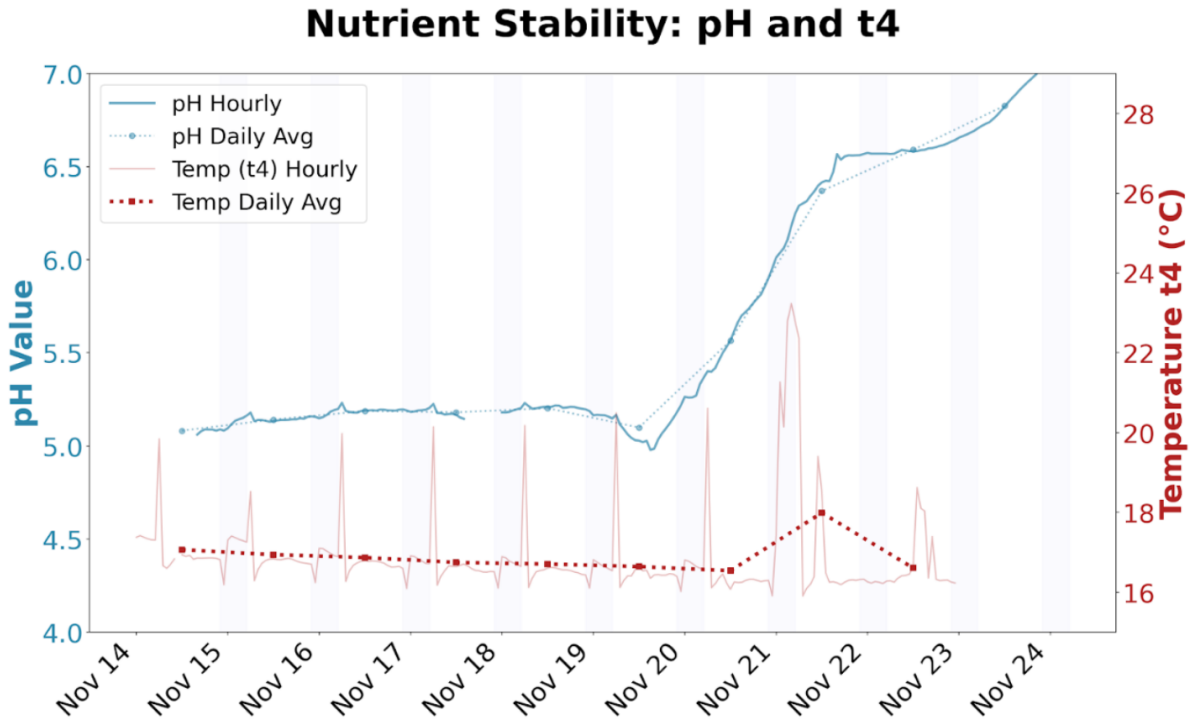

Figure 5.8: Hourly averaged pH time series during the Hoagland solution beaker test. pH remains near 5.1 to 5.2 initially, followed by a sharp increase starting around 20 Nov, consistent with measurement drift caused by probe fouling from biofilm. The test was stopped after the probe was cleaned, and no post cleaning measurements were recorded.

The image shows that the Hoagland solution as well as the Priva shows spikes and a sudden increase after a few days.

5.6.3. First Cultivation Trial (Priva solution: 2.9 μm VMA)

A reservoir-only EC/pH dataset was logged over approximately ten days during a preliminary fogponics run (24 November to 5 December). This trial utilized the 2.9 μm VMA modules in the wick based prototype from Episode 3 in Section 4.2. While the prototype was mechanically connected to a drain pathway, no excess drain volume accumulated for collection, meaning the dataset represents bulk-reservoir behavior exclusively and does not support reservoir–drain attribution.

Table 5.4: Trend-level EC summary (daily averages in mS/cm).

Metric	Start (24 Nov)	End (5 Dec)	Net change
Reservoir pH	7.01	7.42	+0.41
Reservoir EC	2.2	0.5	-1.7

Data processing. Raw logger outputs were screened for non-physical values, such as pH readings outside the 0–14 range or negative EC values. EC values recorded in μS/cm are reported in mS/cm (1 mS/cm $= 1000$ μS/cm) and rounded to one decimal place for trend analysis.

pH development and sensor fouling. Figure 5.9 shows the reservoir pH development. A distinct affected window occurred on 28 November, when the recorded pH dropped to 0.4, coinciding with a

logger input voltage of 1.18 V. Visual inspection confirmed the formation of a biofilm on the pH sensor. After cleaning and restoring the sensor on 1 December, the reading returned to 6.81 (2.925 V). This window is retained in the detailed plot for transparency but excluded from trend reporting. Using daily averages outside this window, the pH increased from 7.01 to 7.42.

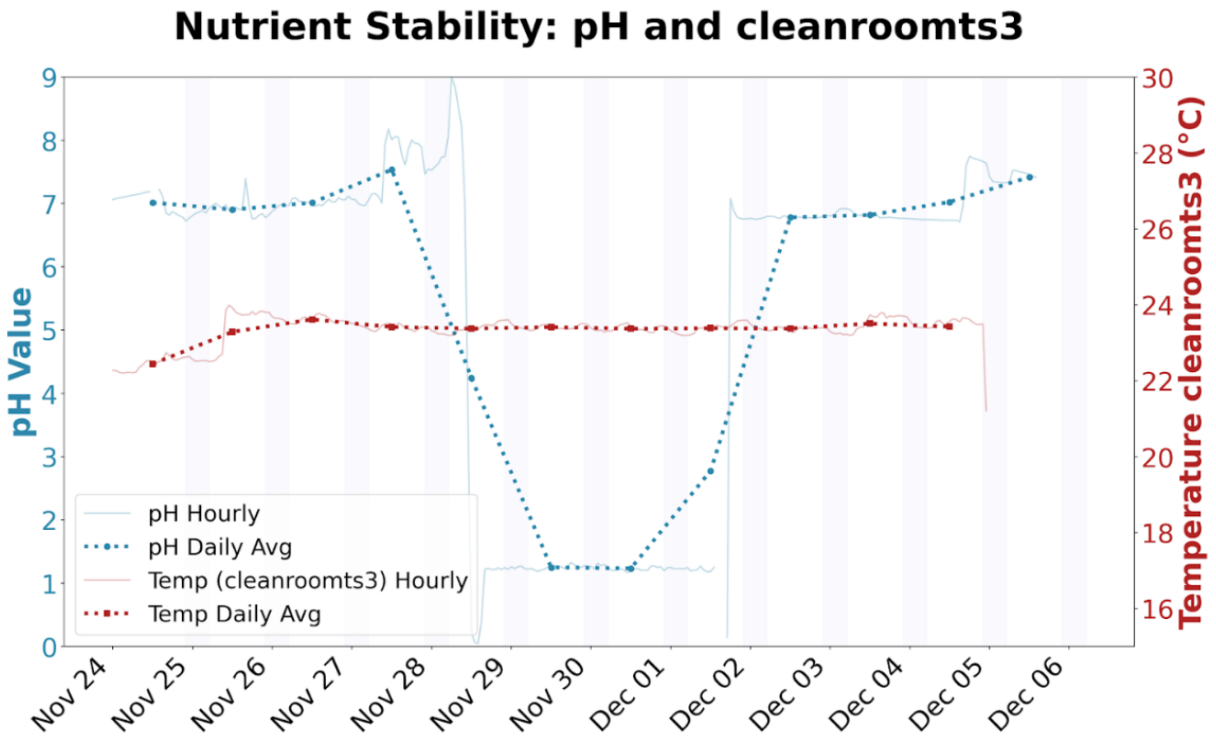

(a) Detailed pH time series showing the drop to 0.4 due to biofilm.

Figure 5.9: pH development during the first cultivation trial using Priva solution and the first wick based fogponics prototype. The plot shows the hourly averaged pH time series and highlights a period of erroneous readings in a sensor artifact window, where the measured pH drops to near zero and later recovers. This event is linked to biofouling of the sensor.

EC development. Figure 5.10 illustrates the EC development. Daily averages remained constant at 2.2–2.4 mS/cm until December 2nd, followed by another sharp decrease to 0.5 mS/cm by 5 December. These sudden drops coincide with checks and taking out the sensors from the reservoir and interpolating the gaps by the post processing. Table 5.4 summarizes the results and is added for completeness. The net change, however, should not be taken into account as real results.

Thermal stability. Temperature was recorded during the final five days of the trial to monitor the thermal impact of the 2.9 μm VMA on the nutrient solution. Figure 5.11 shows that the reservoir temperature remained stable despite the chemical drift observed in the same period.

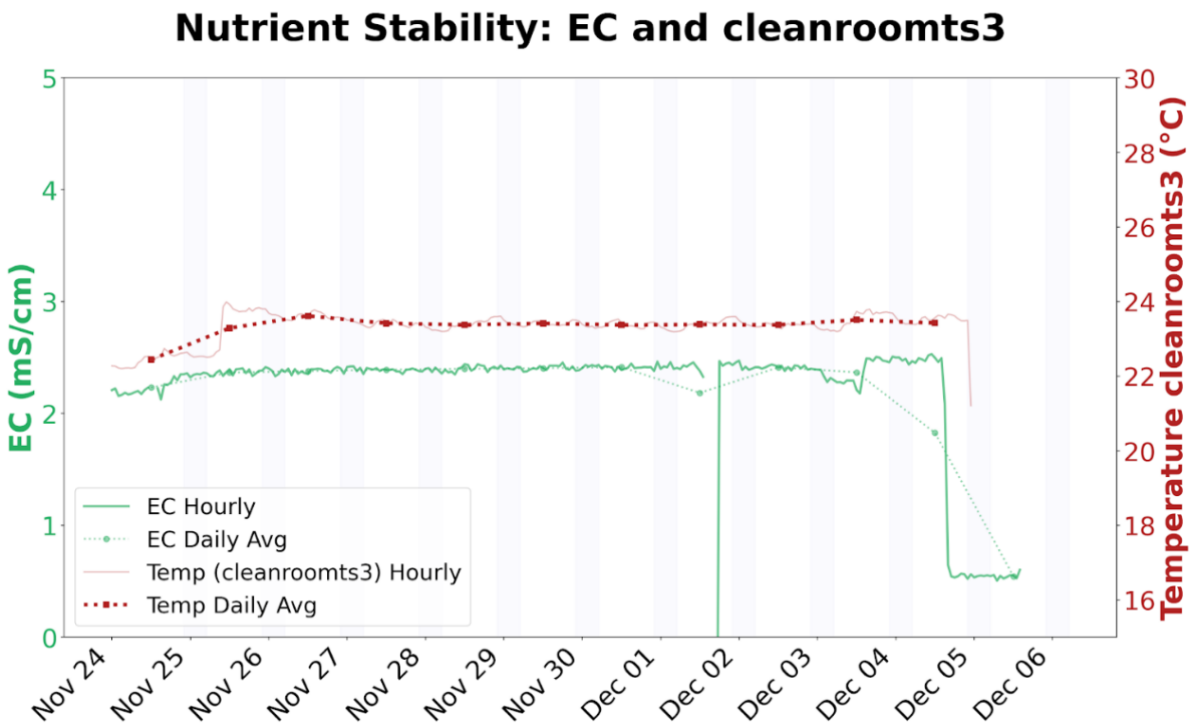

Figure 5.10: Hourly averaged EC time series from the first cultivation trial using Priva solution and the first fogponics prototype. EC stays around 2.2 to 2.4 mS/cm for most of the trial, with a short discontinuity when the probes were out of the solution. The segment between 1 Dec and 2 Dec and the sharp drop at the end coincide with removal of the EC sensor and interpolation during post processing, so they reflect a measurement artifact rather than a reservoir EC collapse.

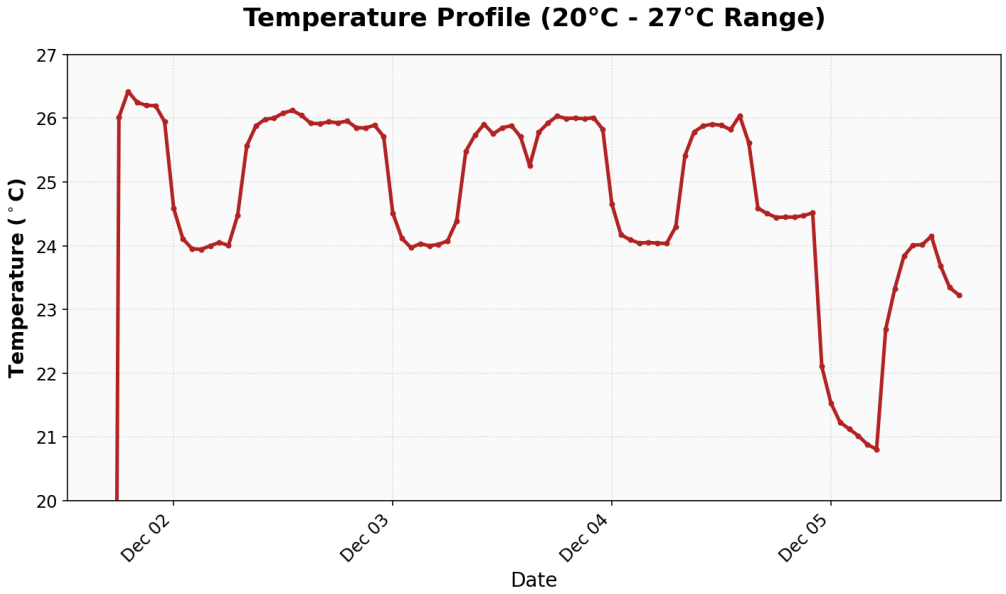

Figure 5.11: Reservoir temperature stability during the final phase of the first trial of the fogponics experiment.

5.6.4. Second cultivation trial (Hoagland; 20 Dec - 5 Jan): qualitative outcomes

The Hoagland-based pilot cultivation trial was initiated on 20 December with seedlings placed in both systems. On 23 December, fogging was observed and the fogponics grow tray was visibly filled with fog, indicating active atomization. At that time, an estimated 2-3 L of liquid had accumulated in the fogponics drain, and the reservoir was refilled. Figure 5.12 shows that by 30 December, the fogponics plants showed severely stunted growth, while in the aeroponics on the left plants appeared comparatively healthy. The environmental logger indicated an air temperature of 25.6 °C in the fogponics enclosure and 23.2 °C in the aeroponics enclosure at that inspection point, with both systems covered by plastic domes.

At the endpoint visit (January 5th), no fog was being produced and no water was observed to be pumped through the fogponics supply lines. The pilot trial, therefore, did not provide a viable fogponics plant dataset for endpoint harvest metrics. Photographs from 30 December (10 days during the trial) are shown in Figure 5.12. Further explanation on the critical stagnation of supply is further discussed in as system anomalies in Section 5.7.

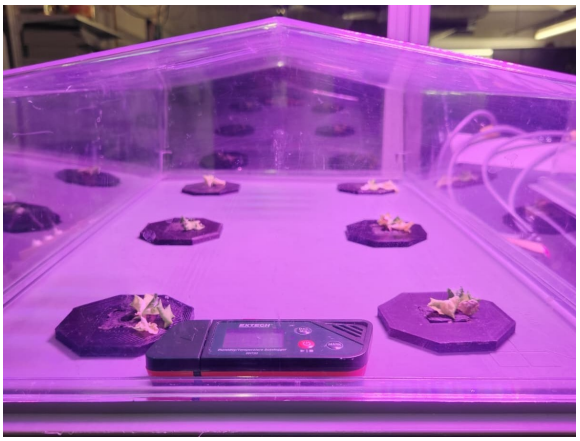

(a) Fogponics

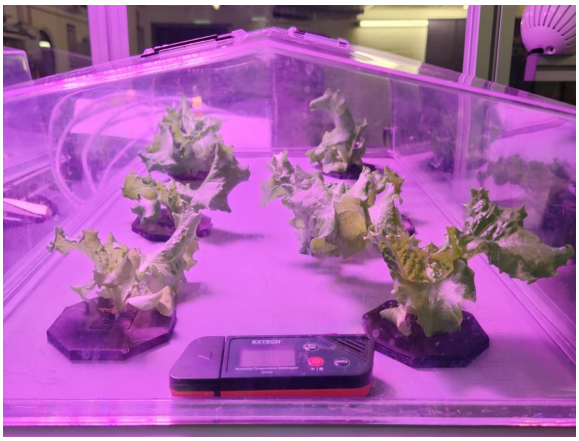

(b) Aeroponics (Baseline)

Figure 5.12: Plant growth comparison on 30 December, 10 days into the Pilot Trial. While both systems show healthy initial development, these represent the final qualitative data points before the system failure observed at the endpoint visit. No quantitative harvest metrics were collected for this trial.

Table 5.5: Evolution of nutrient chemistry: baseline (20 December) versus endpoint spot measurements (5 January). EC is reported in mS/cm and temperature in °C.

Location / Timeframe	pH	EC (mS/cm)	T (°C)
Initial Hoagland Baseline (20 Dec)	6.0	1.1	20
Aeroponics reservoir (Endpoint 5 Jan)	4.0	1.1	19
Fogponics reservoir (Endpoint 5 Jan)	5.89	1.4	19
Fogponics drain collection (Endpoint 5 Jan)	5.7	1.6	19

(a) Lettuce development status after 16 days fogponics set-up. Completely dried out due to unintended workings of system.

(b) Lettuce development static after 16 days in aeroponics baseline set-up.

Figure 5.13: Comparative plant status during the Hoagland based pilot trial. The images document the stunted growth in the fogponics system relative to the aeroponic controls between 30 December and the trial endpoint.

Event log Experiments

Below Table 5.6 summarizes the key events and qualitative observations used as reliability evidence. Where timestamps are approximate (e.g., field estimates of drain volume), this is indicated in the description.

Table 5.6: Event log and operational reliability evidence across the preliminary run (Priva) and the pilot cultivation trial (Hoagland).

Date	Run	Subsystem	Observation / event
24 Nov	Priva	System start	Preliminary fogponics run started (reservoir-only chemistry logging; earlier prototype configuration).
28 Nov	Priva	pH sensor	pH dropped to $\sim$0.4 with corresponding logger voltage $\sim$1.18 V; treated as an affected measurement period in the pH record.
01 Dec	Priva	pH sensor	pH sensor cleaned; pH returned to 6.81 with corresponding logger voltage 2.925 V.
01 Dec	Priva	Grow tray / fog output	Limited fog output observed. Condensate/collected liquid biased to back of tray; tray observed to be slightly slanted. Six-plant degradation overview photographed (to be inserted).
05 Dec	Priva	System endpoint	Salt precipitation observed at end of run; photo evidence recorded (to be inserted).
20 Dec	Hoagland	Trial start	Pilot cultivation trial initiated; seedlings placed in both fogponics and aeroponics systems.
23 Dec	Hoagland	Fog output / drain	Fogging observed; fogponics tray visibly filled with fog. Estimated 2–3 L liquid in drain. Reservoir refilled.
30 Dec	Hoagland	Plant status	Fogponics plants severely stunted; aeroponics plants comparatively healthy. Photo evidence recorded (to be inserted). Environmental logger indicated $T_{\text{fogponics}} = 25.6^{\circ}$C and $T_{\text{aeroponics}} = 23.2^{\circ}$C (both under domes).
03 Jan	Hoagland	Delivery	Fogponics observed not fogging (suspected pump/line clogging reported earlier in the trial narrative).
05 Jan	Hoagland	Delivery / endpoint	Endpoint visit. No fog produced and no water was observed to be pumped through the supply lines. Endpoint spot pH/EC/T measurements recorded.
06 Jan	Hoagland	Endpoint status	Endpoint plant-status photographs recorded (if separate from 5 Jan; to be inserted).

5.7. System Performance Anomalies

Despite the implementation of the logging protocols described in 4.3.3, the final prototype differentiated from its intended behavior. As mentioned in 5.6.4, the system ceased outputting nutrient solution. Furthermore, the data logger failed to commit any information to the SD card. This section covers the investigation into these two primary issues.

5.7.1. Nutrient Solution Supply Anomaly

During the experiment, the system stopped producing fog. Investigation showed that the atomization modules were still turning on, which was confirmed by the audible switching of the control relay and the faint sound of the modules.

This led to an inspection of the nutrient supply to the foggers. The small pump, controlled by the same Arduino, was still activating. However, the strength of the sound of the pump was significantly less than what was observed at the start of the study. Upon further examination of the reservoir tray, it was found that the nutrient solution had accumulated microbial growth in the form of a biofilm. This growth was found around and on the pump itself. The implications are discussed in Chapter 6.

5.7.2. Absence of Data Acquisition

While the data logging functioned correctly in the first trial with three sensors (1x pH, 1x EC, 1x Temp), the system encountered a critical error when the sensor count was increased to eight (2x pH, 2x EC, 4x Temp). This increase in the number of measurements, specifically taking 1,000-sample averages for each sensor every five minutes, significantly increased the calculation and workload for the microcontroller.

Because the system operated autonomously without a serial monitor connection, any ”SD FAIL” warnings would not have been observed. Additionally, the ”safety-first” flush protocol meant that if the initial file handle was not secured due to bus contention, all subsequent data windows would be discarded by the logic. Under this hypothesis, while the Arduino continued to process sensor samples for the live display, the data was never successfully transitioned to storage.

6

Discussion

The purpose of this chapter is to synthesize the knowledge generated through the constructive development and subsequent interrogation of the fogponic prototype. This research utilizes a Research through Design methodology. The NDS is characterized as a ”design thing” to analyze where the material reality of lunar agricultural requirements met the constraints of current technology.

The discussion is structured to tie back to the initial research goal of optimizing nutrient transport for isolated, and low-gravity environments. We evaluate the performance of the prototype through two distinct lenses. First, we conduct a formal verification of the system against the in Section 1.1 mentioned requirements established in the problem space. Second, we reflect on the ”points of resistance” and failure modes encountered during testing. These failures provide critical ”negative heuristics” that define the boundaries of current VMA technology. By bridging the gap between controlled laboratory testing and the requirements of a bio-regenerative life support system, this analysis identifies the chemical-mechanical compatibility necessary for sustainable extraterrestrial food production.

6.1. Verification Analysis

This section evaluates the experimental setup as a research instrument and the prototype as a potential candidate for Lunar agricultural applications. The analysis is divided into the verification of the measurement system and the formal assessment of design requirements.

Research Instrument Verification Results

The verification plan established in Section 4.5.2 was executed to define the reliability and uncertainty bounds for the data presented in Chapter 5. These results provide the technical justification for interpreting the observed system trends.

- **Temperature Consistency:** Co-location testing of the four temperature sensors prior to installation revealed a maximum offset of **1.1°C**. This establishes the system’s uncertainty bound. Any thermal delta reported between the root zone and the reservoir is interpreted relative to this potential sensor variance.
- **Flow-rate Measurement Repeatability :** The gravimetric method mentioned in Section 4.3.2 was verified by performing repeated measurements on fresh modules. For the high-flow 25 μm modules, the fresh mean was 25.5 g/min with a unit-to-unit standard deviation of 2.94 g/min. For the 2.9 μm modules, the baseline measurements showed a mean of 0.45 g/min with a standard deviation of 0.023 g/min. These values confirm that the measurement procedure is repeatable and capable of establishing a reliable performance baseline.
- **Flow-rate Sensitivity:** The method successfully captured the distinct performance decay signatures of both module variants. The 25 μm modules demonstrated a ”graceful” failure after mesh rupture and retained a mean of approximately 75.3% of their initial flow. In contrast, the 2.9 μm modules exhibited a terminal failure mode due to salt precipitation and retained only 21.5% of

their baseline flow. The magnitude of these changes significantly exceeds the repeatability scatter recorded in Item 6. This validates the use of gravimetric flow-rates as a primary health indicator for VMA hardware.

- **Logging Integrity and Manual Validation :** The integrity of the digital logging as presented in Section 4.3.3 for the Pilot Trial suffered issues leading to no data on pH, EC and Temperature of the trial. Independent of the logging system, a handheld meter was used to perform a single-point manual measurement of the nutrient solution at the conclusion of the trial to record the final chemical state. While this prevents a time-series interpretation of the final run, the manual validation provides a verified endpoint for the bulk solution chemistry.
- **Calibration Traceability and Analog Integrity:** To ensure data validity despite firmware updates, the system utilized a hardware-level calibration strategy mapping transmitter outputs to the Arduino ADC. To maintain instrumental transparency and allow for post-hoc verification, five reference datasets of these raw voltage outputs are documented in Appendix D. This inclusion decouples sensor performance from specific software scaling factors and provides a ground-truth electrical baseline independent of the primary logging system.
- **EC probe:** The Electrical Conductivity (EC) monitoring chain encountered a significant resolution constraint due to the mismatch between the hardware's dynamic range and the experimental requirements. The Atlas Scientific K1.0 EC probes used in this setup feature an operational range of 0 to 100 mS/cm. However, the nutrient solutions (Priva and Hoagland) typically operate within a narrow band of 0 to 2 mS/cm, utilizing only 2% of the sensor's total scale. When mapped across the 10-bit Arduino ADC, this narrow range resulted in a coarse digital resolution where small physical fluctuations were lost within a single bit-step. To compensate for this low signal-to-noise ratio, a specialized a trimmed-mean averaging protocol was required to extract meaningful trends from the discretized raw data. However, it is advised to use EC probes with a higher resolution in the specified range. The Atlas Scientific K0.1 will suffice in this case.

Requirements Verification

Table 6.1 summarizes the functional performance of the prototype against the aerospace standards established in the Problem Space. Status is categorized as Met, Partially Met (PM), Not Met (NM), or Out of Scope (OOS).

Table 6.1: Verification matrix for the VMA prototype. Status indicates the degree to which the requirement was satisfied during the experimental trials.

ID	Requirement Description	Status	Notes / Observations
CC	**Contamination Control (CC-01–04)**	*OOS*	Out of scope; research defines the need for future mitigation.
IRR-01	Single-component failure tolerance	**Not met**	Module rupture leads to localized irrigation loss due to 1:1 plume-to-plant mapping.
IRR-02	Minimize failure-prone components	**Met**	Removal of leaking top-reservoirs. Use of a pump was a necessary trade-off for consistent supply.
IRR-03	Prevent leakages	**Met**	No leakages occurred at fluidic interfaces during the 10-day preliminary trial.
IRR-05	Power consumption (< 660 W)	**Met**	Measured draw of VMA modules is well within the allocated mission budget.
SC-01	Minimize part count / mass / volume	**Met**	Design simplification (removal of tubes and wicks) reduced system volume and complexity.
SC-03	Autonomous operation	**Not met**	100% data loss in the Pilot Trial logger indicates a lack of autonomous reliability.
SC-04	Ease of maintenance	**Met**	VMA modules were verified to be easily swappable in the event of failure.
MC-01	Continuous monitoring (pH, EC, T)	**Partially met**	Verified in the Preliminary trial; failed in the Pilot trial due to hardware corruption.
MC-04	Closed-loop control	**Not met**	System operated as an open-loop platform.

Synthesis of Findings

The verification process highlights the trade-off between architectural simplicity and system redundancy. While the prototype successfully satisfied requirements for mass, power, and maintenance (SC-01, IRR-05, SC-04), it remains vulnerable to single-point failures (IRR-01).

The move from the leaking reservoir to a pump-driven direct feed (IRR-02) resolved immediate fluidic failures but increased the reliance on active hardware. Furthermore, the 100% data loss in the Pilot Trial (SC-03) suggests that while the physical delivery mechanism is promising, the data persistence and monitoring sub-systems require a transition from consumer-grade logging to robust, real-time telemetry to support the level of autonomy required for Lunar surface operations.

6.2. System behavior synthesis

In this decontextualized study, the prototype as a ”design thing” translates experimental observations into actionable engineering requirements through the extraction of specific Design Rules (DR). Each subsection follows a consistent logical progression by first identifying a research-based origin, then presenting the subsequent engineering solution, and finally formalizing a Design Rule as a mandatory architectural constraint for reliable lunar agricultural systems.

Chemistry is dynamic and operationally relevant at short timescales

The observed pH behavior demonstrates that nutrient solution chemistry is not a slow, monotonic drift variable but a dynamic state that can change significantly on hourly timescales. The experimental evidence in the beaker trial in Subsection 5.6 shows pH volatility and transient spike behavior, and the measurements demonstrate a coupling between chemistry and temperature. This establishes that chemistry and thermal state must be interpreted as a coupled system response rather than independent monitoring channels.

From an engineering perspective, the primary implication is that stability evaluation and closed-loop control concepts cannot be based on sparse sampling or long averaging windows. The relevant dynamics occur at the operational timescale of the system.

Design rule (DR-02). If pH/EC dynamics are used to evaluate fogponic feasibility or stability, then chemistry must be logged at minute-scale resolution (approximately every 5 minutes) to capture operational transients and spikes that are part of the real system behavior.

Root-zone temperature measurement is required to interpret chemistry behavior

The experimental evidence demonstrates that temperature and chemistry are not separable in interpretation. During this operation a duty cycle of 30 seconds on 30 seconds off was used. Temperature evolution and pH behavior co-vary, indicating that thermal state influences chemical behavior and therefore the chemical state experienced by the root zone. This elevates root-zone temperature from a contextual “environment variable” to an integral variable in the measurement and interpretation chain.

In engineering terms, pH/EC monitoring without temperature monitoring creates an incomplete causal description of the system, because apparent chemical drift can reflect a coupled thermo-chemical response.

Design rule (DR-01). If a fogponic architecture includes separate fluid states (reservoir and drain/return/condensate), then pH, EC, and temperature must be measured in each state along with temperature to preserve interpretability of drift mechanisms and root-zone exposure.

Probe biofilm is a first-order threat to data validity and must be designed against

The documented biofilm formation on probes as shown in Section 5.6.2 demonstrates that sensor fouling is an operational reality. Biofilm on pH/EC probes can silently bias readings while the system remains apparently functional. This produces plausible-looking data with incorrect meaning, and therefore directly threatens the validity of any chemistry-based inference.

The correct engineering conclusion is that probe fouling must be treated as a failure mode of the measurement chain and addressed by design. This includes physical access for inspection, procedures for cleaning, and an explicit validation step integrated into operation (e.g., reference checks, cross-comparison, or scheduled inspection).

Design rule (DR-03). If pH/EC is used as verification evidence, then the system must include probe fouling controls (inspection access, cleaning protocol, and a validation check), because biofilm can invalidate chemistry interpretation without visible system malfunction.

Feed strategy governs whether VMA modules operate inside a valid envelope

The wick-based supply approach from Section 4.2 demonstrated insufficient delivery capacity, creating conditions where modules can enter dry running operating states. The key engineering learning is that VMA integration is not only a question of whether an atomizer functions in isolation, but whether the feed architecture reliably maintains the wet operating condition required for stable atomization. Insufficient supply is not only a performance reduction; it shifts the system into an operating regime where failure becomes plausible.

The design move from wick supply to direct pump supply therefore represents an architectural correction: delivery must be governed by controlled supply rather than passive transport if stable operation is required.

Design rule (DR-04). If VMA modules are used for nutrient delivery, then the feed system must guarantee continuous wetting or minimum supply and include protection against dry operation, because under-supply drives unstable operation and can precipitate early module failure.

Salt deposition is a dominant failure mode and must be treated as expected behavior

Severe salt deposition was observed in Figure 5.5 in Section 5.5.5 as an operational failure mechanism in nutrient-rich operation. The engineering interpretation is that deposition is not a cosmetic artifact but a performance-limiting mechanism that couples chemistry, wetting/evaporation behavior, and module geometry. It directly constrains performance retention and therefore constrains maintainability, replacement frequency, and system availability at scale.

The relevant design conclusion is that deposition must be assumed as a credible mode of degradation and designed around at the architectural level: swappability, isolation, and maintenance logic become first-order design properties.

Design rule (DR-05). If fogponics is implemented with distributed VMA modules, then module failure must be assumed and the architecture must support rapid swap and isolation, because nutrient operation can drive severe deposition and major output loss on operational timescales.

Gravimetric flow-rate is a practical and discriminative health metric

The flow-rate measurements from Section 5.5 demonstrate that gravimetric output provides a direct, discriminative indicator of module delivery performance. The method resolves differences between module variants and captures performance collapse associated with failure signatures. This establishes gravimetric flow rate as an actionable, operationally meaningful health metric, particularly when droplet sizing is not part of the instrument suite.

Engineering significance: when output mass flow is tracked relative to a fresh baseline under standardized conditions, it becomes possible to define health thresholds, compare module variants, and quantify performance retention as a function of operating exposure.

Design rule (DR-06). If droplet sizing is not part of the measurement chain, then gravimetric mass flow (g/min) should be used as the primary quantitative indicator of VMA health and delivery performance, defined by fresh baselines and post-event comparisons.

Plume kinematics and droplet size dictate module orientation and targeting

The characterization of plume behavior in Section 4.2 demonstrates that droplet size fundamentally alters the transport mechanism of the nutrient mist. The $2.9\mu m$ aperture modules produce a suspended fog, whereas the $25\mu m$ variants generate a ballistic, spray-like plume dominated by directional momentum. This divergence in physical behavior confirms that a it's important to take into account the orientation should work with both plume natures.

The engineering redesign toward direct root-zone aiming reflects a shift from volume-filling strategies to targeted delivery. To maximize nutrient capture, the system architecture must acknowledge that larger droplets require line-of-sight ballistic paths. Effective research into varied droplet sizes therefore requires an orientation strategy that is optimized for the specific kinetic energy of the plume.

Design rule (DR-07). If a fogponic system utilizes multiple aperture sizes, then module orientation and distance to the root zone must be tailored to the specific plume nature (suspended fog vs. ballistic spray), to accommodate for effective use of both natures.

6.3. Architectural implications and scaling framing

A practical pathway to contextualize these findings is to translate module-level behavior into per-tray requirements and then propagate to an EDEN-heritage reference architecture. A 40-tray configuration provides a grounded scaling anchor because it aligns with an established controlled-environment cultivation reference system.

In this framing, the system design reduces to three coupled decisions per tray: (i) required delivered

mass flow per tray (driven by plant demand and intended duty cycle logic), (ii) modules per tray (driven by total required flow and redundancy strategy), and (iii) maintenance cadence and spares strategy (driven by failure behavior such as deposition and rupture risk).

A first-order scaling relation can be used as a placeholder for later system sizing:

$$\dot{m}_{\text{total}} = N_{\text{trays}} \cdot N_{\text{modules/tray}} \cdot \dot{m}_{\text{module}} \cdot D, \tag{6.1}$$

where $N_{\text{trays}} = 40$, $\dot{m}_{\text{module}}$ is the measured fresh gravimetric flow rate (g/min), and D is the duty-cycle fraction. This relation links measured module output to system throughput and provides a direct handle to (i) estimate total daily water/nutrient throughput, (ii) define redundancy requirements (modules per tray) for single-failure tolerance, and (iii) translate observed failure behavior into expected maintenance and spare-part demand at system scale. The remaining parameters $N_{\text{modules/tray}}$, $\dot{m}_{\text{module}}$, and D are populated once design choices are fixed.

6.4. Technical Constraints and Defined Research Scope

As mentioned in 5.7, the system suffered from critical anomalies, resulting in the acquisition of less data than intended. The following to paragraphs discuss the causes and implications for further research.

Biofilm Resistance and Component Redundancy are Critical for System Integrity

The investigation indicated that biofilm likely caused the system malfunction, which confirms the necessity of designing specifically against biological contamination. The detrimental effect of biofilm on the nutrient supply suggests that future iterations should incorporate a secondary circulation pump within the reservoir. Maintaining constant movement of the nutrient solution, particularly when the flow is directed toward the supply pump intake, reduces the opportunity for biofilm to accumulate. While adding a circulation pump introduces an extra component and increases system complexity, the potential for reduced biological interference is considered a significant advantage.

Furthermore, the current architecture proved vulnerable to a total system collapse due to the failure of a single component. To prevent such outcomes, future designs should eliminate single-point failures by implementing redundancy, such as utilizing multiple supply pumps. It remains essential to maintain the precise balance between nutrient supply volume and the atomization rate. Designing against single-point failures aligns with Requirement IRR-02 from 1.1, which specifies minimizing reliance on failure-prone components, and CC-01, which requires mitigation measures for biological contamination.

High-Resolution Sensing and Dedicated Computation are Required for Reliable Data Acquisition

The lack of successfully committed data suggests that the computational load, caused by high-frequency averaging, exceeded the capabilities of the Arduino Uno when combined with the SPI-based SD and Ethernet architecture. This averaging protocol was necessary because both probes exhibited significant voltage noise, particularly the EC probe. Because the K1.0 probe is designed for a range of 0 to 100,000 $\mu S/cm$, the operating target of 2,000 $\mu S/cm$ utilized only 2% of the available range. This low utilization resulted in insufficient resolution and high sensitivity to noise, necessitating the 1,000-sample averaging logic.

Future improvements should prioritize the use of a K0.1 EC probe, which measures up to 10,000 $\mu S/cm$ with higher accuracy and better resolution for this specific application. Additionally, a more advanced data logging protocol and a higher-performance computing platform are recommended. The Arduino Uno is not optimized for high-throughput data handling, and a dedicated logging computer would ensure reliable data persistence without the bottlenecks encountered in this prototype.

6.5. Final Synthesis: Design Rules and Research Boundary

Next to successfully finding the architecture implications of using different atomization modules, mapping the relation between chemical properties and the use of VMA technologies, and showing the effect of VMA on rootzone temperature, another aim of this research was to provide comparative results in plant development between state-of-the-art aeroponics and fogponics. However, the development of a research prototype capable of matching the operational reliability of established aeroponic systems

revealed significant engineering challenges. These challenges, which included unexpected rupture, limited module lifespans, and chemical-mechanical interactions, required meticulous documentation and analysis. Consequently, the focus of the technical effort was directed toward resolving and documenting these systemic behaviors to provide the rigorous engineering foundation presented in this thesis.

The prototype yields a coherent set of engineering insights that translate directly into design and validation rules for fogponic nutrient delivery development:

- Thermal state and chemistry are coupled and must be treated as a combined system response (DR-01)
- Chemistry behavior is dynamic and must be monitored at the operational timescale (minutes) to be meaningfully interpreted (DR-02). .
- Probe fouling is a real failure mode of the measurement chain and must be controlled by design (DR-03).
- Liquid feed strategy governs whether VMA modules operate inside a valid envelope; preventing dry operation is advised as it contributes to rupture (DR-04).
- Deposition is a dominant degradation mechanism in nutrient operation; module failure must be assumed and managed through swappability and isolation (DR-05).
- Gravimetric flow rate is a robust and discriminative metric to quantify delivery performance and retention (DR-06).
- Droplet size strongly affects plume characteristics and therefore determines the architecture of the prototype (DR-07).

Together, these findings define a practical, bounded design approach: instrument the right state variables at the right timescale, enforce valid wet operating conditions, treat degradation as expected, and use flow-rate baselining as the core performance metric.

The constraints encountered with the nutrient supply system and data logging architecture are not categorized as project failures, but rather as critical findings in the study of fogponic viability. While fogponics remains a promising candidate for resource-efficient nutrient delivery in lunar agriculture, the current prototype reached a logical conclusion of its development cycle. Further iterations to adapt the hardware and software for a full crop cycle require a significant time of design, engineering and iterations, which falls outside the current project timeline and is therefore recommended in further research.

By concluding the research, the study provides a clearly defined boundary of engineering knowledge and a verified set of design rules. This work serves as the necessary baseline for subsequent research, as a new MSc thesis is currently commencing to build upon these results. The knowledge gained from this prototype informs the specific proposal for future research iterations, which is detailed in Chapter 8.

7

Conclusion

Prior to this research, literature concerning fogponic nutrient delivery lacked a unified research framework, often omitting clear specifications regarding the utilized technology or the relevant operational parameters. This thesis addresses this absence by defining an engineering envelope for VMA-based fogponic nutrient delivery within lunar greenhouse contexts. While challenges in heritage high-pressure aeroponic approaches motivate the need for alternative delivery concepts, the present contribution is not a comparative performance claim. Instead, the work constructs a decontextualized laboratory platform to treat the atomization subsystem as a research instrument and to expose technology-material interactions that define feasibility limits. Within this lab venue, the study quantifies bounded system-level behavior, such as performance retention, degradation signatures, and nutrient chemistry dynamics, providing evidence for conditional boundary statements that can be replicated and extended.

The central contribution of this thesis is the standardized baseline research framework formulated to evaluate VMA-based fogponics as a decontextualized laboratory inquiry. The subsequent sections provide justification and answer on RQ1 to RQ4 from Chapter 3 as bounded evidence supporting specific elements of this framework, before summarizing the framework itself as an answer on the Main Research Question for future replication.

RQ1: How do different VMA module variants influence fogponic nutrient delivery behavior and design implications for a lunar NDS?

While fogponics literature typically uses operating frequency to categorize systems, this approach often ignores the fundamental physics and specific technologies involved in atomization. For VMAs, the aperture size is the critical variable because it determines droplet size and delivery behavior. As discussed in Section 2.3.3, the current lack of a technical framework for these hardware nuances makes system performance difficult to predict. These gaps in the literature necessitate a deeper investigation into how specific module choices impact delivery.

The results indicate that VMA module selection (here represented by nominal aperture class: 2.9 μm vs 25 μm) directly constrains feasible system architectures through differences in delivery morphology and mechanical robustness. Qualitative observations in Section 4.2 show that the 2.9 μm modules produced a fine mist-like plume consistent with fogponic operation, whereas the 25 μm modules behaved more spray-like and therefore require direct, near-root placement to achieve controlled root-zone wetting rather than relying on indirect transport or redistribution. In addition, structural integrity emerged as a limiting boundary condition: the 25 μm modules exhibited mesh rupture during operation as shown in the images in Section 5.5.4, demonstrating that not all commercially available VMA module classes are mechanically compatible with sustained operation in nutrient solutions under the tested configurations. Taken together, these findings imply that an optimal module class for lunar-relevant fogponics must satisfy two coupled constraints: (i) delivery behavior that supports the intended root-zone wetting regime and (ii) sufficient mechanical integrity to maintain repeatable performance over relevant operating durations. The observed plume differences and rupture events provide bounded, system-level

evidence that module choice is a first-order design driver and that feasibility depends on identifying a module configuration that achieves stable operation while remaining within plant-relevant droplet-size requirements discussed in Section 2.2.

RQ2: How does VMA-based fogponic operation influence nutrient solution stability as indicated by pH and EC behavior over time?

Previous studies, as discussed in Section 2.3.3, suggest that fogponic operation leads to a rise in pH as atomization frequency increases, alongside significant drifts in EC. However, these claims are often based on research that uses undistinguished atomization technologies rather than isolating the behavior of VMAs. Because the fundamental physics of different technologies may influence nutrient chemistry in varying ways, it is necessary to determine if these stability issues are inherent to the fogging process or a result of system design.

The measurements reported in this thesis indicate that pH is dynamic and coupled to temperature variations, whereas EC remained comparatively stable over the monitored periods. This was clearly observed in the experimental results in Section 5.6.3. In the preliminary beaker test time series using a Priva nutrient solution, pH exhibited transient excursions (spikes) that track changes in environmental temperature, together with a smaller longer-term drift component that is not explained by temperature alone. A second dataset with a Hoagland-type solution similarly showed pH variability, although less pronounced, supporting that pH stability depends on both thermal conditions and nutrient formulation and is shown in Section 5.6.2. In contrast, EC did not show a strong drift signature in the available datasets, which differs from the magnitude of EC changes reported in parts of the prior fogponics literature. Within the bounds of the executed measurements and logging integrity achieved here, the results therefore support two conclusion-level statements: (i) temperature must be treated as a covariable when interpreting pH trends in VMA fogponics, and (ii) Whereas EC appeared substantially less sensitive than pH under the tested conditions, it should be noted that the sensitivity of the EC probe was not high enough to detect small changes. These statements are reported as observed system-level behavior rather than universal trends, and they remain bounded by the specific prototype configurations, nutrient solutions, and instrumentation used in this work. Meaning the drifts in pH and EC as mentioned in Section 2.3.3 should not be attributed to fogponic technology, but rather the system architecture.

RQ3: To what extent does VMA-based fogponic operation alter root-zone temperature, and how does this relate to observed nutrient chemistry behavior?

Literature in Section 2.3.3 and expert discussions frequently highlight a significant increase in root-zone temperature as a major drawback of ultrasonic fogponics. However, these observations are largely associated with submerged piezoelectric transducers, which transfer significant waste heat directly into the nutrient solution. Because VMAs operate on a different mechanical principle and are not submerged, it is unclear if this thermal burden persists in VMA-based systems.

The available thermal dataset provides limited but relevant evidence that root-zone temperature can remain relatively stable during VMA-based fogponic operation under the tested indoor conditions. Temperature logging was available for a window of approximately four days during the preliminary configuration, during which the recorded root-zone temperature remained within a narrow band of roughly 24–27 °C shown in Section 5.6.3. This supports the conclusion that the prototype did not inherently induce large temperature excursions in the monitored period. Importantly, the chemistry datasets show that pH variations coincide with temperature fluctuations and is shown in Section 5.6, which implies that temperature must be treated as a coupled explanatory variable when interpreting pH behavior in fogponics. In this thesis, the principal conclusion is therefore not that VMA fogponics systematically increases root-zone temperature, but that root-zone temperature measurement is required to contextualize observed pH dynamics and to distinguish thermal-driven fluctuations from longer-term drift processes. This directly motivates treating temperature as a core monitoring channel in any lunar-relevant fogponic research framework.

RQ4: What plant-response outcomes were observed under VMA-based fogponics relative to the aeroponics baseline, and how can these outcomes be interpreted within the bounded evidence of this thesis?

Literature on fogponics, as discussed in Section 2.3.3, consistently reports lower biomass yields and slower growth rates compared to aeroponic and hydroponic baselines. However, these studies often fail to provide a detailed framework for the delivery hardware or the stability of the nutrient supply throughout the trial. Without a clear distinction between the technology used and the reliability of the delivery interface, it is difficult to determine if reduced yields are an inherent biological flaw of fogponics or a consequence of hardware degradation.

The initial phases of both experimental trials of Sections 5.6.3 and 5.6.4 demonstrated that the VMA nutrient delivery concept is fundamentally capable of supporting plant growth. During these early stages, the lettuce plants appeared healthy and showed normal development, indicating that the immediate root-zone environment was initially compatible with plant survival. This suggests that the technology is viable for nutrient delivery when the hardware is operating within its intended parameters.

As the trials progressed, however, the development of the plants could be clearly distinguished through visual observation. While no quantitative yield or biomass measurements were taken, a distinct shift toward stunted growth was visible in the fogponics configuration compared to the reference system. It indicates that this stunting was a direct result of the loss of nutrient solution supply. In the first trial, this was caused by the salt-blinding of the modules and the reduced supply by the wicks and in the second trial, by the complete lack of supply of nutrient solution likely due to biofilm buildup inhibiting the feed pump operations.

These findings suggest that the observed stunting was a consequence of delivery hardware degradation rather than a flaw inherent to the fogponic technology itself. Because the 25 μm modules were unavailable for the full trials due to prior mechanical ruptures, these observations are specific to the 2.9 μm implementation. The conclusion for RQ4 is that plant viability is strictly dependent on the stability of the delivery subsystem. Ensuring a consistent flow rate and a reliable supply interface is therefore a prerequisite for any future research into the quantitative growth performance of lunar fogponics.

Main research question: How can a standardized research framework be developed to evaluate the technical boundaries and impacts of VMA-based fogponics for lunar agricultural applications?

The lack of a standardized approach in fogponics research has resulted in a body of literature characterized by inconsistent claims and a failure to distinguish between various atomization technologies. As demonstrated by the preceding research questions, variables such as module aperture size, thermal coupling, and hardware redundancy are not merely technical details; they are first-order design drivers that determine the success or failure of the system. Without a clear framework that accounts for these technical boundaries, it is impossible to conduct the comparable, long-duration trials necessary for lunar agricultural applications.

This thesis proposes a standardized research framework by treating the fogponic nutrient delivery system as a coupled measurement-and-artifact platform in which technical boundaries are established through controlled decontextualization framework. In this thesis, standardized means a fully specified and repeatable baseline protocol for 1 g laboratory evaluation, including defined controllable parameters, measurement locations, data reduction conventions, and required reliability evidence, such that the same test logic can be replicated across iterations and future studies. The framework is structured around (i) clearly defined controllable parameters for VMA-based fogponics, (ii) a set of system-level performance metrics that can be measured reliably without requiring droplet-size instrumentation, and (iii) an architecture-aware measurement strategy that separates where chemical changes occur in the system.

Within the Research through Design framing of Chapter 3, the hard core of the research program remains the motivation for lunar compatible nutrient delivery, while the protective belt is instantiated as testable auxiliary hypotheses on atomizer module class, duty cycle, nutrient formulation, and measurement placement. The research identifies the negative heuristic as a reliance on passive system architectures and insufficient data acquisition strategies. This includes the failure of capillary wicking

to maintain the atomizer interface and a lack of hardware transparency where aperture size and spray morphology are ignored in favor of simple frequency metrics. Furthermore, the use of underpowered microcontrollers and the absence of intermediate system checkups created undetected single points of failure that compromised the observability of the trials. In contrast, the positive heuristic is established as a framework for researchable infrastructure that prioritizes component accessibility and operational redundancy. This includes the implementation of active liquid supply, the physical separation of the reservoir from the root zone, and the use of interchangeable modules to account for specific aperture characteristics. Finally, the design rules require that pH trends be coupled with thermal monitoring and that data infrastructure be isolated into independent subsystems to ensure the integrity of evidence in autonomous lunar environments. These heuristics are derived from the experiments and documented in Section 5.1

First, in Section 4, the framework defines the key experimental levers for VMA fogponics as module type (mesh/aperture class), duty cycle, and nutrient formulation/chemistry of the applied solution. Second, it defines the primary verification metrics as gravimetric module flow rate (delivery performance and degradation), nutrient solution stability indicators (pH and EC), and root-zone temperature as the thermal state variable. Third, the framework specifies that pH and EC should be measured in both reservoir and drain paths where applicable, because reservoir-only measurements cannot attribute chemical behavior to atomization-driven effects versus accumulation in downstream pathways. The results of this thesis further indicate that pH behavior is coupled to temperature dynamics, motivating root-zone temperature logging as a required co-measurement to interpret pH stability and drift. Finally, the framework explicitly integrates operational reliability evidence (event logs, photographs, and post-event performance checks) as a core output, because failure modes and performance-retention losses define the practical operating envelope of VMA-based fogponics and bound the space of feasible lunar implementations.

In summary, the standardized framework developed here evaluates VMA-based fogponics by (1) parameterizing module type, duty cycle, and nutrient formulation, (2) quantifying delivery performance via gravimetric flow rate, (3) monitoring chemistry stability via pH/EC with architecture-aware placement (reservoir and drain), (4) logging root-zone temperature to resolve thermal–chemical coupling, and (5) using documented failure signatures and post-event performance changes to define technical boundaries. This combination yields a reproducible method directed by design rules described in Chapter 6 to interrogate the feasibility limits of VMA-based fogponics for lunar nutrient delivery.

The framework is validated within the specific technical bounds of this research, which include terrestrial gravity, the implemented prototype architectures, and two nominal VMA aperture classes tested over short-duration cycles. By focusing on these parameters, the research establishes a baseline for how VMA hardware interacts with nutrient chemistry and system architecture under controlled conditions. These boundaries are necessary to isolate the primary engineering drivers and failure modes that define the current technology envelope. Consequently, this work provides a grounded evidence base that serves as the prerequisite for subsequent iterations, which can then extend the framework into reduced gravity behavior, long-duration durability studies, and quantitative droplet size characterization.

8

Recommendations

This chapter translates the bounded evidence generated through the Research-through-Design (RtD) process into a concrete positive heuristic that serves as a guided set of next design moves and experiments. It outlines the immediate recommended steps following this research and provides a strategic outlook on how fogponics systems can be further developed for lunar greenhouses. These recommendations are structured around design rules derived from observed system behavior including negative heuristics defined by failure modes, the hardening of the prototype as a research instrument, and a staged recontextualization path toward lunar-relevant operation. Furthermore, this chapter introduces a proposal for a three-year PhD research project to advance these findings while the preliminary exposé is located in the appendix for a more comprehensive review.

8.1. Immediate steps in fogponics research for lunar agriculture

The next RtD cycle should prioritize interpretability over scope expansion. The current limitation is not the absence of biological tests, but the fragility of the measurement chain and the insufficient control over dominant confounders at the atomizer interface. The immediate next step is therefore to harden the prototype as a research instrument by enforcing an evidence bounded operating envelope and by implementing targeted design moves that convert observed failure modes into controlled and measurable behaviors.

Non negotiable operating envelope

Reliable conclusions require chemistry visibility where the system separates. If the NDS is operated as a one way architecture with a drain or condensate path, then pH, EC, and temperature shall be measured in both reservoir and drain. Reservoir only data are insufficient to interpret root zone exposure and are not suitable to attribute drift mechanisms in architectures that intentionally decouple supply and return.

Chemistry dynamics shall be captured at minute scale. If pH or EC dynamics are used to evaluate fogponic feasibility, then the measurement interval shall be on the order of minutes, for example about 5 min, because behavior can be non smooth and may include spikes and transient dynamics that are not captured by coarse sampling and averaging.

Measurement credibility shall be protected as a first order system requirement. If pH or EC values are used as verification evidence, then probe fouling shall be treated as a first order failure mode of the measurement chain. The system shall include inspection access, a cleaning protocol, and validation checks, because biofilm formation can silently corrupt measurements and invalidate conclusions even when the hardware remains operational.

The architecture shall assume module level failure and prevent propagation. If fogponics is implemented using distributed atomization modules, then the design shall assume module level failure within days as a credible scenario and shall support fast swap and local isolation such that module failure does not propagate to system wide irrigation loss.

Until droplet sizing is available, flow shall be the primary quantitative performance signal. If droplet size distributions are not measured, then gravimetric mass flow rate in g/min shall be treated as the primary health metric for module integrity and delivery performance. Fresh baseline values and post event comparisons shall define operational thresholds and enable detection of degradation.

Highest priority implementation: measurement chain robustness

The first hardware iteration should improve logging and data persistence robustness before increasing sensor count or adding biological complexity. This includes reducing sensor count per microcontroller, using buffered writes, enabling watchdog resets, and implementing explicit data valid flags so that partially corrupted logs are not silently treated as evidence.

Probe handling protocol to protect pH and EC credibility

Probe maintenance shall be treated as traceable experimental procedure. An inspection interval and cleaning schedule should be sized to the observed biofouling susceptibility, and every maintenance action shall be logged to preserve traceability and to avoid mixing maintenance effects with system dynamics.

A cross check strategy shall be implemented to detect silent probe drift. Logged values should be periodically cross checked against a handheld meter at the same reservoir and drain locations. Cross checks are not a calibration replacement, but a credibility control that prevents extended operation on corrupted sensor output.

Targeted design moves for the next prototype iteration

The next iteration should pursue a small number of guided design moves with explicit success criteria, focused on removing confounders and bounding failure mechanisms.

Design move 1: design for salt management at the atomizer interface Salt precipitation should be shifted from an uncontrolled failure mode into a managed maintenance mechanism. The design should include features that reduce accumulation and improve cleanability, including a controlled purge or rinse routine, geometry that avoids stagnant zones near the mesh, and accessible module surfaces for rapid cleaning. The effect shall be quantified through repeated gravimetric flow rate checks. Success is defined as no terminal flow collapse over the target test duration and recovery of flow after a defined cleaning or rinse cycle.

Design move 2: module selection and integrity envelope (aperture versus integrity) Aperture class shall be treated as a design variable bounded by structural integrity rather than as a droplet size proxy. Multiple module types should be tested under identical feed and chemistry conditions, and rupture and salt deposition shall be treated as boundary indicators rather than anomalous events. Success is defined as identification of at least one module specification that operates without rupture over a defined minimum duration while maintaining stable flow and manageable deposition.

Configuration study: optimal number of foggers

To optimize robustness and fault tolerance at system level, configurations with different numbers of foggers shall be compared. Each configuration should be tested across orientations and layouts to identify a robust setup that maintains delivery performance under partial failure and minimizes cross interaction effects. This study is not a scaling exercise, but an architecture selection step that supports modular isolation and prevents single point failures.

Summary of the immediate next step

The immediate RtD next step is to harden the prototype as a research instrument before expanding biological scope. The work shall enforce a validated operating envelope with reservoir and drain chemistry visibility at minute scale, explicit probe fouling control, modular replacement and isolation, and gravimetric flow rate health monitoring. Within this envelope, the next prototype iteration shall prioritize measurement chain robustness, implement a traceable probe handling protocol with cross checks, salt management, and module integrity selection, and perform a configuration study on the number and

layout of foggers.

8.2. Road map for continued fogponics research for lunar agriculture and PhD proposal reference

The immediate steps in fogponics research define the entry condition for follow up work. The next research should not expand biological scope before the artifact produces interpretable evidence. Once the prototype is hardened as a research instrument, follow up research can be structured as a road map across three levels. Component level research targets atomizer physics and measurable performance indicators. Subsystem level research targets one cultivation tray as the first closed unit of plant interaction. System level research targets multi tray integration and long term effects relevant for a lunar crop production facility.

Component level research

Droplet size remains a central indicator of performance, but a predictive relation between VMA geometry and droplet size is not yet established. The first component level objective is therefore to measure droplet size using high resolution imaging and to relate droplet size distributions to aperture geometry and membrane parameters. This relation should be explained through the physics of VMA atomisation and supported by modeling, including CFD based simulation of flow and breakup behavior near the mesh. Gravity effects on fog production and fog behavior should be included as an explicit variable, with reduced gravity validation targeted through parabolic flight. This requires a flight compatible prototype that can activate fogging, switch between atomizer variants, and acquire imagery during manoeuvres.

A second component level direction concerns failure modes and integrity limits. This thesis showed mesh rupture as a credible failure mode, indicating a structural integrity boundary that may be linked to aperture class and membrane design. Follow up work should investigate the mechanics behind vibrating mesh atomizers and map operating conditions to rupture and degradation outcomes. This can be supported by COMSOL based modeling and used to identify an aperture and geometry window that preserves integrity while still enabling the intended mist regime. Silicon based VMA variants can be considered within the same framework and then validated by experiments.

A third component level direction concerns real time performance indicators beyond gravimetric flow checks. Gravimetric mass flow rate is a valid health metric, but it is disruptive and time intensive if modules must be removed. Other measurable signals exist at the actuator level, including current draw and operating frequency near resonance. Follow up work should link these electrical observables to atomization state, wetting state, and failure progression. This includes detection of dry operation, detection of reduced atomization, and long term tracking of degradation and lifetime without interrupting operation.

Subsystem level research

Subsystem level research treats one cultivation tray as the primary unit for plant relevant fogponic behavior. Once a droplet size relation is established at component level, the tray level objective becomes to determine droplet size and delivery strategies that support crop specific uptake and growth targets. This includes tuning duty cycles, fog density, and delivery timing.

A core subsystem objective is the development of one way nutrient delivery without return circulation. In this concept, nutrient delivery is tuned to plant evaporation and uptake rather than recirculating bulk solution. The root system can be treated as a retention and filtration volume that holds a bounded amount of liquid depending on root structure and environmental drivers of evaporation. Follow up work should identify how to achieve stable one way delivery at tray level while maintaining chemistry control and avoiding uncontrolled deposition.

A second subsystem direction is droplet electrostatic charging. Droplets can acquire charge during atomization, which may enable guiding droplets towards the roots or repelling droplets from wall surfaces. This could support improved delivery efficiency and reduced unwanted deposition.

Crop yield experiments can be performed at subsystem level once delivery and monitoring are stable enough to separate plant response from instrument artifacts.

System level integration

System level research integrates multiple cultivation trays into a facility relevant simulator to capture long term effects and system interactions. This enables study of lifetime and maintenance intervals under realistic duty cycles and chemistry regimes. It also enables verification of claimed benefits such as reduced biofilm formation at scale, which must be tested under long term operation rather than assumed from short runs. System level integration also enables quantification of crew time and operational workload, and it creates the basis for yield optimization studies that account for maintenance, reliability, and monitoring overhead.

8.3. Consensus and active traction

The continuation of this work is aligned with an active development trajectory. A new student, Lukas Wagner, is following up on the prototype research and will incorporate the immediate recommendations from this MSc thesis, with the explicit aim to harden the system as a reliable research instrument. This provides continuity for the prototype platform and preserves comparability across iterations.

For continuation beyond the immediate prototype hardening phase, the work has been formulated as a PhD research proposal. Funding is being pursued through an ESA OSIP request, and an internal request for a parabolic flight campaign has been issued to enable reduced gravity validation of fog production and behavior. In parallel, Clorofilab provides support as a supplier and contributes to the development of novelties in VMA technology, enabling access to hardware variants and an applied development pathway alongside the academic characterization.

Exposé summary and appendix reference

The proposed PhD work expands the immediate prototype recommendations into a structured research ladder across component, subsystem, and system levels. At component level, the program targets a predictive relation between VMA geometry and droplet size through high resolution imaging and physics based modeling, and it bounds structural integrity through failure mode mapping supported by simulation and validation experiments. It further develops real time performance indicators based on electrical observables, enabling long term degradation tracking without disruptive gravimetric procedures. At subsystem level, the program translates component characterization into crop relevant delivery strategies within a single cultivation tray, including one way nutrient delivery concepts and droplet electrostatic effects as potential levers for deposition control and uptake efficiency. At system level, the program integrates multiple trays into a facility relevant simulator to quantify lifetime, maintenance, biofilm behavior, and operational workload under long duration operation. The full PhD exposé is provided in Appendix E. The internal parabolic flight request is also included in Appendix F. Here personal contacts are crossed out for privacy reasons. Together, these documents specify the research questions, work packages, prototype requirements, validation logic, and a timeline that operationalizes the roadmap described in this chapter.

References

[1] Encyclopædia Britannica. *Moon - Resources, Exploration, Science*. Accessed: 2025-04-16. 2024. URL: https://www.britannica.com/place/Moon/Lunar-resources.

[2] European Space Agency. *Helium-3 mining on the lunar surface*. Accessed: 2025-04-16. 2022. URL: https://www.esa.int/Enabling_Support/Preparing_for_the_Future/Space_for_Earth/Energy/Helium-3_mining_on_the_lunar_surface.

[3] Statista Research Department. *Missions to the Moon by Country*. https://www.statista.com/chart/18749/missions-to-the-moon-by-country/. Accessed: 2025-04-28. 2023.

[4] China Manned Space Agency. *China's manned lunar exploration program under steady progress*. Accessed: 2025-03-03. Mar. 2025. URL: https://english.www.gov.cn/news/202503/03/content_WS67c57e96c6d0868f4e8f041c.html.

[5] European Space Agency. *ESA Terrae Novae 2030+ Roadmap*. Tech. rep. Accessed: 2025-03-03. European Space Agency, 2016. URL: https://indico.gsi.de/event/6401/images/751-Roadmap_v6.pdf.

[6] German Aerospace Center (DLR). *The EDEN Initiative: Evolution and Design of Environmentally-closed Nutrition-sources*. Accessed: January 4, 2026. Institute of Space Systems. 2024. URL: https://www.dlr.de/en/irs/about-us/departments/system-analysis-space-segment/planetary-infrastructures/eden-initiative-1.

[7] EDEN ISS Consortium. *EDEN ISS: A Mobile Greenhouse for Space Exploration*. Accessed: 2026-01-09. 2020. URL: https://eden-iss.net/.

[8] Paul Zabel et al. "Introducing EDEN ISS: A European project on advancing plant cultivation technologies and operations". In: *45th International Conference on Environmental Systems (ICES)*. Mobile Test Facility concept and Antarctic analogue campaign overview. Bellevue, Washington, 2015.

[9] Daniel Schubert et al. *Bio-regenerative Life Support Systems at DLR: Roadmap in the context of international collaboration 2020 to 2030*. Roadmap 2020-DLR-BLSS-v1.0. Cologne/Bremen, Germany: German Aerospace Center (DLR), June 2020. URL: https://www.dlr.de/de/irs/downloads/images20/eden_initiative/DLR_BLSS_Roadmap_English_final_v1.0.pdf.

[10] German Aerospace Center (DLR). *EDEN Next Generation: Lunar Agricultural Module Ground Test Demonstrator*. Accessed: 2026-01-09. 2023. URL: https://www.dlr.de/en/irs/research-transfer/missions-and-projects/eden-next-generation.

[11] ESA/DLR. *LUNA Analog Facility: Simulation and Testing in a Moon Analog Environment*. Accessed: December 24, 2024. European Space Agency (ESA) and German Aerospace Center (DLR). 2025. URL: https://luna-analog-facility.de/en/.

[12] Gemini Team and Google. *Gemini: A Family of Highly Capable Multimodal Models*. 2023. arXiv: 2312.11805 [cs.CL]. URL: https://arxiv.org/abs/2312.11805.

[13] German Aerospace Center (DLR). *EDEN LUNA: Lunar Greenhouse Simulation Facility*. Accessed: 2026-01-09. 2023. URL: https://www.dlr.de/en/irs/research-transfer/missions-and-projects/eden-luna.

[14] Andre Fonseca Prince et al. "EDEN Versatile End-effector (EVE): An Autonomous Robotic System to Support Food Production on the Moon". In: *2024 IEEE Aerospace Conference*. Big Sky, MT, USA: IEEE, 2024, pp. 1–9. DOI: 10.1109/AERO58975.2024.10521422.

[15] Jens Hauslage et al. "Eu:CROPIS – "Euglena gracilis: Combined Regenerative Organic-food Production in Space" - A Space Experiment Testing Biological Life Support Systems Under Lunar And Martian Gravity". In: *Microgravity Science and Technology* 30 (2018). Open Access; published online 26 Sep 2018, pp. 933–942. DOI: 10.1007/s12217-018-9654-1. URL: https://doi.org/10.1007/s12217-018-9654-1.

[16] Vincent Vrakking et al. “System Design of the EDEN LUNA Greenhouse: Upgrading EDEN ISS for future Moon mission simulations”. In: *53rd International Conference on Environmental Systems (ICES)*. ICES-2024-281. Louisville, Kentucky: International Conference on Environmental Systems, July 2024.

[17] Volker Maiwald et al. “From ice to space: a greenhouse design for Moon or Mars based on a prototype deployed in Antarctica”. In: *CEAS Space Journal* 13 (2021), pp. 17–37. DOI: 10.1007/s12567-020-00318-4. URL: https://doi.org/10.1007/s12567-020-00318-4.

[18] Conrad Zeidler et al. “Crew time and workload in the EDEN ISS greenhouse in Antarctica”. In: *Life Sciences in Space Research* 31 (2021), pp. 131–149. DOI: 10.1016/j.lssr.2021.08.001. URL: https://doi.org/10.1016/j.lssr.2021.08.001.

[19] Satoru Tsukagoshi and Yutaka Shinohara. “Nutrition and nutrient uptake in soilless culture systems”. In: *Plant Factory: An Indoor Vertical Farming System for Efficient Quality Food Production*. Ed. by Toyoki Kozai, Genhua Niu, and Michiko Takagaki. Elsevier, 2020, pp. 221–232. ISBN: 9780128166918. DOI: 10.1016/B978-0-12-816691-8.00014-5.

[20] Philipp Caesar. “Design of a Lunar Greenhouse Nutrient Delivery System”. Space Engineering Track. Master’s thesis. Delft University of Technology, 2023.

[21] G. W. Wieger Wamelink et al. “Can Plants Grow on Mars and the Moon: A Growth Experiment on Mars and Moon Soil Simulants”. In: *PLOS ONE* 9.8 (2014), e103138. DOI: 10.1371/journal.pone.0103138. URL: https://doi.org/10.1371/journal.pone.0103138.

[22] Gioia D. Massa et al. “VEG-01: Veggie Hardware Validation Testing on the International Space Station”. In: *Open Agriculture* 2.1 (2017), pp. 33–41. DOI: 10.1515/opag-2017-0003. URL: https://doi.org/10.1515/opag-2017-0003.

[23] Merle H. Jensen. “Controlled Environment Agriculture in Deserts, Tropics and Temperate Regions - A World Review”. In: *Proceedings of the International Symposium on Tropical and Subtropical Greenhouses*. Ed. by S. Chen and T.-T. Lin. Vol. 578. Acta Horticulturae. Tucson, Arizona, USA: International Society for Horticultural Science (ISHS), 2002, pp. 19–25.

[24] Hydroponic Urban Gardening. *Ebb and Flood Hydroponic Systems*. Accessed: 9 January 2026. n.d. URL: https://www.hydroponic-urban-gardening.com/fileadmin/intern/hydroponik-systeme/Flood-and-Drain-Ebbe-Flut-Technik/Ebb-flood-systems.svg.

[25] Melanie L. Lewis Ivey et al. “Food Safety in Hydroponic Food Crop Production: A Review of Intervention Studies to Control Human Pathogens”. In: *Foods* 14.13 (2025), p. 2308. DOI: 10.3390/foods14132308. URL: https://doi.org/10.3390/foods14132308.

[26] Sasireka Rajendran et al. “Hydroponics: Exploring innovative sustainable technologies and applications across crop production, with Emphasis on potato mini-tuber cultivation”. In: *Heliyon* 10 (2024), e26823. DOI: 10.1016/j.heliyon.2024.e26823.

[27] Ashwini Kumar et al. “A Comprehensive Analysis of Technology in Aeroponics: Presenting the Adoption and Integration of Technology in Sustainable Agriculture Practices”. In: *International Journal of Environment and Climate Change* 14.2 (2024), pp. 872–882. DOI: 10.9734/IJECC/2024/v14i24001. URL: https://www.researchgate.net/publication/378495896.

[28] No Soil Solutions. *Aeroponics*. Accessed: 9 January 2026. n.d. URL: https://nosoilsolutions.com/aeroponics/.

[29] M. Rakib Uddin and M. F. Suliaman. “Energy efficient smart indoor fogponics farming system”. In: *IOP Conference Series: Earth and Environmental Science*. Vol. 673. 1. IOP Publishing, 2021, p. 012012. DOI: 10.1088/1755-1315/673/1/012012.

[30] Hydro Garden Geek. *10 Different Types of Hydroponic Systems*. 2023. URL: https://hydrogardengeek.com/10-types-of-hydroponic-systemss/ (visited on 01/09/2026).

[31] Ilpo Koskinen et al. *Design Research Through Practice: From the Lab, Field, and Showroom*. Waltham, MA: Morgan Kaufmann, 2011. ISBN: 978-0-12-385502-2. DOI: 10.1016/B978-0-12-385502-2.00015-8.

[32] M Rakib Uddin and MF Suliaman. “Energy efficient smart indoor fogponics farming system”. In: *The 3rd International Conference on Smart City Innovation*. Vol. 673. IOP Conference Series: Earth and Environmental Science 1. IOP Publishing, 2021, p. 012012. DOI: 10.1088/1755-1315/673/1/012012.

[33] Amir Hossein Mirzabe et al. “Piezoelectric atomizer in aeroponic systems: A study of some fluid properties and optimization of operational parameters”. In: *Information Processing in Agriculture* 10.4 (2023), pp. 564–580. DOI: 10.1016/j.inpa.2022.05.008.

[34] A G Niam and L Sucahyo. “Ultrasonic atomizer application for Low Cost Aeroponic Chambers (LCAC): a review”. In: *International Conference on Agricultural Engineering for Sustainable Agriculture Production (AESAP 2019)*. Vol. 542. IOP Conference Series: Earth and Environmental Science 1. IOP Publishing, 2020, p. 012034. DOI: 10.1088/1755-1315/542/1/012034.

[35] EU Spray. *Spray Nozzles – Droplet Size Classification and Atomization Regimes*. Accessed: 2026-01-09. 2023. URL: https://www.euspray.com/en/products/spray-nozzles-technical-information/.

[36] Yu Zhang, Songmei Yuan, and Lizhi Wang. “Investigation of capillary wave, cavitation and droplet diameter distribution during ultrasonic atomization”. In: *Experimental Thermal and Fluid Science* 120 (2021), p. 110219. DOI: 10.1016/j.expthermflusci.2020.110219.

[37] Alex Paulo Martins do Carmo et al. “Electrical conductivity of nutrient solutions affects the growth, nutrient levels, and content and composition of essential oils of Acmella oleracea (L.) R. K. Jansen from southeastern Brazil”. In: *Journal of Agriculture and Food Research* 15 (2024), p. 100968. DOI: 10.1016/j.jafr.2024.100968.

[38] Alexios A. Alexopoulos et al. “Effect of Nutrient Solution pH on the Growth, Yield and Quality of Taraxacum officinale and Reichardia picroides in a Floating Hydroponic System”. In: *Agronomy* 11.6 (2021), p. 1118. DOI: 10.3390/agronomy11061118.

[39] Qiansheng Li et al. “Growth Responses and Root Characteristics of Lettuce Grown in Aeroponics, Hydroponics, and Substrate Culture”. In: *Horticulturae* 4.4 (2018), p. 35. DOI: 10.3390/horticulturae4040035.

[40] Alibaba. *FBPZT16808 PZT Material Piezo Ceramic Ring (product page)*. Accessed: 2026-01-09. 2026. URL: https://german.alibaba.com/product-detail/FBPZT16808-PZT-Material-Piezo-Ceramic-Ring-1600056519653.html (visited on 01/09/2026).

[41] Custom Cages. *Ultrasonic Mister (product listing)*. Accessed: 2026-01-09. 2026. URL: https://www.customcages.com/ultasonic-mister.html (visited on 01/09/2026).

[42] Altrasonic. *Ultraschall-Nebeldüse / Ultrasonic atomization (product page)*. Accessed: 2026-01-09. 2026. URL: https://de.altrasonic.com/ultrasonic-atomization_c48_6 (visited on 01/09/2026).

[43] Amir Hossein Mirzabe et al. “Piezoelectric atomizer in aeroponic systems: A study of some fluid properties and optimization of operational parameters”. In: *Information Processing in Agriculture* 10 (2023), pp. 564–580. DOI: 10.1016/j.inpa.2022.05.008.

[44] Abhinav Priyadarshi et al. “New insights into the mechanism of ultrasonic atomization for the production of metal powders in additive manufacturing”. In: *Additive Manufacturing* 83 (2024), p. 104033. DOI: 10.1016/j.addma.2024.104033.

[45] Pallavi Sharma and Nathan Jackson. “Vibration analysis of MEMS vibrating mesh atomizer”. In: *Journal of Micromechanics and Microengineering* 32.6 (2022), p. 065007. DOI: 10.1088/1361-6439/ac69ad. URL: https://doi.org/10.1088/1361-6439/ac69ad.

[46] L. Poulet et al. “Large-Scale Crop Production for the Moon and Mars: Current Gaps and Future Perspectives”. In: *Frontiers in Astronomy and Space Sciences* 8 (2022), p. 733944. DOI: 10.3389/fspas.2021.733944.

[47] Imran Ali Lakhiar et al. “Effects of Various Aeroponic Atomizers (Droplet Sizes) on Growth, Polyphenol Content, and Antioxidant Activity of Leaf Lettuce (Lactuca sativa L.)” In: *Transactions of the ASABE* 62.6 (2019), pp. 1475–1487. DOI: 10.13031/trans.13168.

[48] Mazhar H. Tunio et al. “Effects of droplet size and spray interval on root-to-shoot ratio, photosynthesis efficiency, and nutritional quality of aeroponically grown butterhead lettuce”. In: *International Journal of Agricultural and Biological Engineering* 15.1 (2022), pp. 79–88. DOI: 10.25165/j.ijabe.20221501.6725.

[49] P. Gopinath, P. Irene Vethamoni, and M. Gomathi. “Aeroponics Soilless Cultivation System for Vegetable Crops”. In: *Chemical Science Review and Letters* 6.22 (2017). ISSN 2278-6783, pp. 838–849.

[50] M. Whipple. “Deposition of nutrient mist onto hairy root cultures”. PhD thesis. Worcester Polytechnic Institute, 1995.

[51] Tanuja Buckseth et al. “Methods of pre-basic seed potato production with special reference to aeroponics—A review”. In: *Scientia Horticulturae* 204 (2016), pp. 79–87. DOI: 10.1016/j.scienta.2016.03.041.

[52] Bethany M. Eldridge et al. “Getting to the roots of aeroponic indoor farming”. In: *New Phytologist* 228.4 (2020), pp. 1183–1192. DOI: 10.1111/nph.16780. eprint: https://nph.onlinelibrary.wiley.com/doi/pdf/10.1111/nph.16780. URL: https://nph.onlinelibrary.wiley.com/doi/10.1111/nph.16780.

[53] Imran Ali Lakhiar et al. “Modern plant cultivation technologies in agriculture under controlled environment: a review on aeroponics”. In: *Journal of Plant Interactions* 13.1 (2018), pp. 338–352. DOI: 10.1080/17429145.2018.1472308.

[54] C.J. Rosen and R.M. Carlson. “Influence of root zone oxygen stress on potassium and nitrogen accumulation by potatoes”. In: *Journal of Plant Nutrition* 7.9 (1984), pp. 1261–1270. DOI: 10.1080/01904168409363257.

[55] Eni Sumarni et al. “Temperature Distribution in Aeroponics System with Root Zone Cooling for the Production of Potato Seed in Tropical Lowland”. In: *International Journal of Scientific & Engineering Research* 4.6 (2013), pp. 799–803. ISSN: 2229-5518.

[56] Wenxin Yang et al. “Sustainable Soilless Cultivation Mode: Cultivation Study on Droplet Settlement of Plant Roots under Ultrasonic Aeroponic Cultivation”. In: *Sustainability* 14.23 (2022), p. 15844. DOI: 10.3390/su142315844.

[57] Amin Reza Jamshidi, Ahmad Ghazanfari Moghaddam, and Ahmad Reza Ommani. “Effect of Ultrasonic Atomizer on the Yield and Yield Components of Tomato Grown in a Vertical Aeroponic Planting System”. en. In: *International Journal of Horticultural Science and Technology* 6.2 (Dec. 2019). DOI: 10.22059/ijhst.2019.278366.284. URL: https://doi.org/10.22059/ijhst.2019.278366.284 (visited on 04/20/2025).

[58] Sensors & Probes. *Industrial pH Transmitter*. Accessed: 2026-01-09. n.d. URL: https://sensorsandprobes.com/products/industrial-ph-transmitter?srsltid=AfmBOooaZDsrQWosfsA4dwxUPZ_S-0YL9ljDv5lZiPNdfnOmIRRkm5rV (visited on 01/09/2026).

[59] Smart Citizen. *Atlas pH (documentation)*. Accessed: 2026-01-09. n.d. URL: https://docs.smartcitizen.me/knowledge/soil-water/pH/Atlas_pH/ (visited on 01/09/2026).

[60] MG Super Labs. *Atlas Scientific IXIAN Conductivity Transmitter*. Accessed: 2026-01-09. n.d. URL: https://www.mgsuperlabs.co.in/estore/Atlas-Scientific-IXIAN-Conductivity-Transmitter (visited on 01/09/2026).

[61] Sensors & Probes. *Conductivity Probe K = 1.0*. Accessed: 2026-01-09. n.d. URL: https://sensorsandprobes.com/products/conductivity-probe-k-1-0?srsltid=AfmBOooNiteLCiD-NGN7Rq3Mh2fQMQ8A_SUs60w7lX7_Ns3lJxzok9Lf (visited on 01/09/2026).

A

Morphological Chart

The morphological chart starts on the next page.

1. Core Nutrient Mist Generation & Delivery							
Function							
The system shall convert nutrient solution into fine droplets.	**Vibrating**	**Ultrasoni**	Surface Acoustic	Electrostatic ultrasonic hybrid atomizers			
The system shall guide the droplets to the plant roots.							
The system shall provide controllable spray intervals.	 Raspberry pi	 Arduino	 Directly to pc	 Manual switch	 ESP32		
The system shall ensure that mist is being produced when the mister is active (mist verification).	 Humidifier senso	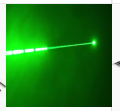 Laser	 Rain Sensor	Feedback from circuit			
2. Nutrient Solution Management							
Function							
The system shall collect and guide excess water to the reservoir tank.	 Fog tube	 Condensed tube	 Fog collection net				
The system shall filter solid particles from the drain before recycling.	 Filter	 membrane	 second condens	 Sieve	 Aquarium filter		
The system shall recycle the nutrient solution back to the mister.	Same as current	 Directly into rese	Extra tank for cleaning Ns				
The system shall replenish the nutrient solution in the reservoir when needed.	 Valve	 Constant flow	 Manual				
3. Nutrient Composition & Environment Control							
Function							
The system shall maintain Temperature	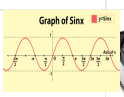 Alternating in fog interval	 Active cooling	 Active heating	 Heating the fog			

The system shall measure pH	 Hand Helt	 Automated					
The system shall measure EC	 Hand Helt	 Automated					
The system shall measure Temperature	 Analog	 Hand Helt	 Automated				
The system shall monitor EC, pH, and temperature in the drain tray (to detect nutrient dynamics and losses).	 Hand helt sensor	 Continual sensor					
4. Monitoring & Validation							
Function							
The system shall provide the possibility to measure droplet size (even if external method).							
The system shall measure water usage over time.	 Flow meter on er	 Calculate by fogg	 Water level sensor				
The system shall measure power usage over time.	 Outlet measurem	 Through Arduino					
5. Operational & Safety Support							
Function							
The system shall detect failures (fogger not working, fan not working, sensor failures, etc.).	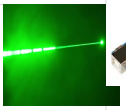 Laser through fo	 By Arduino feedback on sensor readings					
The system shall provide easy maintenance (easy access, modularity, cleaning).	 Lid on the tray	 3d printed mounts for parts					
The system shall posess of a redundant fail safe to prevent overflowing	valve close by de	Mechanical stop like in toilet					
The system shall allow wireles data transmitting	Connect to lab in	Connect with sep	bluetooth				
The system shall provide an evenly distributed fog to all plantroots	from different sid	Maybe one side is sufficient.					

The system shall constantly mix/stirr the nutrient solution	Water pump	Mixing unit withh	Blender like thing	Stirring with a stick			
The system shall provide enough room for the roots (Ask Jess how much room they might need)							
The system shall measure them water usage up to an accuracy of up to at least 0.3 L/m^2 (1% of the irrigational water use of aeroponic system) Source: Improving water use efficiency.... Laura Carotti							
The system shall not be connected to the drain of the lab and be a standalone technology.	Needle system	Tweak incoming NS before entering					

B

NDS Requirements

The table with requirements starts on the next page.

ID	Requirement Description	Source
P-01	The system shall automatically detect internal failures resulting in loss of irrigation.	EDEN LUNA Requirements
P-03	The system shall monitor and control EC and pH levels of the nutrient solution before and after fogging.	FR-NC-010 (EDEN NEXT GEN)
P-04	The runoff nutrient solution shall be recirculated into the reservoir.	FR-TI-070 (EDEN NEXT GEN)
P-05	The system shall include access points for manual and automatic solution sampling.	EDEN LUNA Requirements
P-06	The reservoir tank shall be equipped with level sensors.	EDEN LUNA Requirements
P-07	The system shall provide data logging with time indication for control and analysis.	EDEN LUNA Requirements
P-08	The system shall include filtering to prevent solid particles from clogging the drain.	EDEN LUNA Requirements
P-09	All fluid-contact components must be chemically compatible with nutrients and cleaning agents.	FR-TI-110 (EDEN NEXT GEN)
P-10	Components shall be designed for accessibility and ease of servicing.	FR-OP-010 (EDEN NEXT GEN)
P-11	The system shall allow misting frequency to be changed.	
P-18	The system shall have redundancy built in to reduce the chance of failure resulting in loss of irrigation.	EDEN LUNA Requirements
P-19	The system shall store enough water for at least 3 days to allow for unattended operation during weekends.	User Requirement
P-20	The refill mechanism shall include a fail-safe to prevent overflow, using either mechanical or mechatronic methods.	Meeting with Daniel (26/05/2025)
P-21	The system shall support inline Temperature, pH and EC sensors for continuous monitoring.	Meeting with Daniel (26/05/2025)
P-22	The foggers shall produce droplets in the optimal size range for nutrient absorption.	Meeting with Daniel (26/05/2025)
P-23	The tray shall accommodate 40x60 cm dimensions and ensure a minimum root zone height.	Meeting with Daniel (26/05/2025)
P-24	The drain shall be positioned to avoid root congestion, preferably at the tray's edge.	Meeting with Daniel (26/05/2025)
P-25	The system shall prevent root intrusion into the drain using sponge or equivalent barrier.	Meeting with Daniel (26/05/2025)
P-26	The system shall include a datalogging solution capable of time-stamped EC and pH recordings.	Meeting with Jess (27/05/2025)
P-27	The system shall monitor PAR, temperature, and humidity continuously at height of the foliage.	Meeting with Jess (27/05/2025)
P-28	The system shall allow for fixed-position imaging of plant roots and leaves.	Meeting with Jess (27/05/2025)
P-29	The system shall support two control conditions in Experiment 1: RO water and nutrient solution only.	Meeting with Jess (27/05/2025)
P-30	The system shall support adjustable plant density per tray (6 or 12 plants based on growth duration).	Meeting with Jess (27/05/2025)
P-31	The system shall support switching plant positions between repetitions to minimize positional bias.	Meeting with Jess (27/05/2025)

Table B.1: Consolidated Prototype-Specific System Requirements

C

Environmental Parameters Cultivation Lab

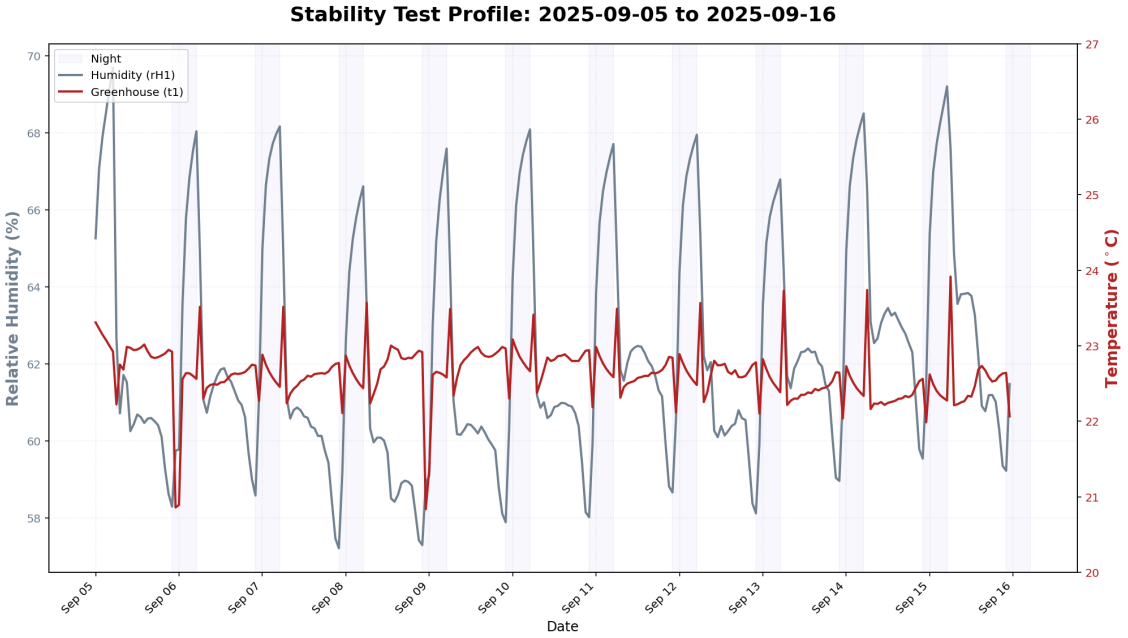

Figure C.1: Operating environment time series during the Priva beaker test (05 to 16 Sep), showing air temperature and relative humidity in the cultivation area together with the day night light state. The data show a clear daily cycle, with temperature varying from about 21 to 24 degrees Celsius and a corresponding alternating pattern in relative humidity.

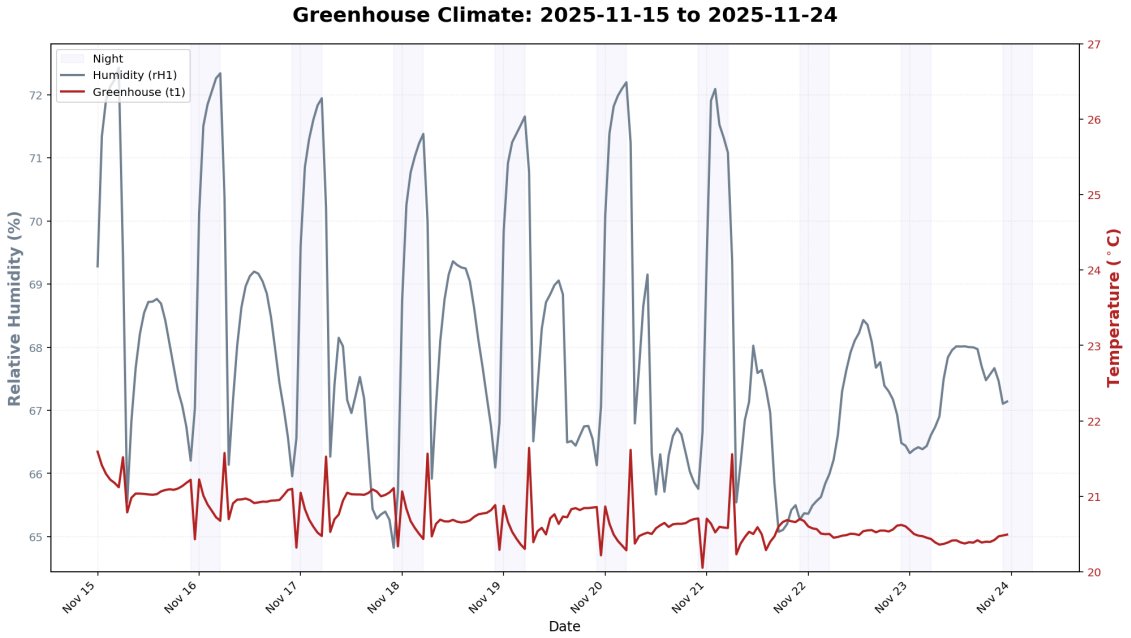

Figure C.2: Operating environment time series during the Hoagland beaker test (15 to 24 Nov), showing air temperature and relative humidity in the cultivation area together with the day night light state. The data show a clear daily cycle for most of the period, but this pattern degrades in the final days as the temperature and humidity signals become less periodic, marking the onset of a malfunction in the cultivation room system.

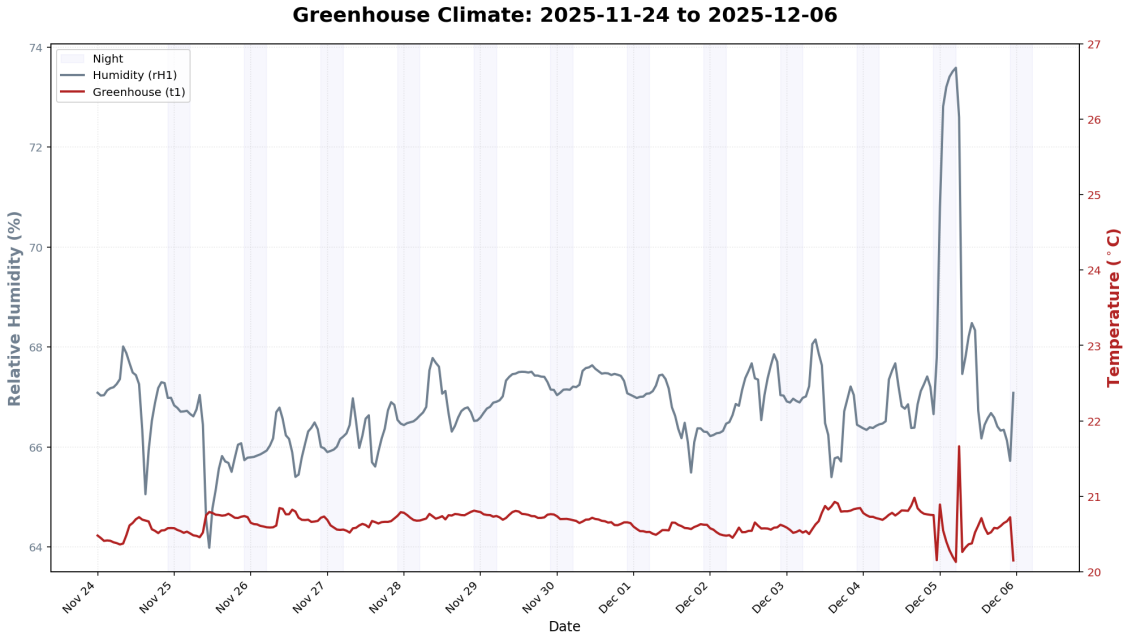

Figure C.3: Operating environment time series (24 Nov to 06 Dec) during the first trial with Priva solution and the wick based prototype, showing air temperature and relative humidity in the cultivation area together with the day night light state. In contrast to the earlier periods, the expected daily alternation is largely absent, indicating that most of the cultivation room climate control was not operating correctly during this interval.

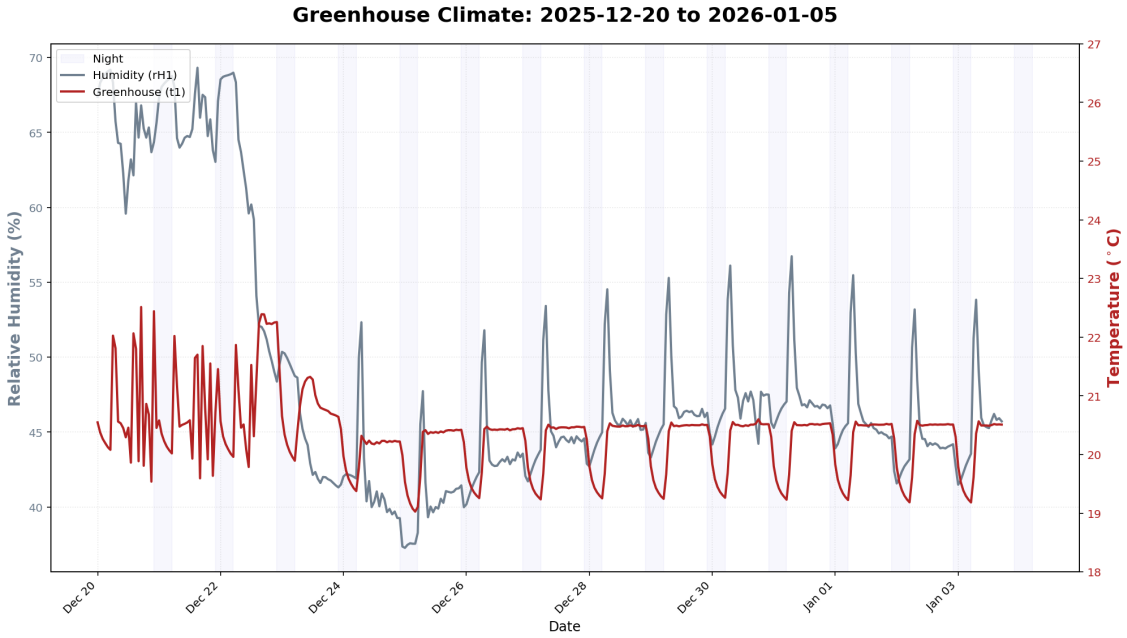

Figure C.4: Operating environment time series (20 Dec to 05 Jan) in the second trial with Hoagland solution and the final prototype, showing air temperature and relative humidity in the cultivation area together with the day night light state. The data again show a clear daily alternation, but with a different signal shape than earlier periods, indicating that the climate control behaviour had changed while maintaining a day night driven cycle.

D

Raw Sensor Voltage Datasets

This appendix provides the raw analog-to-digital converter (ADC) voltage outputs for the primary experimental phases. These datasets represent the hardware-level ”ground truth” before the application of digital filtering or software-side calibration scaling. Documenting these signals ensures instrumental transparency and allows for the independent verification of sensor behavior, signal noise, and potential drift encountered during the trials.

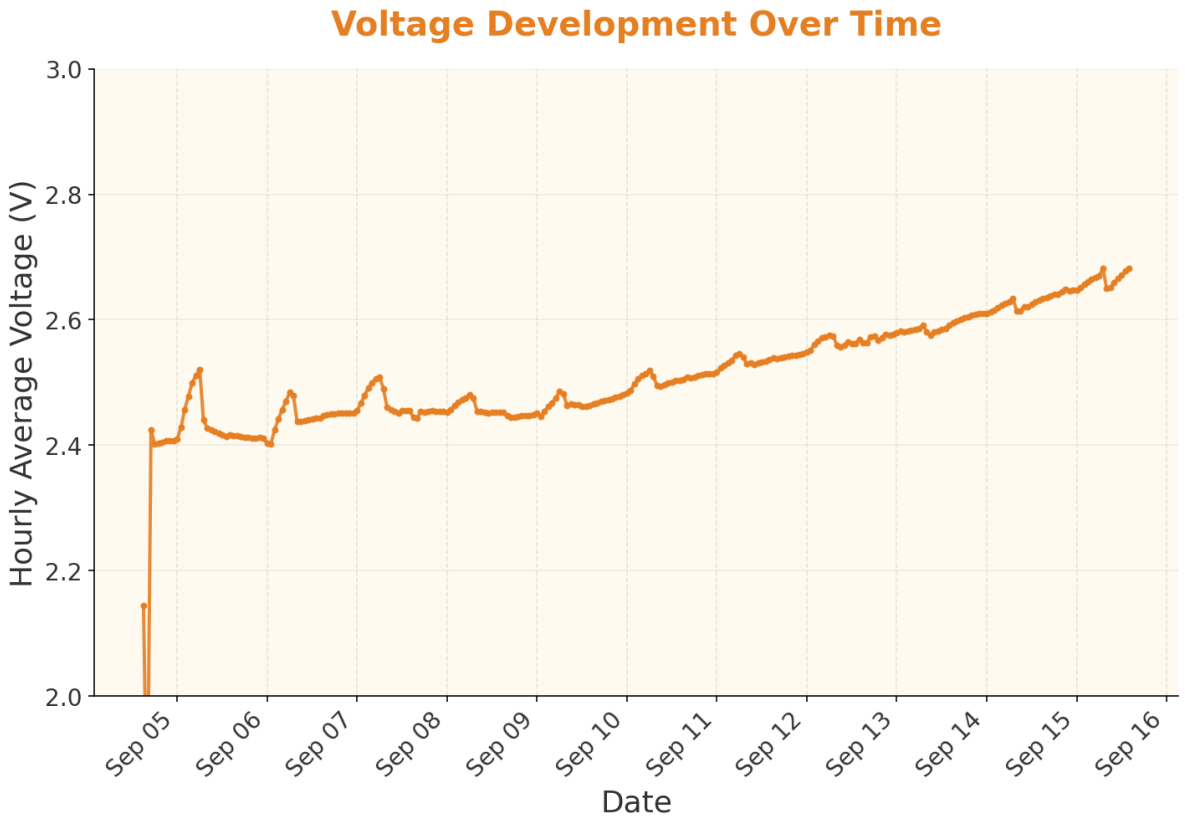

Figure D.1: Raw voltage output for the static pH beaker test using 800 mL of Priva nutrient solution (5 to 16 September). The fluctuations correspond to the unmixed, open reservoir state. Short term voltage spikes are visible and are discussed in Chapter 6 as artifacts related to laboratory environmental conditions.

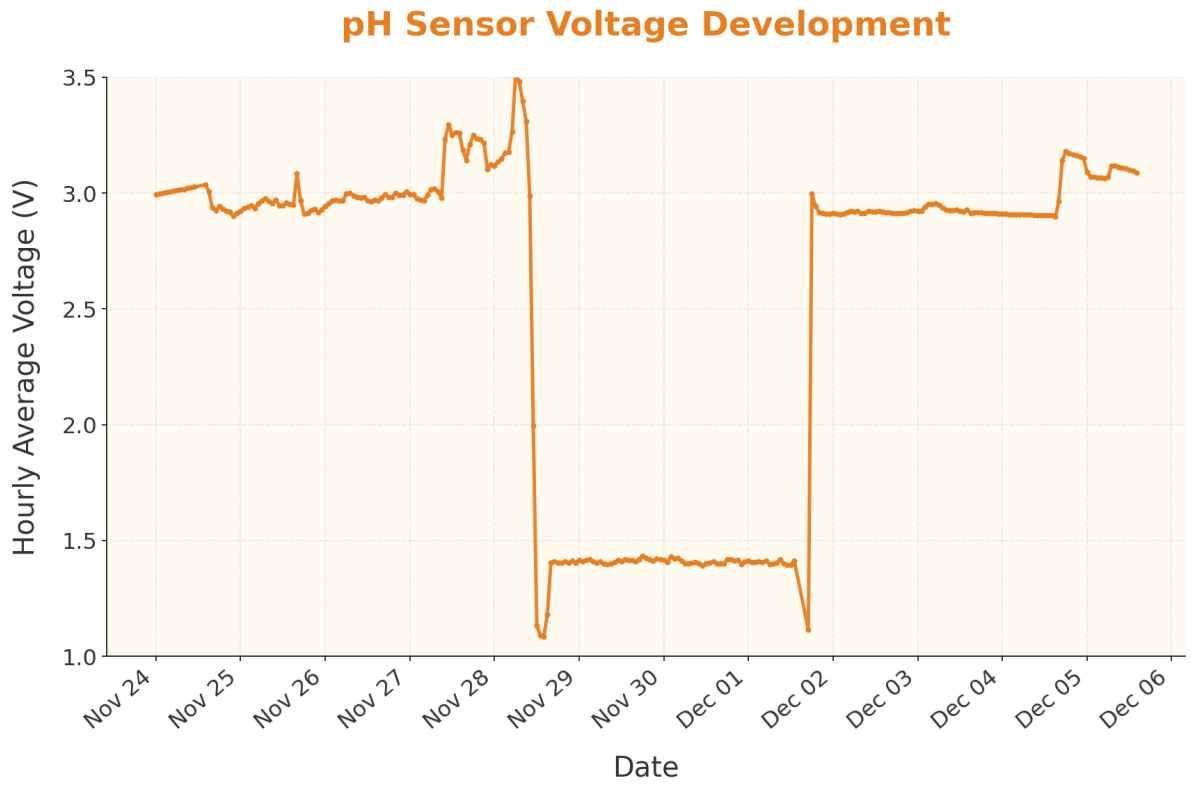

Figure D.2: Raw voltage output for the fogponics reservoir pH during the preliminary run (24 Nov - 5 Dec).

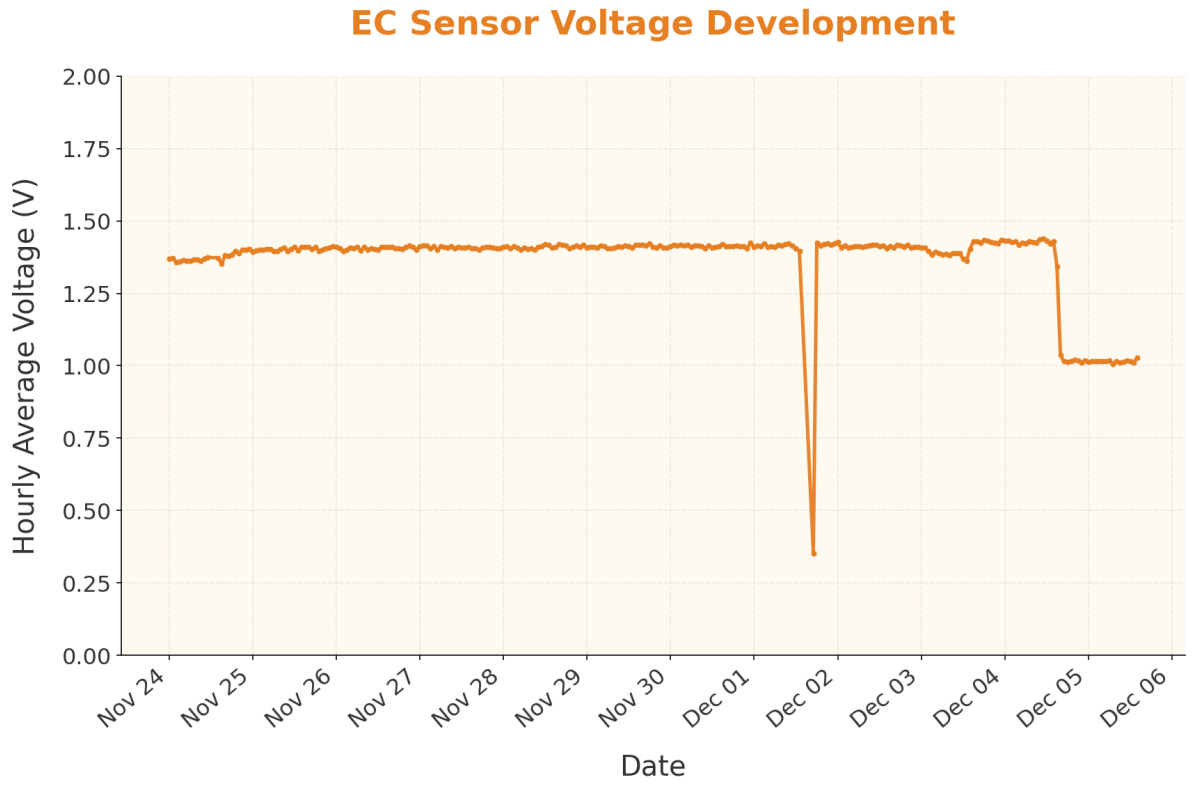

Figure D.3: Raw voltage output for the fogponics reservoir EC during the preliminary run (24 Nov - 5 Dec).

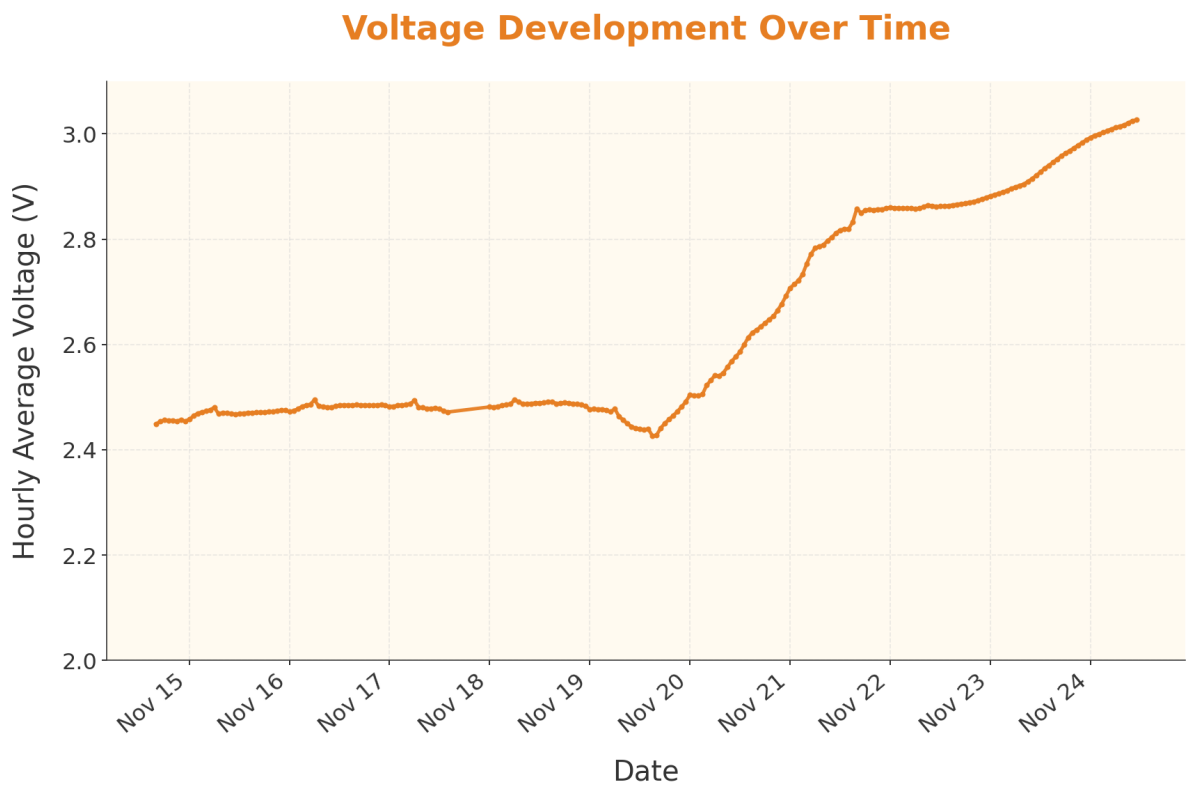

Figure D.4: Raw voltage output for the static EC beaker test utilizing Hoagland nutrient solution (15 to 24 November). This dataset defines the baseline voltage mapping used for the second nutrient formulation phase.

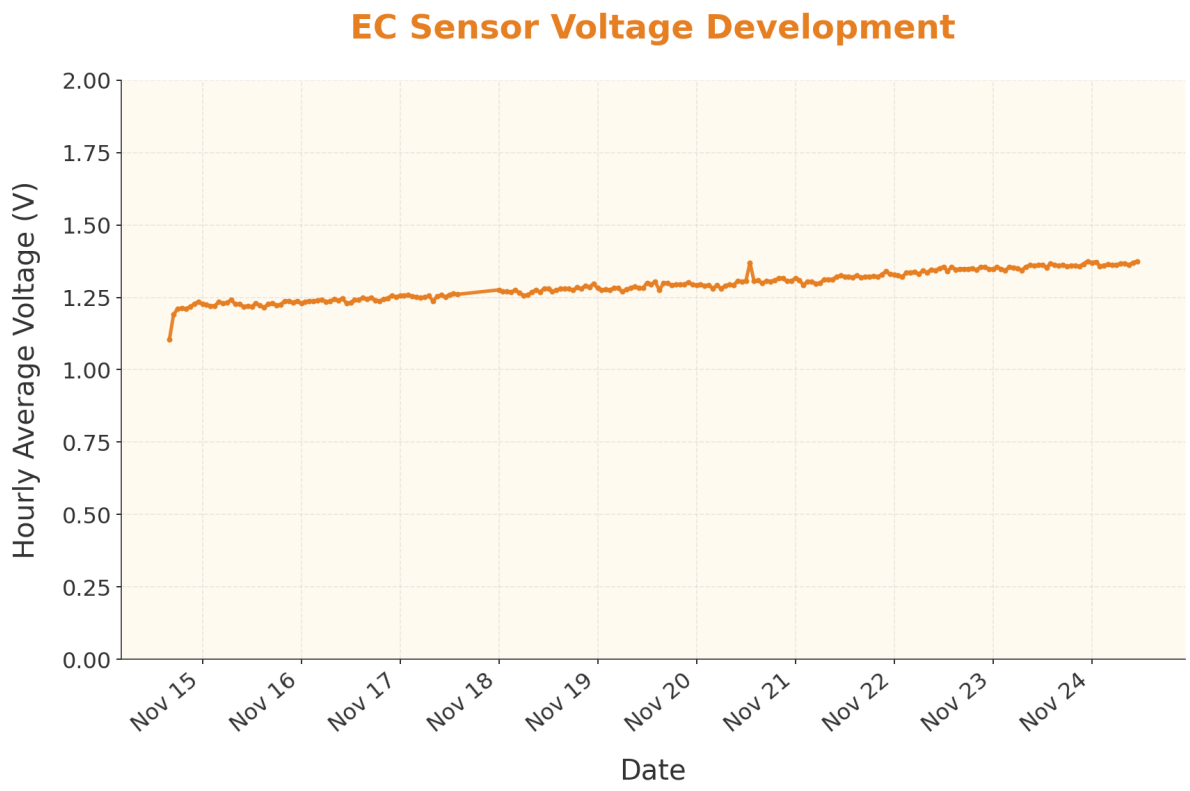

Figure D.5: Raw voltage output for the static EC beaker test utilizing Hoagland nutrient solution (15 to 24 November). This dataset defines the baseline voltage mapping used for the second nutrient formulation phase.

Voltage-to-Physical Conversion

The raw voltages (V_{raw}) presented in this appendix can be converted back to the reported chemical values using the linear relationship defined in Section 4.3.

E

PhD 3-Year Research Proposal

The research proposal starts on the next page.

Research proposal: Characterisation of droplet size, fog plume behaviour, and failure modes in VMA based fogponics for lunar agriculture

Measurement and modelling framework for cross gravity validation of fogponic atomization

by

Siert Hamers

—

Instructor: [TBD]
Faculty: [TBD]

TU Delft

1 Introduction

The establishment of a sustained human presence on the Moon requires life support architectures that reduce dependence on resupply and enable predictable, long duration operation. Bioregenerative Life Support Systems (BLSS) address this requirement by recycling resources and producing food in situ. Within BLSS, the Nutrient Delivery System (NDS) is the engineering interface that determines whether plant growth can be maintained with acceptable crew time, mass, power, and reliability. The NDS is therefore not only a crop production subsystem but also a reliability critical element in the overall habitat design.

1.1. Operational heritage and problem framing

The German Aerospace Center (DLR) has advanced Controlled Environment Agriculture (CEA) for extreme environments through the EDEN initiative. The EDEN ISS project in Antarctica demonstrated long duration crop production, producing more than 1,000 kg of fresh crops. It also provided operational evidence on the strengths and limits of current aeroponic implementations. In particular, long duration operation revealed that shared reservoirs and recirculating loops can promote extensive biofilm growth that restricts flow and requires periodic manual cleaning. In parallel, high pressure pumps and biofilm mitigation measures include mass and complexity. These observations motivate a shift toward nutrient delivery architectures that reduce contamination risk and complexity, and provide predictable reliability with minimal crew intervention.

1.2. Engineering bottleneck motivating the research questions

Fogponics is a promising nutrient delivery approach for lunar agriculture because it can, in principle, deliver water and nutrients with high efficiency while keeping the root zone well aerated. However, current fogponic implementations based on vibrating mesh atomizers have low technology readiness for long duration lunar use. The primary limiting factor is hardware unreliability, including rupturing and performance degradation of atomization modules during operation. This unreliability is compounded by two measurement gaps. First, droplet size and droplet size distribution are rarely quantified as a function of atomizer geometry and operating conditions, which prevents physically grounded design rules for lunar applications. Second, current performance assessment often requires removing the atomizer module for inspection, which interrupts operation and makes it difficult to detect degradation early, quantify lifetime, or validate mitigation strategies.

A further challenge is that reduced gravity can change fluid transport, droplet generation, fog behavior and propagation, and droplet settlement and coalescence. As a result, design choices that appear robust under Earth gravity may express differently under lunar relevant conditions. There is therefore a need for a validated, geometry linked framework that connects atomizer design and operating conditions to droplet output, degradation signatures, and time to failure, with monitoring approaches that work in situ and without dismantling the system. Solving this would directly increase technology readiness by enabling predictive operation planning, early fault detection, and evidence based lifetime extension strategies for lunar fogponic hardware.

This gap leads directly to the first set of research questions: how droplet size distribution and delivered

mass flux depend on geometry and operating conditions, how different gravity levels influence droplet behavior, and whether electrical observables can serve as real time indicators of performance and degradation.

2

Research Questions

This research addresses the low technology readiness of VMA based fogponic nutrient delivery for long duration lunar agriculture. The thesis focuses on the atomization module as a reliability critical component and on the operational requirement to predict performance, detect degradation, and extend lifetime without removing the module during operation. Reduced gravity is treated as a key environmental variable that can alter droplet formation and failure progression. Nozzle based aeroponics is used as a baseline for comparison under matched boundary conditions.

2.1. Main research question

How can the reliability and predictability of vibrating mesh atomizer based fogponic nutrient delivery be increased to improve technology readiness for lunar agriculture under reduced gravity?

2.2. Research questions

1. *Geometry to droplets:* How do vibrating mesh geometric parameters, including aperture size, pore pattern, membrane thickness, and active area, influence droplet size distribution and fog output rate across relevant operating conditions?
2. *Degradation and failure mechanisms:* Which physical failure modes dominate in long duration operation, including rupture and progressive performance loss, and how are these modes linked to mechanical loading, fluid film behavior, and operating conditions?
3. *In situ performance determination:* Which measurable in situ signals can serve as reliable proxies for droplet output and atomizer health state without removing the module, and how can they be translated into a quantitative condition monitoring method?
4. *Reduced gravity effects:* How does reduced gravity change droplet formation at the mesh, fog transport near the module, fluid supply dynamics, and the onset and progression of the identified failure modes?
5. *Predictive modelling and validation:* Can a model that uses atomizer geometry and operating parameters predict droplet size distribution, fog output, and time to failure, and does experimental validation confirm the model under Earth gravity and reduced gravity conditions?
6. *Comparative baseline relevance:* Compared with nozzle based aeroponics under matched boundary conditions, what reliability and performance trade offs emerge, and which requirements determine when fogponics is the preferred solution for lunar operations?

3

Methods and tools

This chapter defines how each research question will be answered through a traceable evidence chain. The approach follows a Science Cycle: models produce falsifiable predictions, predictions are translated into measurable observables, data are acquired with calibrated instruments, and predictions are accepted or rejected using predefined decision criteria. The work combines modeling and experiments. Models support deduction and design space exploration. Experiments provide validation and parameter identification. Reduced gravity testing is used as boundary validation after 1g maturity is achieved.

The chapter is structured into four work packages. Work package 1 addresses geometry to droplets and plume propagation (RQ1, RQ4, part of RQ5). Work package 2 addresses degradation and failure mechanisms (RQ2, part of RQ5). Work package 3 addresses in situ performance determination and condition monitoring (RQ3, part of RQ5). Work package 4 addresses reduced gravity validation and baseline relevance (RQ4, RQ6, completion of RQ5). Each work package specifies the model outputs, the measurement chain, and the decision criteria used to claim validation.

3.1. Key outputs, observables, and failure definitions

The methods are centered on a small set of outputs that are shared across models and experiments. These outputs define what will be predicted, measured, and used for verification.

3.1.1. Core outputs and observables

The core observables are:

- droplet size distribution moments (X_{10}, X_{50}, X_{90}) and Span
- fog output rate as delivered mass flux
- plume propagation metrics, including a residence time and a spatial spread metric in a defined observation volume
- electrical observables for in situ monitoring, including resonance frequency shift, quality factor, and selected impedance magnitude and phase features or current draw
- environmental boundary conditions used for interpretation, including temperature, relative humidity, and airflow velocity

3.1.2. Failure and degradation definitions

Two failure endpoints are used to quantify reliability. Catastrophic failure is defined as loss of atomization due to membrane rupture or electrical failure. Functional failure is defined as a performance drop below an operational threshold, expressed as delivered mass flux falling below a defined fraction of nominal or a sustained shift of droplet spectrum outside an acceptable range. Degradation states are tracked through time to clog, blockage progression indicators, and changes in electrical observables. These definitions enable time to failure and remaining useful life estimation and provide common endpoints for model validation and comparison across operating conditions.

3.2. Overall methodological structure

The methodology is organized into four work packages that map to the research questions and the required evidence. Each work package specifies the model outputs, the measurement chain, and the decision criteria needed to claim validation.

Work package 1: geometry to droplets and plume propagation

This work package builds the quantitative mapping from VMA geometry and operating conditions to droplet size distribution and fog output rate, and extends it to near field plume propagation metrics. It addresses RQ1, RQ4, and part of RQ5.

Work package 2: degradation and failure mechanisms

This work package identifies the dominant degradation mechanisms during long duration operation and converts them into lifetime models that predict functional failure and catastrophic failure. It addresses RQ2 and part of RQ5.

Work package 3: in situ performance determination and condition monitoring

This work package develops a quantitative method to infer fog output and health state from in situ electrical signals, enabling monitoring without module removal. It addresses RQ3 and part of RQ5.

Work package 4: reduced gravity validation and baseline relevance

This work package applies a validation ladder to test gravity sensitivity and model credibility under reduced gravity boundary conditions, and it establishes the operational trade offs relative to nozzle based aeroponics under matched conditions. It addresses RQ4, RQ6, and completes RQ5.

3.3. Key outputs, observables, and failure definitions

This section lists the main tools only in relation to the observables defined in Section 3.3.

Droplet size distributions and plume propagation metrics are obtained using an optical measurement chain based on stroboscopic imaging or laser diffraction, with calibrated length scales and controlled measurement volumes. Fog output rate is measured gravimetrically and used as ground truth for model validation and for calibration of in situ proxies. Electrical observables are acquired using impedance spectroscopy or resonance tracking during operation, synchronized with excitation settings. Environmental boundary conditions are recorded using temperature, humidity, and airflow sensors. Modelling is performed using multiphysics and structural dynamics software for electromechanical response, fluid transport, and fatigue estimation, supported by reduced order models where full coupling is not feasible.

3.4. Data management and reproducibility

All tests generate version controlled datasets with standardized metadata that link each run to geometry, excitation settings, fluid condition, and environmental boundary conditions. Raw data, processed data, calibration files, and analysis scripts are stored together to ensure traceability from reported metrics back to measurements. Processing pipelines for droplet sizing, flux estimation, and electrical feature extraction are documented and kept consistent across test campaigns. Reduced gravity boundary tests use preregistered hypotheses and decision criteria, and the same uncertainty reporting format is applied across 1g and reduced gravity datasets.

4

Workplan

This chapter presents a phased workplan to develop predictive and monitorable VMA based fogponic nutrient delivery for lunar agriculture. Each phase has a clear objective, a concrete set of activities, and defined deliverables. Effort is estimated in person months at 1.0 FTE. All effort ranges are multiplied by a factor 1.5 relative to the initial estimates.

Overview of phases and effort

Phase	Focus	Duration (months)	Months
A	Literature foundation, measurement method selection, reduced gravity experiment definition, and early campaign planning	4	1 to 4
B	Baseline modelling and analysis pipeline, prototype requirements, and experimental design maturity aligned with reduced gravity constraints	5	5 to 9
C	Protocol finalisation and flight ready hardware definition, including documentation and integration requirements	3	10 to 12
D	Prototype build, integration, calibration, and repeatability verification for droplet, plume, and electrical measurements	10	13 to 22
E	1 g baseline campaign using the flight measurement chain, plus data processing and model calibration	6	23 to 28
F	Reduced gravity campaign execution and immediate processing, plus growth trial with electrical monitoring if feasible	5	29 to 33
G	Cross gravity synthesis, model validation, operational monitoring framework, and final reporting consolidation	3	34 to 36

Table 4.1: Three year workplan model in calendar months from project start. The structure prioritises reduced gravity by defining the reduced gravity experiment early and aligning prototype development, measurement chains, and 1 g baselining with the reduced gravity campaign.

Phase A, literature foundation and metrology definition (4 months)

Objective

Build a defensible knowledge base and define measurement and analysis methods that will later be implemented experimentally. The outcome is a clear map of what is known, what is missing, and which measurement and modelling approaches are feasible.

Key activities

- Review and compare droplet sizing methods for the expected VMA droplet range, including reported calibration steps and uncertainty sources.
- Review and compare fog plume propagation measurement methods, including definition of observation volumes and plume metrics.
- Synthesize literature on droplet formation as a function of VMA geometry, excitation frequency, and physicochemical properties of the nutrient solution.
- Synthesize literature on plume propagation as a function of droplet statistics, gravity level, settling, coalescence, and transport processes.
- Map failure modes of VMAs with emphasis on fatigue driven rupture, including crack initiation mechanisms and progression drivers.
- Identify electrical observables for in situ monitoring, including resonance frequency tracking, impedance, current, voltage, and power, and map expected signatures for failure modes and performance drift.

Phase deliverables

- D-A1: Report on droplet sizing methods with trade offs based on resolution, frame rate, measurement volume, and suitability for VMA droplets. Includes validation discussion by comparison to published studies.
- D-A2: Report on plume propagation measurement methods and plume metric definitions for a defined observation volume.
- D-A3: Report and preliminary model outline for VMA droplet formation, including geometry, frequency, and fluid property dependencies, and a gravity sensitivity framing.
- D-A4: Report and preliminary model outline for plume propagation linked to droplet size distribution and gravity.
- D-A5: Report and preliminary model outline for fatigue driven rupture in VMAs, including dominant parameters and expected measurable outcomes.
- D-A6: Electrical monitoring concept and measurement plan, including required electronics, sampling requirements, synchronisation requirements, and expected signal signatures.

Decision gate A

Proceed only if the selected measurement approaches and validation route are feasible with available facilities and resources, and if the model outlines can be converted into implementable formulations with measurable inputs.

Phase B, modelling and experimental design maturity (5 months)

Objective

Convert Phase A model outlines into implementable computational models and define executable experiment plans that directly support validation and rupture quantification.

Key activities

- Implement a droplet formation model that predicts droplet size distribution and output from VMA geometry, excitation frequency, and selected fluid properties.
- Define model calibration parameters and the experiments required to identify them.
- Implement a fatigue and crack propagation model for VMA rupture using literature based fatigue formulations and explicit loading assumptions.
- Define an experiment plan for electrical proxy measurement during degradation and rupture tests, including data schema, timestamps, synchronisation, and analysis pipeline.

Phase deliverables

- D-B1: Droplet formation model implementation with defined inputs, outputs, calibration parameters, and uncertainty handling approach.

- D-B2: Fatigue and crack propagation model implementation with defined material assumptions, loading assumptions, and predicted outcomes.
- D-B3: Executable experiment plan for electrical proxies during degradation and rupture, including instrumentation list, sampling rates, synchronisation plan, and analysis method.

Decision gate B

Proceed only if both models can produce testable predictions and if the experimental plans define measurable quantities that can be evaluated against the model assumptions.

Phase C, experiment definition and hardware readiness planning (3 months)

Objective

Convert modelling and plans into fully specified experimental protocols and hardware designs that can be built and executed.

Key activities

- Define the droplet size and plume propagation validation campaign in 1 g, including test matrix, replication strategy, calibration steps, and data acceptance criteria.
- Define the reduced gravity campaign concept, including target gravity levels, required metrics, and constraints imposed by the platform.
- Define the rupture experiment protocol, including parameter sweeps intended to initiate cracks, measurable outcomes, and replication strategy.
- Finalise electronics and integration design for electrical observables, including wiring, sampling, grounding, and synchronisation with optical and other observables.

Phase deliverables

- D-C1: Executable experiment plan for droplet size and plume propagation with defined metrics, calibration steps, replication plan, and data acceptance criteria.
- D-C2: Executable experiment plan for rupture and fatigue progression with defined parameters, measurable outcomes, and replication plan.
- D-C3: Hardware and integration package for electrical proxy measurements, including electronics specification and data logging specification.

Decision gate C

Proceed only if the protocols are executable end to end and if the hardware designs can be built within the project constraints.

Phase D, build, integration, verification, and first rupture dataset (10 months)

Objective

Build and verify the experimental setups, then execute initial rupture experiments with synchronised electrical logging and a clean dataset.

Key activities

- Build the droplet sizing and plume measurement setup and verify calibration procedures and repeatability.
- Build and verify the electrical measurement chain for resonance and impedance observables and ensure time synchronisation with optical and other data streams.
- Execute pilot rupture tests to confirm the protocol can produce repeatable crack initiation and progression signals.
- Execute the first rupture dataset generation with structured metadata and consistent storage.

Phase deliverables

- D-D1: Working and verified measurement prototype, including calibration records and repeatability checks.
- D-D2: Rupture dataset with time to crack initiation, time to rupture, rupture location, rupture geometry where measurable, and synchronised electrical observables.

Decision gate D

Proceed only if repeatability is sufficient to support statistical comparisons and if the dataset structure supports traceable analysis.

Phase E, 1 g baseline campaign and readiness for reduced gravity and plant trial (6 months)

Objective

Generate validated 1 g droplet and plume datasets across geometries, derive electrical proxy relationships from rupture data, and prepare systems for reduced gravity and plant trials.

Key activities

- Execute a structured 1 g campaign across selected VMA geometries and operating conditions to measure droplet size distribution, fog output rate, and plume metrics.
- Process the rupture and electrical proxy data to derive relationships between physical failure progression and electrical observables.
- Freeze a flight capable configuration and a plant trial capable configuration, including procedures and checklists.

Phase deliverables

- D-E1: 1 g droplet size and plume propagation results across geometries, including distribution metrics and fog output rate metrics.
- D-E2: Electrical proxy relationship for rupture progression, including recommended indicators and candidate detection thresholds.
- D-E3: Reduced gravity ready prototype configuration package and plant trial ready prototype configuration package.

Decision gate E

Proceed only if the 1 g results provide a stable baseline for cross gravity comparison and if the system is operationally stable enough for extended runs.

Phase F, reduced gravity campaign and growth trial with electrical monitoring (5 months)

Objective

Collect reduced gravity droplet and plume data, consolidate rupture and electrical proxy findings, and demonstrate electrical monitoring during a growth relevant operational trial.

Key activities

- Execute reduced gravity tests for droplet size and plume propagation with matched metrics to the 1 g campaign.
- Consolidate rupture and electrical proxy findings into a report suitable for publication level reporting.
- Execute a growth trial with electrical logging and at least one independent operational observable, such as flow rate or mass balance, and record operational events.

Phase deliverables

- D-F1: Reduced gravity droplet size and plume propagation dataset for 0 g and lunar g segments with consistent metrics and metadata.
- D-F2: Report on rupture and electrical proxies, including operational implications and limitations.
- D-F3: Growth trial dataset linking electrical metrics to operational observables and recorded operational events.

Schedule risk note

Reduced gravity access can introduce additional calendar waiting time. Preparation and re qualification work is included in the phase duration.

Phase G, synthesis, cross gravity validation, and operational monitoring framework (3 months)

Objective

Close the loop between models and experiments and deliver a cross gravity prediction capability and an operational monitoring method for VMA health state.

Key activities

- Validate droplet formation and plume propagation models against 1 g, lunar g, and 0 g datasets and update uncertainty bounds.
- Validate the fatigue and rupture model against measured crack and rupture outcomes and update parameter sensitivities.
- Formalise an operational monitoring method based on electrical observables, including recommended metrics, thresholds, and decision logic for condition based maintenance.

Phase deliverables

- D-G1: Final cross gravity synthesis report with model validation results, residuals, uncertainty bounds, and limitations.
- D-G2: Final operational monitoring framework report, including instrumentation requirements and recommended monitoring logic.

Phase	Focus	Duration (months)	Months
A	Literature foundation, method selection, reduced gravity experiment definition, and early campaign planning	4	1 to 4
B	Modelling and experimental design maturity aligned with reduced gravity constraints	5	5 to 9
C	Protocol finalisation and flight ready hardware definition	3	10 to 12
D	Prototype build, integration, calibration, and repeatability verification	10	13 to 22
E	1 g baseline campaign using the flight measurement chain and model calibration	6	23 to 28
F	Reduced gravity campaign execution, immediate processing, and growth trial with electrical monitoring if feasible	5	29 to 33
G	Cross gravity synthesis, model validation, operational monitoring framework, and reporting consolidation	3	34 to 36

Table 4.2: Three year workplan model in calendar months from project start.

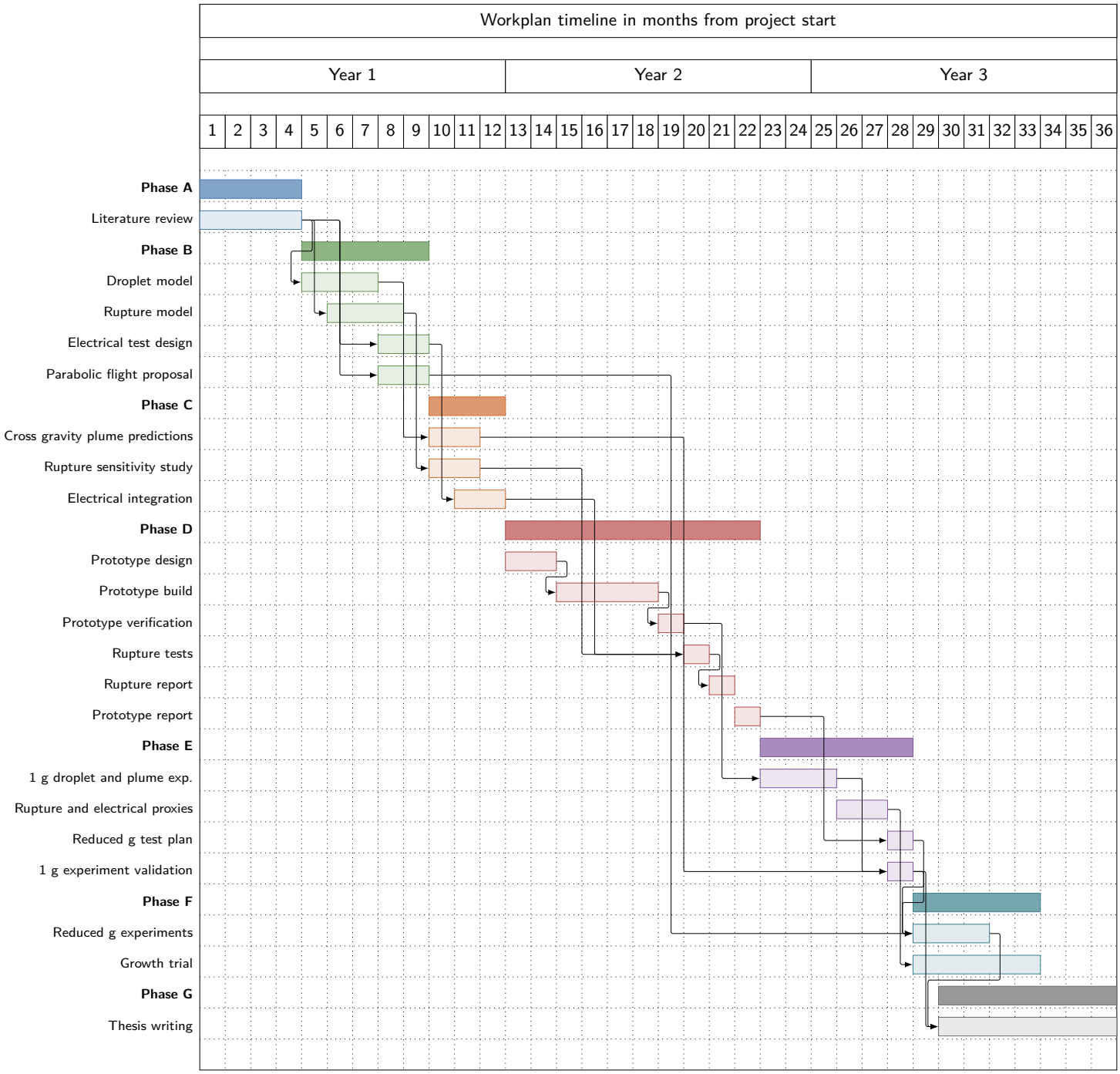
Workplan timeline in months from project start
Year 1
Year 2
Year 3
1 2 3 4 5 6 7 8 9 10 11 12 13 14 15 16 17 18 19 20 21 22 23 24 25 26 27 28 29 30 31 32 33 34 35 36
Phase A
Literature review
Phase B
Droplet model
Rupture model
Electrical test design
Parabolic flight proposal
Phase C
Cross gravity plume predictions
Rupture sensitivity study
Electrical integration
Phase D
Prototype design
Prototype build
Prototype verification
Rupture tests
Rupture report
Prototype report
Phase E
1 g droplet and plume exp.
Rupture and electrical proxies
Reduced g test plan
1 g experiment validation
Phase F
Reduced g experiments
Growth trial
Phase G
Thesis writing

5

Risk Management

5.1. Main risks and likely consequences

Reduced gravity access. The reduced gravity campaign depends on external platforms, most likely parabolic flight. Access is competitive and subject to schedule changes, modified flight profiles, and last minute cancellation. If access is delayed, the cross gravity dataset cannot be collected on the intended timeline. This delays model validation across gravity levels and shifts the final synthesis and reporting that depend on reduced gravity results.

Procurement and facility availability. The experimental programme depends on specific hardware and facility access, including measurement equipment, instrumentation, and atomizer modules. Long lead times, supplier delays, or limited lab availability can delay prototype integration and baseline experiments. If key hardware is late, the build and verification phase expands and the 1 g baseline dataset is delayed. This cascades into reduced gravity readiness because the flight configuration and test plan rely on verified 1 g performance and stable measurement chains.

5.2. Mitigation and contingency plan

Reduced gravity access. Submit the parabolic flight proposal early and define a minimal reduced gravity configuration that targets only the measurements required for cross gravity comparison. Separate the programme into a complete 1 g baseline campaign and a reduced gravity validation campaign with identical metrics and analysis. Start reduced gravity planning during Phase B and Phase C and freeze the flight configuration early to reduce rework. If reduced gravity access is delayed, proceed with full completion of the 1 g dataset, model calibration, and prototype readiness, and treat reduced gravity as a targeted validation step that can be executed when access becomes available.

Procurement and facility availability. Create a long lead item list early and order critical components in advance of prototype build. Identify at least one alternative supplier or substitute component for high risk items. Use a modular prototype design so missing parts do not block all integration work. Define a minimum viable measurement chain that can produce the baseline dataset even if higher end equipment is delayed. Maintain a short buffer in the build and integration phase to absorb late delivery without shifting all downstream experiments.

6

Novelty and expected advancement

6.1. Where the field is now

Current VMA based fogponic research provides limited support for predictive engineering and lunar operations planning. In most studies, fog generation is demonstrated, but droplet size distributions and delivered mass flux are not quantified in a way that links output to atomizer geometry, excitation settings, and nutrient solution properties. As a result, module selection and operating settings are often based on trial and error rather than prediction.

Performance assessment is also typically intrusive and discontinuous. Health state is commonly inferred through post test inspection or by removing the module, which interrupts operation and prevents early detection of degradation. This makes it difficult to quantify lifetime, compare modules consistently, and evaluate mitigation strategies in a controlled manner.

Hardware unreliability is widely reported, including degradation and rupture, but failure is usually described as an observed outcome rather than treated as a reliability problem with measurable drivers, repeatable tests, and a predictive failure model. This limits the ability to define operating envelopes, predict time to failure, or separate different failure modes such as fatigue driven rupture and chemical blinding.

Finally, reduced gravity effects remain insufficiently validated for VMA fogponics. Even when reduced gravity is recognised as important, there is limited cross gravity evidence that links droplet generation and plume transport to metrics that matter for a lunar root zone, such as droplet statistics, propagation behaviour, and settling dynamics. Without this, design choices that appear robust at 1 g cannot be justified for lunar conditions.

6.2. Where this research will bring the field

This project advances VMA based fogponics from demonstration level operation toward predictive and monitorable operation suitable for lunar use. The first outcome is a validated measurement and metric framework for droplet sizing, fog output, and plume propagation. The measurement chain is defined with calibration steps, uncertainty sources, and repeatability targets so results are comparable across module geometries, operating conditions, and gravity levels.

The second outcome is a geometry linked predictive model chain for droplet output and plume behaviour. The model takes atomizer geometry, excitation parameters, and selected fluid properties as inputs and predicts droplet size distributions and plume metrics. It is calibrated using 1 g experiments and validated using reduced gravity data. This creates a tool that can support planning and design decisions under lunar relevant constraints.

The third outcome is a controlled reliability dataset and modelling approach for failure progression. Rupture and degradation are investigated with repeatable test protocols and synchronised observations. A fatigue and failure progression model is developed and confronted with measured outcomes such as time to crack initiation, time to rupture, and changes in performance indicators. This shifts the discussion from failure anecdotes to quantified lifetime behaviour and sensitivity to key parameters.

The fourth outcome is non intrusive condition monitoring through electrical observables. Electrical measurements such as resonance related features and impedance related metrics are evaluated as

indicators of performance drift and failure progression. The novelty is not only measuring these signals, but establishing their relationship to physical output and degradation using synchronised experiments and independent observables. This provides a route to monitoring without dismantling the system.

The fifth outcome is an operational method for sustained fog generation over extended durations. The project delivers a defined operating envelope, a monitoring logic based on electrical and operational observables, and decision rules for intervention. This directly increases technology readiness by enabling predictable operation planning, early fault detection, and evidence based strategies to extend module lifetime under lunar relevant constraints.

6.3. Novel contributions

The novel contributions of this research are:

- A standardised metrology and analysis framework for VMA fog output, including uncertainty and repeatability, enabling comparable datasets across hardware variants and gravity levels.
- A geometry linked prediction capability for droplet statistics and plume behaviour, calibrated in 1 g and validated with reduced gravity data.
- A repeatable experimental and modelling approach for failure progression, including fatigue driven rupture, that supports lifetime estimation and operating envelope definition.
- A non intrusive monitoring concept that links electrical observables to measured performance and degradation, enabling condition monitoring during operation.
- A practical pathway from trial and error hardware testing to predictive operation planning for lunar fogponic nutrient delivery.

6.4. Conclusion

This proposal addresses a clear bottleneck for VMA based fogponics in lunar agriculture: droplet size distribution, fog output, and plume propagation are not yet characterised with consistent metrics and uncertainty, and their dependence on atomizer geometry and gravity level is not validated. This limits the ability to define operating envelopes and to justify design choices for lunar greenhouse operation.

The work is structured as a three year programme that first establishes defensible metrology and model formulations, then delivers a verified measurement prototype and a replicated 1 g baseline dataset, and finally executes a reduced gravity validation campaign to close the cross gravity evidence gap. Reduced gravity is treated as a boundary condition that shapes the modelling, prototype requirements, and baseline experiments, rather than a late stage add on.

The expected outcome is a measurement and metric framework with calibration, uncertainty reporting, and repeatability targets, together with a predictive model chain that links atomizer geometry and operating parameters to droplet statistics and plume behaviour. This will provide an engineering basis for selecting VMA geometries, defining operating settings, and comparing fogponics against nozzle based aeroponics under matched conditions when needed.

By producing comparable datasets across 1 g and reduced gravity, the project will support technology maturation by turning fogponics from demonstration level operation into a system that can be specified, tested, and justified for lunar greenhouse constraints. The deliverables are designed to be reusable by future lunar agriculture programmes as validated data products and as a practical test protocol for continued development.

F

Parabelflug Experiment Proposal

The proposal document starts on the next page

Deutsches Zentrum
DLR für Luft- und Raumfahrt

Template für einen Experimentvorschlag „DLR-Parabelflug“

Bei einer DLR-Standardkampagne stehen drei Flugtage mit je 31 Schwerelosigkeits-Parabeln zur Verfügung.

Basisinformationen finden Sie hier:
http://www.dlr.de/rd/desktopdefault.aspx/tabid-2282/3421_read-5230/
http://www.novespace.fr/

[redacted]

In **englischer Sprache,** dient nach Auswahl für einen Parabelflug auch zur Information für die Firma Novespace (Organisator der Parabelflüge).

Ausgefüllte Form bitte an [redacted] schicken
Please return [redacted]

1) Date of proposal submission	
2) Title/Titel (auch in Deutsch) *“Cross gravity characterisation of VMA droplet output and fog plume propagation using parabolic flight for lunar agriculture.”* *„Schwerkraftübergreifende Charakterisierung des VMA-Tröpfchenausstoßes und der Nebelfahnenausbreitung mittels Parabelflug für die Landwirtschaft auf dem Mond.“*	
3) Author Name, address (institution), phone number, e-mail Siert Hamers, Robert Hooke Str. 7, 28359 Bremen, [redacted]	
4) Partners: Name, address (institution), phone number, e-mail [redacted]	

Deutsches Zentrum
DLR für Luft- und Raumfahrt

5) Abstract (app. 250-300 words)

Fogponics based on vibrating mesh atomizers can support lunar agriculture by supplying water and nutrients while keeping the root zone aerated. At present, droplet size distribution and fog plume behaviour are seldom measured with consistent metrics, and their dependence on atomizer geometry, operating settings, and gravity level is not validated. This proposal develops a measurement and modelling framework to predict and verify droplet and plume behaviour across gravity levels.

The work first establishes metrology for droplet sizing and plume characterisation. Droplet measurements target the micrometre range and include calibration steps, uncertainty sources, and repeatability criteria. Plume behaviour is quantified in a defined observation volume using a fixed set of metrics such as plume boundary position over time and spread angle. One processing pipeline is defined and used for all datasets.

A computational model is then developed. The droplet model links gravity, mesh aperture geometry, excitation frequency, and nutrient solution properties such as surface tension and density to droplet size distributions and fog output rate. The plume model links droplet statistics to transport and settling processes and includes a gravity sensitivity formulation for 1 g, lunar g, and 0 g.

Validation proceeds in two stages. First, a controlled 1 g campaign generates replicated droplet and plume datasets across selected geometries and operating conditions, enabling model calibration and quantified residuals. Second, a parabolic flight experiment acquires time resolved imagery of droplet formation and plume evolution during repeated 1 g, 0 g, and lunar g segments using matched settings and identical metrics. The resulting cross gravity dataset tests model transfer between gravity levels.

The outcome is a validated capability to predict and measure fogponic droplet and plume behaviour for lunar agriculture, with quantified uncertainty and clear limits, enabling selection of atomizer geometry and operating settings for future lunar greenhouse systems.

6) **Description of experiment hardware and experiment conduction**
(including photos, sketches as available)

The experiment hardware consists of a compact fogponic prototype with three main elements: a water reservoir, a VMA based fog generation unit, and a dedicated spray chamber that acts as the optical observation volume.
The reservoir is filled with reverse osmosis water to keep the fluid conditions stable and to reduce variability from dissolved salts or contaminants. The reservoir supplies the fogponic unit, which atomizes the water using a vibrating mesh atomizer.
The spray chamber is an inflatable enclosure. It is transported in a packed state and inflated shortly before the experiment. This approach provides a larger observation volume while keeping the stowed volume low. The chamber includes defined optical access regions for imaging. Inside the chamber, two measurement methods are used.

First, stroboscopic imaging is used for droplet characterisation. Short duration light pulses freeze droplet motion so that droplet images can be processed to obtain droplet size statistics within a defined measurement region.
Second, a laser based imaging method is used to capture fog propagation in the chamber. The aim is to quantify plume development and propagation behaviour over time in a defined observation volume.
A fan is included to clear the chamber after each run. The goal is to return to a fog free initial condition before the next trial. The fan is used only between trials, and it is switched off during measurement windows to avoid disturbing the observed fog field.

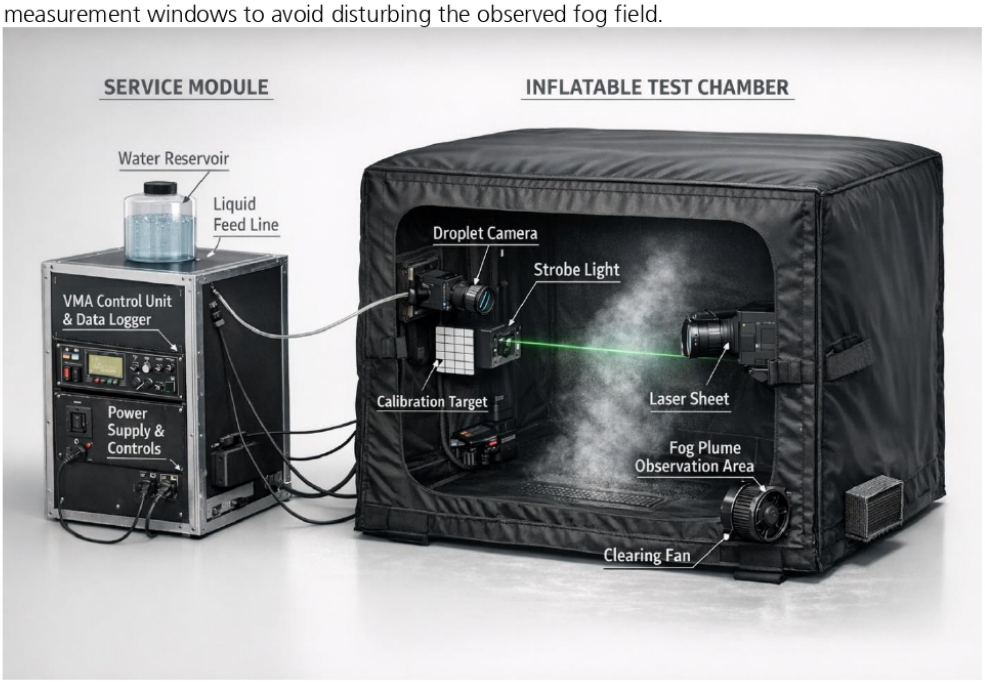

Experiment execution

Each trial starts from a cleared, fog free chamber condition. The VMA is activated at a fixed operating point. Droplet images are taken at defined times after initiation to capture early transient behaviour and near steady behaviour. The planned time points are immediately after initiation, 2 seconds after initiation, and 10 seconds after initiation.
Fog propagation measurements require a longer observation window. For each trial, the plume evolution is recorded for approximately 20 seconds after initiation to capture the development of the fog field within the chamber.
The same sequence is executed under two reduced gravity conditions: microgravity (0 g) and lunar gravity (about 1/6 g). The same VMA operating point and the same timing are used across gravity levels to enable direct comparison using identical metrics and processing.
The sequence is repeated across multiple reduced gravity segments to obtain replicates. The number of replicates is limited by the available reduced gravity windows, time required for chamber clearing, and overall flight schedule. The test plan prioritises replicated measurements at one configuration over many parameter changes, to maximise data quality and comparability between gravity conditions.

Deutsches Zentrum
DLR für Luft- und Raumfahrt

7) Scientific or technical goals and objectives (references, publications as available)

Goal 1:Quantify droplet size distributions produced by vibrating mesh atomizers under controlled conditions and define repeatable metrics with uncertainty estimates.
Goal 2:Quantify fog plume development and propagation in a defined observation volume and define plume metrics that remain comparable across gravity levels.
Goal 3: Develop a predictive model chain that links atomizer geometry, excitation settings, and fluid properties to droplet statistics and plume metrics, and validate it with 1 g and reduced gravity datasets.
Goal 4: Create a cross gravity dataset for fogponic droplet and plume behaviour in 1 g, lunar g, and 0 g, suitable for use as a reference for lunar agriculture system design.

MSc thesis
Title: Development and Experimental Validation of a Fogponic Nutrient Delivery System for Lunar Greenhouses
Institution: Delft University of Technology
Year: 2026

This research is part of doctoral research as follow up on the MSc thesis

8) Technical information (estimations)

Size / dimensions	0.7mx0.7mx0.4m (0.7m x 0.7m x 1.5m inflated)
Weight of racks	13 kg.
Power consumption	Max. 200 Watts
Operators/ mandatory personnel on board per day	2
Number of flight days needed	1/2
Special requirements	

9) Potential of the expected results for relevant applications in space/on earth

Space agriculture fogponics, predictable droplet output
A validated link between mesh geometry, drive settings, and droplet size distribution enables selection and tuning of VMAs to deliver a target droplet range and output rate. This supports predictable nutrient delivery and reduces trial and error during system design and operation.

VMA based medical aerosol production, better control of particle size and delivery
The same geometry linked modelling and validated droplet sizing methods can be used to improve prediction and control of aerosol size distributions in VMA based inhalation devices, where droplet size strongly affects deposition location in the respiratory tract.

Deutsches Zentrum
DLR für Luft- und Raumfahrt

Standardised testing that accelerates technology maturity A repeatable measurement framework with defined metrics enables direct comparison of VMA designs across labs and applications, supporting verification for space hardware and development testing for commercial devices.
10) Finances (if applicable) Budget and cost-effectiveness of the project (rational distribution of resources in relation to project's activities, time frame)

Ausgefüllte Form bitte [redacted] schicken
Please return to [redacted]